

## INFORMATION TO USERS

The most advanced technology has been used to photograph and reproduce this manuscript from the microfilm master. UMI films the original text directly from the copy submitted. Thus, some dissertation copies are in typewriter face, while others may be from a computer printer.

In the unlikely event that the author did not send UMI a complete manuscript and there are missing pages, these will be noted. Also, if unauthorized copyrighted material had to be removed, a note will indicate the deletion.

Oversize materials (e.g., maps, drawings, charts) are reproduced by sectioning the original, beginning at the upper left-hand corner and continuing from left to right in equal sections with small overlaps. Each oversize page is available as one exposure on a standard 35 mm slide or as a 17" × 23" black and white photographic print for an additional charge.

Photographs included in the original manuscript have been reproduced xerographically in this copy. 35 mm slides or 6" × 9" black and white photographic prints are available for any photographs or illustrations appearing in this copy for an additional charge. Contact UMI directly to order.



300 North Zeeb Road, Ann Arbor, MI 48106-1346 USA



8803027

**BICARBONATE REVERSIBLE ANIONIC INHIBITION OF THE QUINONE REDUCTASE  
IN PHOTOSYSTEM II**

Eaton-Rye, Julian John, Ph.D.

University of Manchester, 1987

**U·M·I**  
300 N. Zeeb Rd.  
Ann Arbor, MI 48106

---



BICARBONATE REVERSIBLE ANIONIC  
INHIBITION OF THE QUINONE REDUCTASE  
IN PHOTOSYSTEM II

BY

JULIAN JOHN EATON-RYE

B.Sc., University of Manchester, 1981

THESIS

Submitted in partial fulfillment of the requirements  
for the degree of Doctor of Philosophy in Biology  
in the Graduate College of the  
University of Illinois at Urbana-Champaign, 1987

Urbana, Illinois

UNIVERSITY OF ILLINOIS AT URBANA-CHAMPAIGN

THE GRADUATE COLLEGE

May 27, 1987

WE HEREBY RECOMMEND THAT THE THESIS BY

JULIAN JOHN EATON-RYE

ENTITLED BICARBONATE REVERSIBLE ANIONIC INHIBITION

OF THE QUINONE REDUCTASE IN PHOTOSYSTEM II

BE ACCEPTED IN PARTIAL FULFILLMENT OF THE REQUIREMENTS FOR

THE DEGREE OF DOCTOR OF PHILOSOPHY

*Covindjai*  
Director of Thesis Research  
*Samuel G. ...*  
Head of Department

Committee on Final Examination†

*Covindjai* . . . . . Chairperson  
*H. W. ...*  
*Shitmarsh*  
*Raymond E. Zelik*

† Required for doctor's degree but not for master's.

BICARBONATE REVERSIBLE ANIONIC  
INHIBITION OF THE QUINONE REDUCTASE  
IN PHOTOSYSTEM II

Julian John Eaton-Rye, Ph.D.  
Department of Biology  
University of Illinois at Urbana-Champaign, 1987  
Govindjee, Advisor

The  $\text{HCO}_3^-$  anion regulates photosynthetic electron transport from  $\text{H}_2\text{O}$  to a Hill oxidant.  $\text{HCO}_3^-$  depletion in the presence of inhibitory anions depresses the electron transport rates by as much as ten-fold. All the inhibitory effects of  $\text{HCO}_3^-$  removal were found to be reversible by the addition of 5 mM  $\text{HCO}_3^-$  unless prolonged depletion procedures were used where the inhibitory anion had been omitted. This study investigated contradictory conclusions regarding the site of  $\text{HCO}_3^-$  action in the electron transport chain. Using methyl viologen as the electron acceptor and various artificial electron donors to different regions in the electron transport chain, the major site of  $\text{HCO}_3^-$  action was located on the acceptor side of photosystem II (PS II). The oxidation of  $\text{Q}_\text{A}^-$  (the primary quinone acceptor of PS II) by  $\text{Q}_\text{B}$  or  $\text{Q}_\text{B}^-$  ( $\text{Q}_\text{B}$  is the secondary quinone acceptor of PS II) exhibited a smaller overall half-time at pH 7.5 than at pH 6.5 in  $\text{HCO}_3^-$ -depleted or treated membranes. However, the slowest oxidation of  $\text{Q}_\text{A}^-$  in these membranes, as indicated by the overall half-time parameter, depends on the flash number and the flash frequency in addition to the pH. The operating redox potential for the  $\text{Q}_\text{B}/\text{Q}_\text{B}^-$  couple was found to be pH independent in treated membranes and the equilibrium for the sharing of an electron between  $\text{Q}_\text{A}^-$  and  $\text{Q}_\text{B}$  was decreased by a factor of 4 at pH 6.0. Also in treated membranes the back reaction between  $\text{Q}_\text{A}^-$  and the  $\text{S}_2$  state of the oxygen evolving complex was inhibited four-fold below pH 7.0 but was unaffected above pH 7.5 in the presence of DCMU. A  $\text{HCO}_3^-$  sensitive back reaction with a

half-time of  $< 100 \mu\text{s}$  was observed at pH 8.0 in the presence of DCMU in approximately half of the PS II centers. The kinetic stability of  $Q_B^-$  also appeared to be reduced in  $\text{HCO}_3^-$ -depleted samples. It was concluded that  $\text{HCO}_3^-$  is a ligand to  $\text{Fe}^{2+}$  in the PS II reaction center, and that the rate-limiting step introduced in the linear electron flow by  $\text{HCO}_3^-$  depletion was the protonation of  $Q_B^-$ .

To my parents

#### ACKNOWLEDGMENTS

I would like to thank my thesis advisor, Dr. Govindjee, for his support and direction throughout the course of this project. I would also like to thank Drs. A.R. Crofts, D.R. Ort and H.H. Robinson for support and extensive discussions throughout my graduate training. I am very grateful to Drs. H.H. Robinson and A.R. Crofts for their generous help with the construction of the kinetic fluorimeter used in this study.

Finally, I wish to thank my wife, Elizabeth, for her help and support in the completion of this thesis.

TABLE OF CONTENTS

CHAPTER	PAGE
I. ELECTRON TRANSFER THROUGH PHOTOSYSTEM II ACCEPTORS· INTERACTION WITH ANIONS.....	1
A. Introduction... ..	1
B. The Bicarbonate Effect. ....	10
C. Anionic Interactions on PS II Acceptor Side Chemistry.....	12
D. The Binding Constant for Bicarbonate at the Anion Site.....	19
E. Possible Physiological Roles for Bicarbonate.....	21
F. Objectives of this Thesis.....	22
References.....	23
II. THE SITE OF ACTION OF $\text{HCO}_3^-$ REVERSIBLE ANIONIC INHIBITION.....	30
A. Introduction.....	30
B. Materials and Methods ..	31
1. Preparation of $\text{HCO}_3^-$ -depleted Samples.....	31
2. Steady-state Measurements of Electron Transport. . . .	32
3. Fluorescence Instrumentation . . . . .	35
C. Results and Discussion.....	38
1. Steady-state Electron Transport from Water to Methyl Viologen. ....	38
2. Steady-state Electron Transport to Methyl Viologen from Artificial Electron Donors ..	41
3. The $\text{HCO}_3^-$ Effect in the Presence of $\text{NO}_2^-$ . . . . .	46
4. The $\text{HCO}_3^-$ Effect in the Absence of Inhibitory Anions.....	52
5. Rate-limitation in $\text{HCO}_3^-$ -depleted and Restored Samples.....	58
D. Summary and Conclusions.....	60
References.....	61
III. ELECTRON TRANSFER THROUGH THE QUINONE ACCEPTOR COMPLEX OF PS II IN BICARBONATE-DEPLETED OR ANION INHIBITED THY- LAKOID MEMBRANES AS A FUNCTION OF ACTINIC FLASH NUMBER AND FREQUENCY.....	65
A. Introduction.....	65
B. Materials and Methods.....	67
C. Results.....	68
1. The Effect of pH on Flash 1 in Treated Membranes.....	68
2. The Effect of pH and Flash Number in Treated Membranes.....	74

3. The Effect of pH and Flash Frequency in Treated Membranes.....	89
D. Discussion.....	93
E. Summary.....	99
References.....	99
IV. THE EFFECT OF pH ON ELECTRON TRANSFER THROUGH THE QUINONE ACCEPTOR COMPLEX OF PS II AFTER 1 OR 2 FLASHES IN BICARBONATE-DEPLETED OR ANION INHIBITED THYLAKOIDS.....	103
A. Introduction.....	103
B. Materials and Methods.....	105
C. Results.....	106
1. Oxidation of $Q_A^-$ in the Absence of an Inhibitor.....	106
2. Oxidation of $Q_A^-$ in the Presence of DCMU... ..	121
D. Discussion.....	130
1. $HCO_3^-$ -reversible Changes in Thermodynamic and Kinetic Parameters of the Two-electron Gate.....	130
2. $HCO_3^-$ and the $Fe^{2+}/Fe^{3+}$ Couple....	140
E. Summary and Conclusions... ..	142
References.....	145
V. SUMMARY AND FINAL CONCLUSIONS.. ..	150
A. The Site of Action of $HCO_3^-$ in Electron Transport .. ..	150
B. The Participation of $HCO_3^-$ in Electron Transfer Through the Two Electron Gate.....	154
1. The Two Site Hypothesis.....	156
2. The Single Site Hypothesis.....	169
VITA.....	173

LIST OF TABLES

TABLE	PAGE
1. EFFECT OF BICARBONATE ON VARIOUS ELECTRON TRANSPORT SYSTEMS SUPPORTED BY METHYL VIOLOGEN.....	43
2. ESTIMATED HALF-TIMES AND AMPLITUDES FOR THE INITIAL LINEAR COMPONENT OF $Q_A^-$ OXIDATION AFTER A SINGLE FLASH.....	120
3. ESTIMATED HALF-TIMES AND AMPLITUDES FOR THE INITIAL LINEAR COMPONENT OF $Q_A^-$ OXIDATION AFTER TWO ACTINIC FLASHES SPACED 1 S APART.....	122
4. THE EFFECT OF $HCO_3^-$ -DEPLETION OR ANION INHIBITION ON $K_0$ , $K_{app}$ AND THE OPERATING REDOX POTENTIAL OF THE $Q_B/Q_B^-$ COUPLE.....	132
5. MAJOR CONCLUSIONS.....	151

LIST OF FIGURES

FIGURE	PAGE
1. Pathway of noncyclic electron flow from H <sub>2</sub> O, the electron donor of photosynthesis, to nicotinamide adenine dinucleotide phosphate (NADP <sup>+</sup> ), the physiological electron acceptor.....	2
2. A stylized model of the electron transport chain with most of the light-harvesting pigment-protein complexes omitted.....	4
3. Diagrammatic presentation of the possible reactions associated with the secondary quinone binding site or the Q <sub>B</sub> site .....	7
4. Decay of variable Chl <u>a</u> fluorescence after one actinic flash... ..	13
5. Decay of variable Chl <u>a</u> fluorescence after three actinic flashes spaced at 1 s.....	16
6. Schematic diagram of the kinetic fluorimeter for monitoring Q <sub>A</sub> <sup>-</sup> reoxidation as a function of variable Chl <u>a</u> fluorescence.....	33
7. The linear response of the kinetic fluorimeter... ..	36
8. Bicarbonate stimulation of photosynthetic electron transport supported by methyl viologen.. ..	39
9. Decay of the variable Chl <u>a</u> fluorescence after the third actinic flash in a series of flashes spaced 1 s apart with 15 mM hydroxylamine acting as the electron donor to PS II.....	44
10. Decay of the variable Chl <u>a</u> fluorescence after the third actinic flash in a series of flashes spaced 1 s apart in nitrite incubated thylakoids.....	48
11. The variable Chl <u>a</u> fluorescence at 1 ms after an actinic flash plotted against the nitrite concentration on a logarithmic scale.....	50
12. Decay of variable Chl <u>a</u> fluorescence, in formate-free samples, after the third actinic flash in a series of flashes spaced 1 s apart with water acting as the natural electron donor to PS II.....	53
13. The influence of inhibitory anions in the HCO <sub>3</sub> <sup>-</sup> -depletion medium.....	56
14. Decay of variable Chl <u>a</u> fluorescence after a single actinic flash at pH 6.5 and pH 7.5.....	69

15.	Variable Chl $a$ fluorescence as a function of flash number.....	75
16.	Variable Chl $a$ fluorescence as a function of flash number in different samples from those used for Fig. 15.....	78
17.	Plot of the overall half-time of $Q_A^-$ oxidation as a function of flash number in treated, restored and control membranes... ..	80
18.	Plot of the overall half-time of $Q_A^-$ oxidation in treated membranes with measurements at pH 6.5 and pH 7.5.....	83
19.	Variable Chl $a$ fluorescence yield as a function of flash number at two frequencies (1 or 5 Hz) and at pH 6.5 and pH 7.5.....	85
20.	Oxidation of $Q_A^-$ after the fifth actinic flash in a train of 5 flashes spaced at 5 Hz or 1 Hz.... .	87
21.	Plot of the overall half-time of $Q_A^-$ oxidation in treated, restored, and control membranes after the fifth actinic flash in a train of five flashes.....	91
22.	Decay of variable Chl $a$ fluorescence after a single actinic flash at pH 6.5 and pH 7.5. ....	107
23.	Decay of variable Chl $a$ fluorescence at pH 6.5 and pH 7.5 after 2 actinic flashes spaced at 1 s.. ....	109
24.	Semi-logarithmic plots of the decay of $[Q_A^-]$ after a single actinic flash calculated from the Chl $a$ fluorescence decays in Fig. 22 .....	113
25.	Semi-logarithmic plots of the decay of $[Q_A^-]$ after two actinic flashes spaced 1 s apart calculated from the Chl $a$ fluorescence decays in Fig. 23.....	115
26.	Plot of the overall half-time for $Q_A^-$ oxidation as a function of pH after 1 and 2 flashes.....	117
27.	Decay of variable Chl $a$ fluorescence after a single actinic flash at pH 6.5 and pH 7.5 in the presence of 5 $\mu$ M DCMU.....	123
28.	The reciprocal of the overall half-time of $Q_A^-$ oxidation, in the presence of 5 $\mu$ M DCMU, plotted as a function of pH.....	125
29.	Decay of variable Chl $a$ fluorescence at pH 8.0 in the presence of 5 $\mu$ M DCMU.....	128

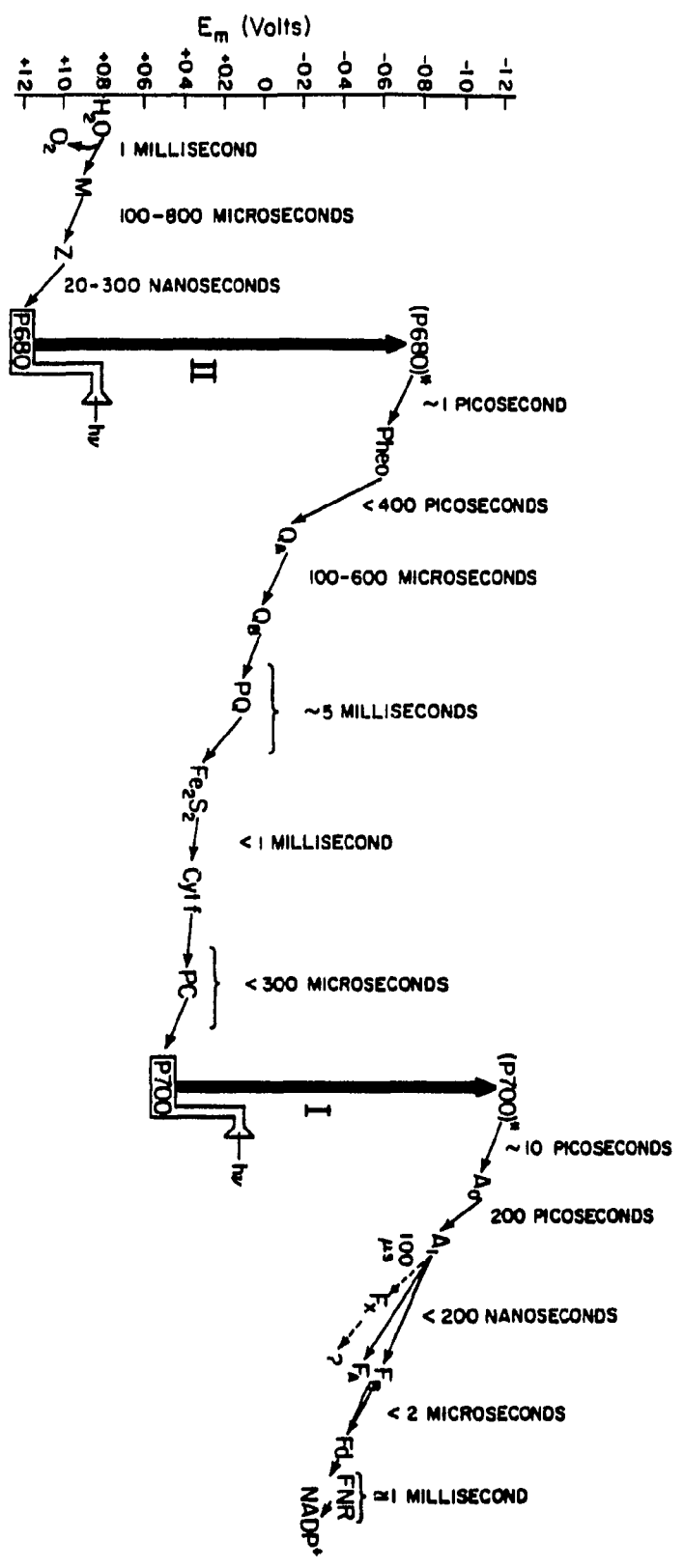
## I. ELECTRON TRANSFER THROUGH PHOTOSYSTEM II ACCEPTORS: INTERACTION WITH ANIONS

### A. Introduction

Much information regarding the complexity of photosynthesis has been drawn from studies of the variable chlorophyll (Chl) a fluorescence yield [1]. Govindjee et al. [2] and Butler [3] showed that the variable fluorescence yield excited by Photosystem II (PS II) light could be quenched by simultaneous excitation by PS I light suggesting its relationship to a two photosystem-two light reaction scheme of photosynthesis. Kautsky et al. [4] explained the Chl a fluorescence transient in terms of the oxidation state of a member of the electron transport chain; fluorescence was suggested to be quenched when this component was oxidized by one light reaction, while its photochemical reduction by another light reaction gave rise to an increase in fluorescence. The designation of this acceptor as Q, for "quencher," arose from the work of Duysens [5] and Duysens and Sweers [6] (see Butler [7]). Q may be identified as  $Q_A$ , the primary quinone acceptor of PS II, in the electron transfer scheme of photosynthesis shown in Figs. 1 and 2.

A heterogeneous population of electron acceptors seems to be present in PS II. Q does not represent a single chemical entity [8,9]. Redox potentiometric titrations have revealed two components,  $Q_H$ , which has an  $E_{m,7}$  (midpoint potential at pH 7) of about 0 mV, and  $Q_L$ , which has an  $E_{m,7}$  of about -250 mV [10,11]. Parallel measurements on C550 (an absorbance change at 550 nm [12]) and variable Chl a fluorescence following single saturating flashes, in DCMU (3-(3,4-dichlorophenyl)-1,1-dimethylurea)-treated samples, revealed the existence of two Q's,  $Q_1$  and  $Q_2$ , where  $Q_1$  was related to all of C550 and to 70% of variable fluores

Figure 1. Pathway of noncyclic electron flow from  $H_2O$ , the electron donor of photosynthesis, to nicotinamide adenine dinucleotide phosphate ( $NADP^+$ ), the physiological electron acceptor.  $E_m$  on the ordinate stands for midpoint redox potential at pH 7.0. Light quanta ( $h\nu$ ) are absorbed in two sets of antenna chlorophyll molecules, the excitation energy is transferred to the reaction center chlorophyll a molecules of photosystem II (P680) and photosystem I (P700) forming (P680)\* and (P700)\*, and the latter two initiate electron transport. M stands for an all-purpose complex, the "M complex" or the oxygen evolving complex (OEC), but it specifically reflects the electron carriers that undergo redox reactions and charge accumulation; Z, a plastoquinol, is the electron donor to P680; Pheo represents pheophytin;  $Q_A$ ,  $Q_B$  and PQ are plastoquinone molecules (see Fig. 3);  $Fe_2S_2$  represents the Rieske iron-sulphur center, Cyt f stands for cytochrome f, PC is plastocyanin;  $A_0$  is suggested to be a chlorophyll molecule,  $A_1$  is possibly vitamin K;  $F_A$ ,  $F_B$  and  $F_X$  are thought to be 4Fe-4S centers and FNR is ferredoxin NADP oxidoreductase. Estimated or directly measured times for various reactions are also indicated. In the case of PS II these are taken from [13] and for PS I from [14]. The values for the intersystem chain are from [15]. In the case of PS I it has also been suggested that  $A_1$  directly reduces  $F_A$  and/or  $F_B$  in approximately 200 ns while  $F_X$  reduction, in approximately 100 us by  $A_1$ , represents a side pathway. For a detailed discussion, see [14]. The figure is redrawn from an earlier presentation by the author [16].



4

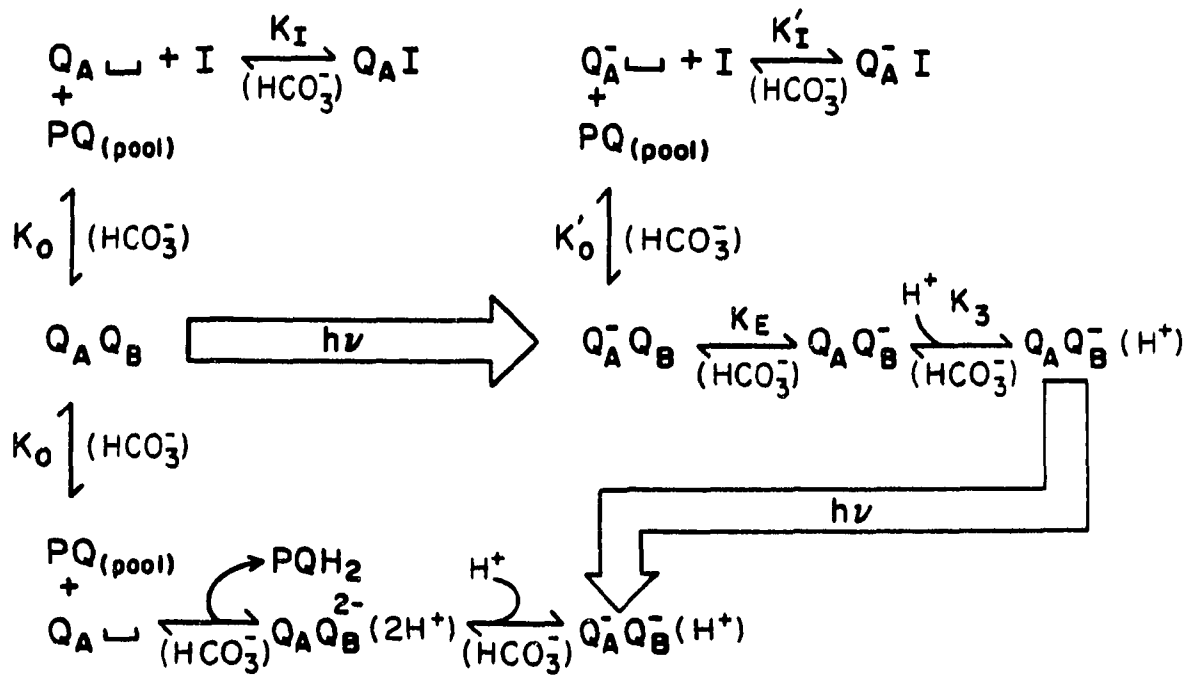
**Figure 2.** A stylized model of the electron transport chain with most of the light-harvesting pigment-protein complexes omitted. The depiction of PS II is adapted from [17] and the organization of the plastoquinol-plastocyanin oxidoreductase or cytochrome  $b_6/f$  complex is based on [18] and [19]. The organization of PS I is adapted from recent overviews given in [19] and [20]. The organization of the  $H^+$ -ATPase ( $CF_1$ - $CF_0$ ) is highly schematic. The hydrophobic  $CF_0$  appears to contain 4-6 copies of the DCCD (N,N'-dicyclohexylcarbodiimide) binding protein or subunit III but  $CF_0$  has not yet been purified [21]. A model for isolated  $CF_1$  has recently been proposed [22]. The subunit stoichiometry shown here is  $3\alpha : 3\beta : \gamma : \delta : \epsilon$  [21]. The figure is modified from that presented earlier by the author in [16].



cence yield [23,24]. Reduction of  $Q_H$  and  $Q_1$  is associated with the creation of a membrane potential ( $\Delta A$  515), whereas reduction of  $Q_2$  and  $Q_L$  is not [25,26]. Furthermore,  $Q_1$  gives a semiquinone signal X-320, whereas  $Q_2$  does not [27]. It appears that  $Q_1$  and  $Q_H$  are the same acceptor located on a side different from that of  $Q_2$  and  $Q_L$ .

$Q_B$ , the secondary quinone acceptor of PS II (Figs. 1-3), is thought to function in a two-electron gating mechanism [28,29]. Electrons are first transferred from reduced pheophytin ( $\text{Pheo}^-$ ) to  $Q_A$ , which can only be reduced to the semiquinone form.  $Q_A^-$  is then oxidized by  $Q_B$  (Fig 3). After two such events,  $Q_B$  is reduced to plastoquinol ( $Q_B^{2-}(2H^+)$ ), which then exchanges with a plastoquinone (PQ) from the plastoquinone pool (PQ pool). Independently, Velthuys [30] and Wraight [31] proposed that the mode of action of a number of PS II herbicides (e.g., DCMU in plants) is to compete with the quinone for the secondary acceptor binding site, the  $Q_B$ -site. Following a single actinic flash an equilibrium for an electron is set up between the two quinone acceptors. While  $Q_B$  and plastoquinol ( $Q_B^{2-}(2H^+)$ ) are bound loosely at the  $Q_B$ -site,  $Q_B^-$  is bound tightly and the equilibrium (see Fig. 3) is displaced towards  $Q_B^-(H^+)$ . A value of 20 for this parameter has been estimated at pH 7.6 [32]. In the presence of a non-electron accepting herbicide (I), such as DCMU,  $Q_A^-I$  is produced (Fig. 3);  $K_O$  and  $K_I$  are the association constants for  $Q_B$  and I respectively when  $Q_A$  is reduced. When  $K_I'$  is  $\gg K_O'$  centers become stable in the state  $Q_A^-I$ . Since  $Q_A^-$  is not a quencher of fluorescence, the presence of  $Q_A^-I$  may be detected by measurements of the variable Chl  $a$  fluorescence yield. In the presence of DCMU, however, the formation of centers in the state  $Q_A^-I$  appears to be present only in 50-70% of PS II [33-37]. This apparent partial displacement of  $Q_B$  has been attributed to heterogeneity of PS II electron acceptors

Figure 3. Diagrammatic presentation of the possible reactions associated with the secondary quinone binding site or the  $Q_B$ -site. Photochemical reactions are shown as open arrows;  $\square$  represents the empty  $Q_B$ -site.  $K_O$  and  $K_I$  are the association constants for plastoquinone and herbicide respectively when  $Q_A$  is oxidized, and  $K_O'$  and  $K_I'$  are the association constants when  $Q_A$  is reduced.  $K_E$  is the equilibrium constant for the sharing of an electron between  $Q_A$  and  $Q_B$ , and  $K_3$  is the equilibrium constant for a proton in association with  $Q_B^-$ . The reactions apparently influenced by  $HCO_3^-$  are indicated (see [38] and text for details). The figure is redrawn from an earlier presentation by the author [16].



rather than equilibrium between the possible states indicated in Fig. 3. Centers which do exhibit electron back-transfer from  $Q_B^-$  to  $Q_A$  in the presence of DCMU are known as B-type; those accounting for the remainder of the variable fluorescence are described as non-B-type. Lavergne [35] has suggested that non-B-type centers are not connected to the main electron transfer pathway; further B-type centers possess many characteristics of  $Q_1$  centers while non-B-type centers resemble  $Q_2$  centers [8].

There is an additional complexity. PS II $\alpha$  and PS II $\beta$  centers are characterized by kinetic components of the steady-state fluorescence induction curve. The Chl a transient, in the presence of DCMU, exhibits a fast sigmoidal phase corresponding to PS II $\alpha$  and a slower exponential phase corresponding to PS II $\beta$  [39,40]. The sigmoidicity of the  $\alpha$  phase has been suggested to arise as a consequence of interconnected antennae serving these centers. In this matrix model [41] the  $\alpha$ -centers exist in a statistical pigment bed (see also [42]). Energy transfer is allowed between PS II units such that an exciton arriving at a closed reaction center is able to visit other centers until it encounters an open trap. The first-order kinetics of PS II $\beta$  centers, by contrast, arise from centers where energy transfer from closed to open centers is not possible. It has been proposed that PS II $\alpha$  are associated with stacked appressed thylakoid membranes and PS II $\beta$  is present in the stroma lamellae (see e.g., [43]). Studies employing absorbance difference spectroscopy have shown that while  $\alpha$ -centers contain  $Q_1$ ,  $\beta$ -centers contain both  $Q_1$  and  $Q_2$  [44,45].

Recently, a population of PS II centers have been identified that are able to evolve oxygen in the presence of halogenated benzoquinones,

artificial electron acceptors for PS II, but are not connected to the main electron transport pathway [46]. These centers appear to represent about 40% of the total PS II present. The relationship of these centers to other PS II heterogeneities has yet to be fully characterized, but it has been argued that PS II $\beta$  -centers comprise a subset of these inactive centers [46].

For further details of PS II the reader is referred to published reviews [1,8,9,13,47].

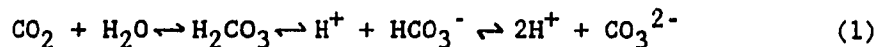
In the remainder of this overview some of the studies that have explored the effects of anions on the acceptor side of PS II will be discussed. Electron transfer at the level of the two-electron gate has been shown to be inhibited by the presence of formate and NO<sub>2</sub><sup>-</sup> [38, 40-50]. Whether this effect is due to the removal of bound HCO<sub>3</sub><sup>-</sup> or due to a direct inhibitory effect is not yet clear. However, this inhibition is uniquely reversed by the addition of HCO<sub>3</sub><sup>-</sup> (see e.g., [51,52]) Furthermore, a wide range of monovalent anions have been shown to be competitive inhibitors of HCO<sub>3</sub><sup>-</sup> binding [52; cf. 51]. These findings suggest the existence of an anion binding site on PS II that, when occupied by HCO<sub>3</sub><sup>-</sup>, facilitates electron transport into the PQ pool. This thesis will investigate the possibility that formate and NO<sub>2</sub><sup>-</sup> inhibit electron flow by displacing HCO<sub>3</sub><sup>-</sup>. An alternative approach is that the stimulation of electron transport by HCO<sub>3</sub><sup>-</sup> is simply due to the removal of inhibitory anions [53,54].

#### B. The Bicarbonate Effect

Warburg and Krippahl [55] discovered the stimulatory effect of HCO<sub>3</sub><sup>-</sup> on the Hill reaction. Originally, it was assumed by Warburg that this effect was on the oxygen evolving mechanism, i.e., he assumed that

O<sub>2</sub> was evolved from CO<sub>2</sub>. Recent studies have shown [56-58] that a large effect is on the electron acceptor side of PS II. Reports of small HCO<sub>3</sub><sup>-</sup>-reversible effects on the donor side of PS II (e.g., [54,59,60]) are not necessarily in contradiction with this assertion. It is entirely possible that such effects result from a relay of changes through the transmembrane helices perturbing a function of the D1 protein on the donor side. This possibility has been suggested by Trebst and Draber [61] to account for donor side effects attributed to phenolic herbicides and DCMU

Good [51] studied the conditions necessary for HCO<sub>3</sub><sup>-</sup>-depletion and found that the presence of anions, particularly formate, acetate and chloride, facilitated the depletion process. Since HCO<sub>3</sub><sup>-</sup> in solution sets up the following equilibria:



the nature of the active species involved has been the subject of several studies. The most effective pH to stimulate the Hill reaction in HCO<sub>3</sub><sup>-</sup>-depleted thylakoids, upon addition of HCO<sub>3</sub><sup>-</sup>, was found to be in the pH 6-7 range [62,63]. In confirmation of this, the maximal HCO<sub>3</sub><sup>-</sup>-restored/HCO<sub>3</sub><sup>-</sup>-depleted ratio of Hill reaction rates was found to be at pH 6.5 [64]. Furthermore, addition of CO<sub>2</sub> to HCO<sub>3</sub><sup>-</sup>-depleted samples was found to stimulate Hill activity more readily than addition of HCO<sub>3</sub><sup>-</sup> to HCO<sub>3</sub><sup>-</sup>-depleted samples at 5°C and pH 7.3 [65,66]. Since the pK for the overall reaction (CO<sub>2</sub> + H<sub>2</sub>O ↔ H<sup>+</sup> + HCO<sub>3</sub><sup>-</sup>) is 6.4, it was suggested (e.g., [64]) that CO<sub>2</sub> was the species required for diffusion to the active site in HCO<sub>3</sub><sup>-</sup>-depleted membranes, but that HCO<sub>3</sub><sup>-</sup> was the active species in restoring the activity. That the active species is indeed HCO<sub>3</sub><sup>-</sup> has been recently shown ([67]; also see [38]) by taking advantage of the pH dependence of the [CO<sub>2</sub>]/[HCO<sub>3</sub><sup>-</sup>] ratio at equilibrium. The

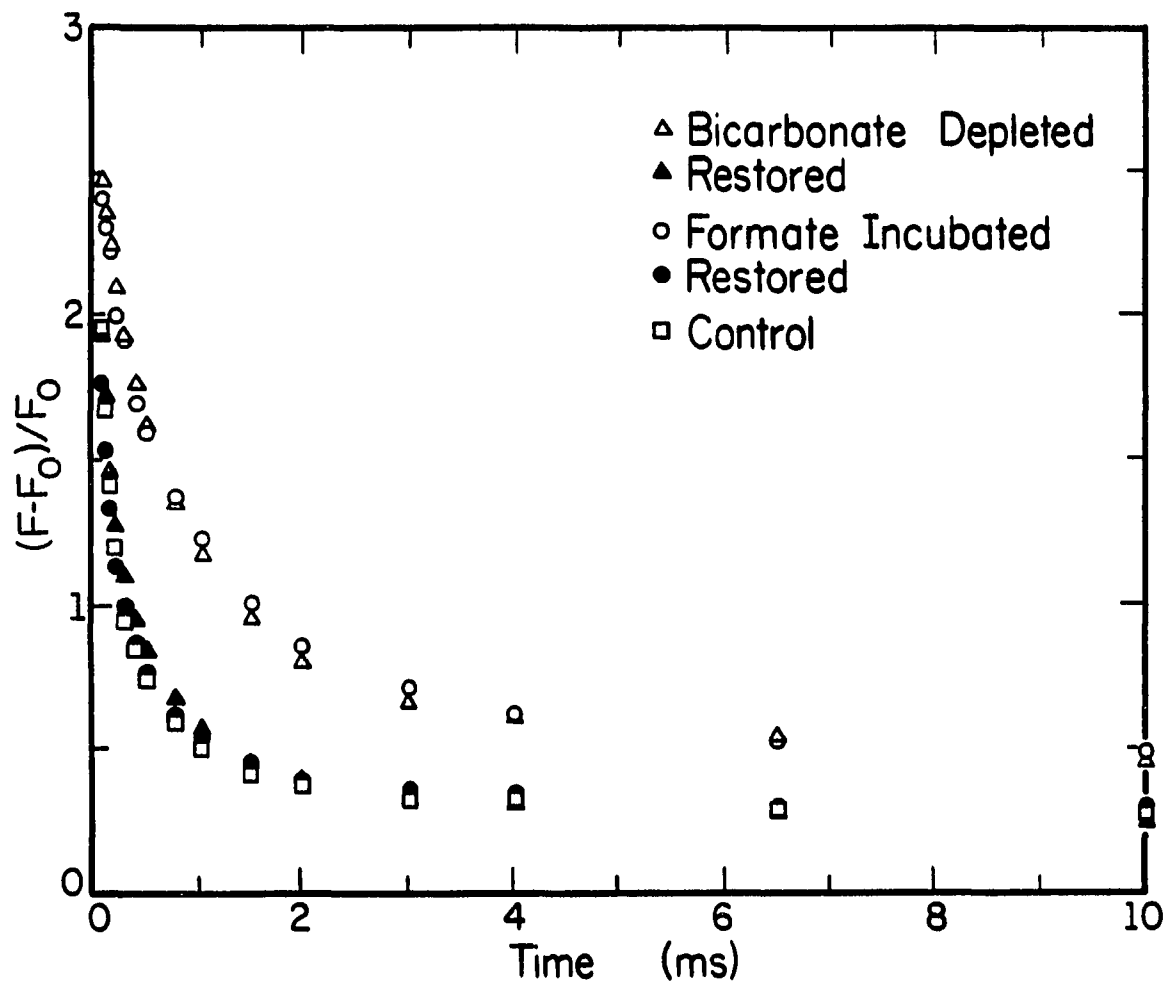
rate of restored electron transport, in  $\text{HCO}_3^-$ -depleted membranes in the presence of formate, was found to depend on the  $\text{HCO}_3^-$  concentration when the  $\text{CO}_2$  concentration was held constant. This work also demonstrated that  $\text{H}_2\text{CO}_3$  and  $\text{CO}_3^{2-}$  have no direct involvement in reversing  $\text{HCO}_3^-$ -depletion.

The location of the  $\text{HCO}_3^-$  effect in the electron transport chain has been identified through several approaches. Wydrzynski and Govindjee [68] studied the effect of this phenomenon on the Chl *a* fluorescence induction kinetics and observed an accelerated rise in  $\text{HCO}_3^-$ -depleted samples. This demonstrated that the reoxidation of  $\text{Q}_\text{A}^-$  had been impaired in the depleted samples. Employing specific inhibitors and electron donors and acceptors, which enabled the electron transport chain to be dissected into a number of clearly defined partial reactions, the  $\text{HCO}_3^-$  effect was located on the electron acceptor side of PS II ([62]; also see [69]). Competitive binding studies with several PS II herbicides, which bind near  $\text{Q}_\text{B}$ , also support this view [70-75]. It is therefore anticipated that a study of the  $\text{HCO}_3^-$  specific reversal of anionic inhibition will add to our understanding of PS II acceptor side chemistry.

### C. Anionic Interactions on PS II Acceptor Side Chemistry

Kinetics of  $\text{Q}_\text{A}^-$  reoxidation may be followed by monitoring the decay of Chl *a* variable fluorescence by a double-flash technique [76]. Following a single-turnover actinic flash, a second weak flash, sampling approximately 1% of the centers [77], is given at specified times. The fluorescence yield from the weak analytical flash is a function of  $[\text{Q}_\text{A}^-]$ , the relationship being non-linear [41,78]. Adoption of this technique has shown  $\text{Q}_\text{A}^-$  reoxidation to be inhibited identically in

Figure 4. Decay of variable Chl a fluorescence after one actinic flash. Restored decays were after the addition of 10 mM  $\text{HCO}_3^-$ .  $F_0$  is the chlorophyll a fluorescence yield from the measuring flash when all  $Q_A$  was oxidized and  $F$  was the yield at the indicated time after the actinic flash. The half-times for  $Q_A^-$  oxidation were: for  $\text{HCO}_3^-$ -depleted membranes, 1.2 ms; for formate-incubated membranes, 1.2 ms and for control membranes, 230  $\mu\text{s}$ . The figure is redrawn from [49].

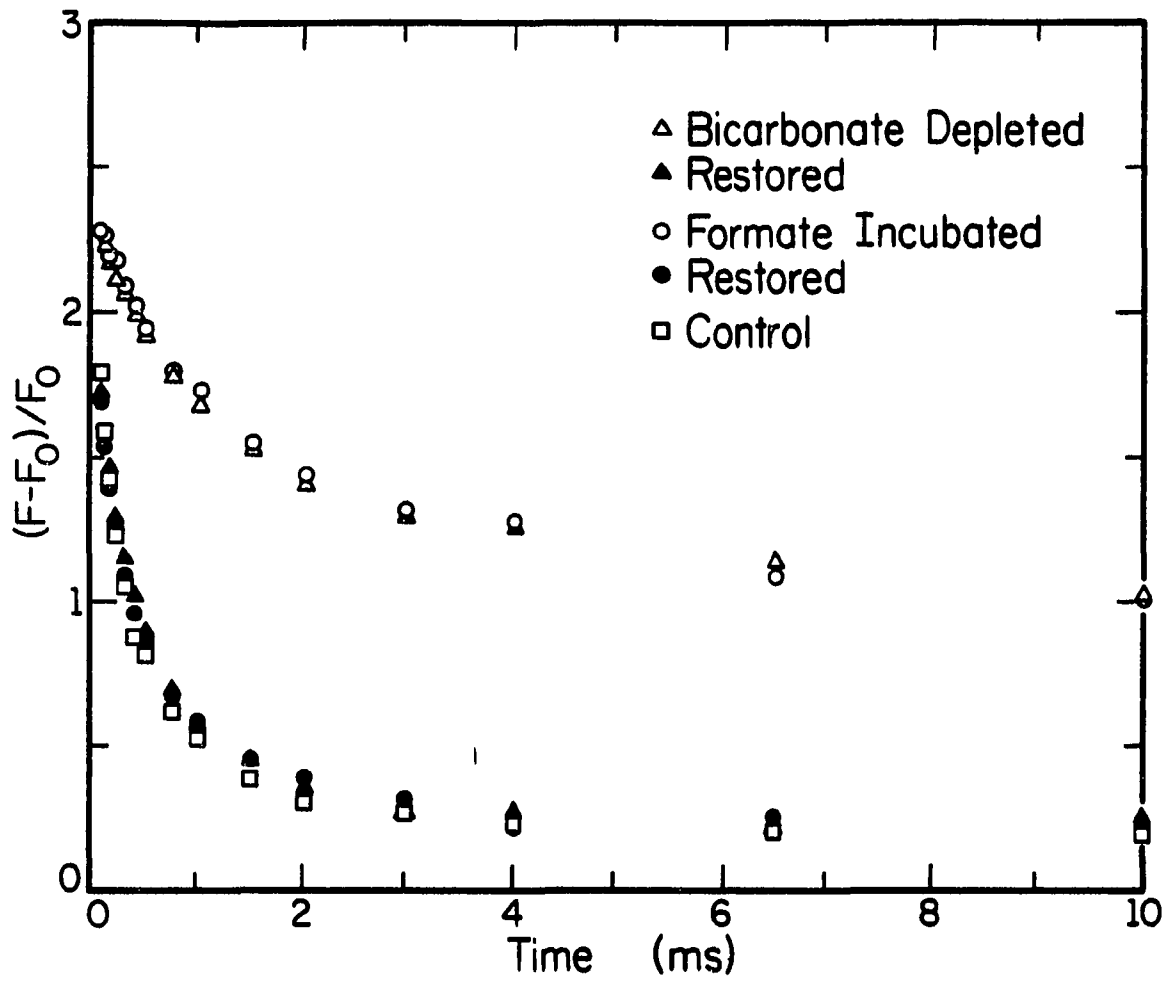


samples  $\text{HCO}_3^-$ -depleted in the presence of formate [48,49,79,80], and similar samples even in the presence of atmospheric  $\text{CO}_2$  (390  $\mu\text{l/l}$ ) (Fig. 4, and see author's work in [49]).

The extent of the anionic interaction is dependent upon flash number [48]. Using Chl *a* fluorescence, the author in collaboration with Dr. H.H. Robinson *et al.* [49] has measured half-times for  $Q_A^-$  reoxidation of 1.2 ms for  $\text{HCO}_3^-$ -depleted and formate-incubated samples equilibrated with 390  $\mu\text{l/l}$   $\text{CO}_2$  and 230  $\mu\text{s}$  for control and  $\text{HCO}_3^-$ -restored thylakoids after a single flash. After the third flash, we obtained half-times of 13 ms for  $\text{HCO}_3^-$ -depleted, 10 ms for formate-incubated equilibrated with 390  $\mu\text{l/l}$   $\text{CO}_2$  and 360  $\mu\text{s}$  for  $\text{HCO}_3^-$ -restored samples. The half-times after flash 2 were intermediate between flash 1 and 3; subsequent flashes yielded results similar to flash 3 (see Figs. 4 and 5). This phenomenon has also been measured by the absorbance change at 320 nm [81,82] and by the 515 nm absorbance change both in thylakoids [79] and in intact chloroplasts [83]. No specific measurements have been made yet to address the differential effects, if any, of this inhibition upon the various PS II heterogeneous populations. However, it is evident from the correlation between the fluorescence and absorption measurements that this phenomenon is associated with  $Q_1$ , *i.e.*, the  $\text{HCO}_3^-$  effect is in the major PS II centers.

The kinetics of  $Q_A^-$  reoxidation for flash 3 are expected to resemble those of flash 1 [84] since, following the formation of plastoquinol after the second flash,  $Q_B^{2-}(2\text{H}^+)$  should readily exchange with a PQ from the PQ pool and  $Q_A^-$  should be oxidized by this PQ species (see Fig. 3). The exchange reactions at the  $Q_B$ -site have been determined to occur with a half-time  $< 2.5$  ms (Robinson, H.H. and Crofts, A.R., personal communication). We have found [38] that the inhibition for the third flash in

Figure 5. Decay of variable Chl a fluorescence after three actinic flashes spaced at 1 s. Other details are as in Figure 4. The half-times for  $Q_A^-$  oxidation were: for  $HCO_3^-$ -depleted membranes, 13 ms; for formate-incubated, 10 ms; and for control membranes, 360  $\mu$ s. The figure is redrawn from [49].



$\text{HCO}_3^-$ -depleted/anion inhibited centers is large and is the same when the dark time between the second and third flashes is 30 ms or 1 s; this result indicates that the exchange reactions are greatly decreased in the inhibited or  $\text{HCO}_3^-$ -depleted case.

A possible explanation for the above observations is that the binding of inhibitory anions to PS II may alter the association constant,  $K_0$ , for  $Q_B$  (see Fig. 3). Although there is no direct measure of the value for  $K_0$ , a number of methods for estimating a value are available [85]. One method is to analyze the decay kinetics of  $Q_A^-$  by monitoring the variable Chl *a* fluorescence after a single flash. Biphasic kinetics are observed for this decay; 60-70% of centers undergo oxidation by a first-order process with a half-time of approximately 150  $\mu\text{s}$  and the remainder by slower processes of indeterminate order [85]. If it is assumed that the centers exhibiting first-order kinetics represent centers in the state  $Q_A Q_B$  before the flash, a value of  $500 \text{ M}^{-1}$  for  $K_0$  can be calculated [85]. This approach is applied to  $\text{HCO}_3^-$ -depleted or anion inhibited membranes in Chapter IV of this thesis.

A shift in the equilibrium for the sharing of an electron between  $Q_A$  and  $Q_B$  (see Fig. 3) has been reported in the thylakoids that have been  $\text{HCO}_3^-$ -depleted in the presence of formate [86]. A two-fold shift in this equilibrium towards  $Q_A^-$  was observed by comparing the rates of the back reaction with the  $S_2$  state (for a discussion of S-states, see [13]) of the oxygen evolving complex both in the presence and absence of DCMU. In the presence of DCMU, the back reaction from  $Q_A^-$  to  $S_2$  was inhibited two-fold, but the back reaction from  $Q_B^-$  in the absence of an inhibitor was found to be unchanged in  $\text{HCO}_3^-$ -depleted membranes [86].

The equilibrium (see Fig. 3,  $K_E$  and  $K_3$ ) for the sharing of an electron between  $Q_A$  and  $Q_B$  is pH dependent [84]. It has, therefore,

been suggested that the presence of a proton in association with the  $Q_B^-$  site stabilizes the electron on  $Q_B^-(H^+)$ . It is therefore possible that  $HCO_3^-$ -depletion inhibits protonation at the  $Q_B^-$ -site. In addition, the fraction of centers decaying through the rapid first-order process after a second flash, has been shown to be proportional to the fraction of centers in which  $Q_B^-(H^+)$  is present [84]. Therefore the inhibition on the  $Q_B^-(H^+)$  protonation suggested above may also account for the inhibited kinetics of  $Q_A^-$  reoxidation observed after the second flash [48,49]. By analogy, the maximal inhibition observed after the third flash could result from  $Q_B^{2-}$  not becoming protonated and therefore not able to exchange with the PQ pool. This interpretation suggests that the rate-limiting step introduced by  $HCO_3^-$ -depletion and/or anion inhibition is the rate of protonation of  $Q_B^{2-}$ . A role for  $HCO_3^-$  in protonation reactions associated with PS II has also been proposed as a result of comparative studies with carbonic anhydrase [54,59]. This topic is addressed in Chapters III and IV.

#### D. The Binding Constant for Bicarbonate at the Anion Site

Given the unique ability of  $HCO_3^-$  to reverse the anion inhibition of quinone mediated acceptor side electron transfer, studies have been performed to determine its dissociation constant. A value of 80  $\mu M$  has recently been obtained using  $H^{14}CO_3^-$  in maize thylakoids with 1 binding site per PS II [72,87].  $H^{14}CO_3^-$  binding has been shown to be competitive with  $HCO_2^-$ ,  $NO_3^-$ ,  $CH_3CO_2^-$  and  $F^-$  [52]. This list is almost certainly not exhaustive.  $NO_2^-$  is of particular interest. Formate has routinely been employed in  $HCO_3^-$ -depletion procedures since the work of Good [51]. This reflects, in part, its structural homology with  $HCO_3^-$  as well as its specificity.  $NO_2^-$ , however, has the same degree of

charge delocalization as does  $\text{HCO}_3^-$ . Blubaugh and Govindjee [67] have discussed the significance of this homology suggesting that the unique behavior of  $\text{HCO}_3^-$  may result from the hydroxyl group on this anion. A similar suggestion was made earlier by Good [51]. Stemler and Murphy [52] have demonstrated that  $\text{NO}_2^-$  is an even more effective competitor of  $\text{H}^{14}\text{CO}_3^-$ -binding than formate, and Jursinic and Stemler [50] have demonstrated, using identical experimental conditions as employed for the  $\text{H}^{14}\text{CO}_3^-$ -binding constant determination, an  $80 \mu\text{M } K_m$  (concentration required to restore half-maximal activity) for  $Q_A^-$  reoxidation as monitored by the decay of variable Chl a fluorescence following a single actinic flash. These findings therefore appear to confirm that the  $80 \mu\text{M}$  dissociation constant measured for  $\text{H}^{14}\text{CO}_3^-$  represents  $\text{HCO}_3^-$  binding that facilitates electron transfer through PS II in the presence of inhibitory anions.

However, it is difficult, if not impossible, to be sure that there is only one binding site and only one binding constant. A hint of at least two separate binding sites was presented by Blubaugh and Govindjee [88]. The existence of a tight binding site may have been overlooked since none of the experiments show data on the amount of intrinsic bound  $\text{HCO}_3^-$  in the sample. Furthermore, the binding studies performed have always been restricted to a concentration range between  $50 \mu\text{M}$  and  $0.5 \text{ mM}$  [72,87]. The possibility of detecting a binding site in the nanomolar range is therefore precluded by these studies. In addition, atrazine and DCMU binding to PS II has been observed to suppress half of the  $\text{HCO}_3^-$  binding noncompetitively when these herbicides bind to an apparent low affinity binding site [59,72].

### E. Possible Physiological Roles for Bicarbonate

The specificity of  $\text{HCO}_3^-$  in reversing the inhibition induced by anions on PS II acceptors has led to speculation regarding an in vivo role for  $\text{HCO}_3^-$ . The phenomenon is clearly associated with PS II- $Q_1$ - $Q_B$ -type centers and therefore is a characteristic of the principal electron transport pathway. Bound  $\text{HCO}_3^-$  has also been suggested [70] to produce a conformational change in the 32 kD herbicide/quinone binding protein or D1 (Fig. 2), facilitating efficient reduction of  $Q_B$  [89], and of exchange of  $Q_B^{2-}(2\text{H}^+)$  with a PQ molecule of the PQ pool (Fig. 3). Indeed, the phenomenon is irrefutably associated with the oxidation of  $Q_A^-$  in these centers and strong evidence suggesting a direct involvement on the exchange reactions of the two-electron gate has been collected [38,48,49,90]. Herbicide action has even been proposed to result from the displacement of  $\text{HCO}_3^-$  from its binding site [64,74].

Another proposal suggests that following  $\text{CO}_2$  exhaustion the accumulation of NADPH would reduce the  $\text{NADP}^+$  concentration, permitting  $\text{O}_2$  to act as an alternative acceptor. The resulting formation of  $\text{H}_2\text{O}_2$  and the superoxide radical  $\text{O}_2^-$  could then inflict serious damage across a wide range of chloroplast functions thus threatening the survival of the whole plant [57]. The shutting down of electron transport in the absence of  $\text{CO}_2$  would avoid this possibility. A further hypothesis regarding the role of  $\text{HCO}_3^-$  in vivo is that bound  $\text{HCO}_3^-$  may be necessary to protect against inhibitory levels of formate produced via photorespiration [53]. This hypothesis may be extended to include other anions such as  $\text{CH}_3\text{CO}_2^-$ ,  $\text{NO}_2^-$  and  $\text{Cl}^-$ .

Arguments against a physiological role for  $\text{HCO}_3^-$  have been based upon the  $80 \mu\text{M}$  binding constant [87]. This claim stems from an estimated in vivo  $\text{CO}_2$  concentration of  $< 5 \mu\text{M}$  [91] which, it has been sugges-

ted, would result in the  $\text{HCO}_3^-$  binding site being unoccupied. However, Blubaugh and Govindjee [67] have pointed out that while the  $\text{CO}_2$  concentration may be quite low in the chloroplast, at pH 8.0, the approximate pH of the stroma, the  $\text{HCO}_3^-$  concentration may be as high as 220  $\mu\text{M}$ . This is well above the estimated binding constant [38,67]. Furthermore, a  $\text{CO}_2$  reversible inhibition of  $\text{Q}_\text{A}^-$  oxidation in intact wheat leaves has been reported by Ireland *et al.* [92]. This therefore suggests a significant role for  $\text{HCO}_3^-$  in the reactions of PS II.

#### F. Objectives of this Thesis

Throughout this chapter the site of action of  $\text{HCO}_3^-$  has been presented as facilitating the passage of electrons through the plastoquinone acceptors of PS II. Despite the extent and breadth of the evidence supporting this conclusion, conflicting results exist in the literature indicating that the rate-limiting step introduced by  $\text{HCO}_3^-$ -depletion is not at the level of the two-electron gate. Fischer and Metzner [93] found that the  $\text{H}_2\text{O}$  to methyl viologen reaction was insensitive to  $\text{HCO}_3^-$ . In addition, these workers found that linear electron transport from artificial electron donors to PS II, supported by methyl viologen as electron acceptor, was also insensitive to  $\text{HCO}_3^-$ . Fischer and Metzner concluded that the major site of  $\text{HCO}_3^-$  action was in fact associated with the oxygen evolving complex. The first objective of this thesis, therefore, was to reinvestigate the specific effect of  $\text{HCO}_3^-$  on electron transport in the presence of methyl viologen and to remove any ambiguity regarding the major site of  $\text{HCO}_3^-$  action. This work is described in Chapter II.

The second and major objective of the thesis was aimed directly at developing an understanding of the mechanism of the  $\text{HCO}_3^-$  effect. In

the preceding pages two principal hypotheses addressing the mechanism of this phenomenon have been advanced. These are: (1) that  $\text{HCO}_3^-$  is directly involved in the protonation reactions associated with plastoquinone reduction at the  $\text{Q}_B$ -site and (2) that  $\text{HCO}_3^-$  is required in maintaining the conformational integrity of PS II to allow for efficient transfer of electrons through the quinone acceptor complex to the plastoquinone pool. Chapters III and IV are directed at the question of mechanism and also address the final objective which is to learn how an understanding of the  $\text{HCO}_3^-$  effect, associated with PS II, can advance our understanding of the operation of the two-electron gate.

#### References

1. Govindjee, Amesz, J. and Fork, D.C., eds. (1986) Light Emission by Plants and Bacteria, Academic Press, Orlando.
2. Govindjee, Ichimura, S., Cederstrand, C.N. and Rabinowitch, E. (1960) Arch. Biochem. Biophys. 89, 322-323
3. Butler, W.L. (1962) Biochim. Biophys. Acta 64, 309-317
4. Kautsky, H., Appel, W. and Amann, H. (1960) Biochem. Z. 332, 277-292
5. Duysens, L.N.M. (1963) Proc. Roy. Soc. B157, 301-313
6. Duysens, L.N.M. and Sweers, H.E. (1963) in Microalgae and Photosynthetic Bacteria (Japanese Society of Plant Physiologists, ed.), pp. 353-372, University of Tokyo Press, Tokyo
7. Butler, W.L. (1966) in Current Topics in Bioenergetics (Sanadi, D.R., ed.), Vol. I, pp. 49-73, Academic Press, New York
8. Black, M.T., Brearley, T.M. and Horton, P. (1986) Photosynthesis Res. 8, 193-207
9. Vermaas, W.F.J. and Govindjee (1981) Photochem. Photobiol. 34, 775-

10. Cramer, W.A. and Butler, W.L. (1969) *Biochim. Biophys. Acta* 172, 503-510
11. Horton, P. and Croze, E. (1979) *Biochim. Biophys. Acta* 545, 188-201
12. Erixon, K. and Butler, W.L. (1971) *Biochim. Biophys. Acta* 234, 381-389
13. Govindjee, Kambara, T. and Coleman, W. (1985) *Photochem. Photobiol.* 42, 187-210
14. Rutherford, A.W. and Heathcote, P. (1985) *Photosynthesis Res.* 6, 295-316
15. Haehnel, W. (1984) *An. Rev. Plant Physiol.* 35, 659-693
16. Govindjee and Eaton-Rye, J.J. (1986) *Photosynthesis Res.* 10, 365-379
17. Mathis, P. (1987) in *Progress in Photosynthesis Research* (Biggins, J., ed.), Vol. I, pp. 151-160, Martinus Nijhoff, Dordrecht
18. Mansfield, R.W. and Anderson, J.M. (1985) *Biochim. Biophys. Acta* 809, 435-444
19. Ort, D.R. (1986) in *Encyclopedia of Plant Physiology: Photosynthetic Membranes* (Staehlin, A. and Arntzen, C.J., eds.), New Series, Vol. 19, pp. 143-196, Springer-Verlag, Berlin
20. Malkin, R. (1986) *Photosynthesis Res.* 10, 197-200
21. McCarty, R.E. and Nalin C.M. (1986) in *Encyclopedia of Plant Physiology: Photosynthetic Membranes* (Staehlin, A. and Arntzen, C.J., eds.), New Series, Vol. 19, pp. 576-583, Springer-Verlag, Berlin
22. Tiedge, H., Schafer, G. and Mayer, F. (1983) *Eur. J. Biochem.* 132, 37-45
23. Joliot, P. and Joliot, A. (1973) *Biochim. Biophys. Acta* 305, 302-

24. Joliot, P. and Joliot, A. (1981) in *Photosynthesis II, Electron Transport and Photophosphorylation* (Akoyunoglou, G. ed.), pp. 885-889, Balaban, Philadelphia
25. Diner, B.A. and Delosme, R. (1983) *Biochim. Biophys. Acta* 722, 443-451
26. Joliot, P. and Joliot, A. (1979) *Biochim. Biophys. Acta* 546, 93-103
27. Joliot, P. and Joliot A. (1981) *FEBS Lett.* 134, 155-158
28. Bouges-Bocquet, B. (1973) *Biochim. Biophys. Acta* 314, 250-256
29. Velthuys, B.R. and Amesz, J. (1974) *Biochim. Biophys. Acta* 333, 85-94
30. Velthuys, B.R. (1981) *FEBS Lett.* 120, 277-281
31. Wraight, C.A. (1981) *Israel J. Chem.* 21, 348-354
32. Robinson, H.H. and Crofts, A.R. (1983) *FEBS Lett.* 153, 221-226
33. Lavergne, J. (1982) *Photobiochem. Photobiophys.* 3, 257-271
34. Lavergne, J. (1982) *Photobiochem. Photobiophys.* 3, 273-285
35. Lavergne, J. (1982) *Biochim. Biophys. Acta* 682, 345-353
36. Lavergne, J. and Etienne, A.L. (1980) *Biochim. Biophys. Acta* 593, 136-148
37. Wollman F-A. (1978) *Biochim. Biophys. Acta* 503, 263-273
38. Eaton-Rye, J.J., Blubaugh, D.J. and Govindjee (1986) in *Ion Interactions in Energy Transfer Biomembranes* (Papageorgiou, G.C., Barber, J. and Papa, S., eds.), pp. 263-278, Plenum Publication Corporation, New York
39. Melis, A. and Homann, P.H. (1975) *Photochem. Photobiol.* 21, 431-437
40. Melis, A. and Homann, P.H. (1976) *Photochem. Photobiol.* 23, 343-350
41. Joliot, P. and Joliot, A. (1964) *C.R. Acad. Sci. Paris Ser. D* 258, 4622-4625

42. Butler, W.L. (1980) Proc. Natl. Acad. Sci. USA 77, 4697-4701
43. Anderson, J.M. and Melis, A. (1984) Proc. Natl. Acad. Sci. USA 80, 745-749
44. Melis, A. and Duysens, L.N.M. (1979) Photochem. Photobiol. 29, 373-392
45. Melis, A. and Homann, P.H. (1979) Biochim. Biophys. Acta 547, 47-57
46. Graan, T. and Ort, D. R. (1986) Biochim. Biophys. Acta 852, 320-330
47. van Gorkom, H.J. (1985) Photosynthesis Res. 6, 97-112
48. Govindjee, Pulles, M.P.J., Govindjee, R., van Gorkom, J.H. and Duysens, L.N.M. (1976) Biochim. Biophys. Acta, 449, 602-605
49. Robinson, H.H., Eaton-Rye, J.J., van Rensen, J.J.S. and Govindjee (1984) Z. Naturforsch. 39C, 382-385
50. Jursinic. P. and Stemler, A. (1986) Photochem. Photobiol. 43, 205-212
51. Good, N.E. (1963) Plant Physiol. 38, 298-304
52. Stemler, A. and Murphy, J.B. (1985) Plant Physiol. 77, 974-977
53. Snel, J.F.H. and van Rensen, J.J.S. (1984) Plant Physiol. 75, 146-150
54. Stemler, A. and Jursinic, P. (1983) Archiv. Biochem. Biophys. 221, 227-237
55. Warburg, O. and Krippahl, G. (1958) Z. Naturforsch. 13B, 509-514
56. Govindjee and van Rensen, J.J.S. (1978) Biochim. Biophys. Acta 505, 183-213
57. Vermaas, W.F.J. and Govindjee (1981) Proc. Indian Natl. Sci. Acad. B47, 581-605
58. Vermaas, W.F.J. and Govindjee (1982) in Photosynthesis: Development, Carbon Metabolism and Plant Productivity (Govindjee, ed.),

Vol. II, pp. 541-558, Academic Press, New York

59. Stemler, A. (1985) in *Inorganic Carbon Transport in Aquatic Photosynthetic Organisms* (Berry, J. and Lucas, W., eds.), pp. 377-387, American Society of Plant Physiologists
60. Saygin, O., Gerken, S., Meyer, B. and Witt, H.T. (1986) *Photosynthesis Res.* 9, 71-78
61. Trebst, A. and Draber, W. (1986) *Photosynthesis Res.* 10, 381-392
62. Khanna, R., Govindjee and Wydrzynski, T. (1977) *Biochim. Biophys. Acta* 462, 208-214
63. Stemler, A. and Govindjee (1973) *Plant Physiol.* 52, 119-123
64. Vermaas, W.F.J. and van Rensen, J.J.S. (1981) *Biochim. Biophys. Acta* 636, 168-174
65. Sarojini, G. and Govindjee (1981) in *Photosynthesis II, Electron Transport and Photophosphorylation* (Akoyunoglou, G., ed.), pp. 143-149, Balaban, Philadelphia
66. Sarojini, G. and Govindjee (1981) *Biochim. Biophys. Acta* 636, 168-174
67. Blubaugh, D.J. and Govindjee (1986) *Biochim. Biophys. Acta* 848, 147-151
68. Wydrzynski, T. and Govindjee (1975) *Biochim. Biophys. Acta* 384, 403-408
69. Eaton-Rye, J.J. and Govindjee (1984) *Photobiochem. Photobiophys.* 8, 279-288
70. Khanna, R., Pfister, K., Keresztes, A., van Rensen, J.J.S. and Govindjee (1981) *Biochim. Biophys. Acta* 634, 105-116
71. Snel, J.F.H. and van Rensen, J.J.S. (1983) *Physiol. Plant.* 57, 422-427
72. Stemler, A. and Murphy, J.B. (1984) *Plant Physiol.* 76, 179-182

73. van Rensen, J.J.S. and Vermaas, W.F.J. (1981) in Photosynthesis II, Electron Transport and Photophosphorylation (Akoyunoglou, G., ed.), pp. 151-156, Balaban, Philadelphia
74. van Rensen, J.J.S. and Vermaas, W.F.J. (1981) *Physiol. Plant.* 51, 106-110
75. Vermaas, W.F.J., van Rensen, J.J.S. and Govindjee (1982) *Biochim. Biophys. Acta* 681, 242-247
76. Mauzerall, D. (1972) *Proc. Nat. Acad. Sci. USA* 69, 1358-1362
77. Joliot, A. (1974) in Proceedings of the Third International Congress on Photosynthesis (Avron, M., ed.) Vol. I, pp. 315-322, Elsevier, Amsterdam
78. Forbush, B. and Kok, B. (1968) *Biochim. Biophys. Acta* 162, 243-253
79. Jursinic, P. and Stemler, A. (1982) *Biochim. Biophys. Acta* 681, 419-428
80. Jursinic, P., Warden, J. and Govindjee (1976) *Biochim. Biophys. Acta* 440, 322-330
81. Farineau, J. and Mathis, P. (1983) in The Oxygen Evolving System of Photosynthesis (Inoue, Y., Crofts, A.R., Govindjee, Murata, N., Renger, G. and Satoh, K., eds.), pp. 317-325, Academic Press, New York
82. Siggel, U., Khanna, R., Renger, G. and Govindjee (1977) *Biochim. Biophys. Acta* 462, 196-207
83. van Rensen, J.J.S. and Snel, J.F.H. (1985) *Photosynthesis Res.* 6, 231-246
84. Robinson, H.H. and Crofts, A.R. (1984) in Advances in Photosynthesis Research (Sybesma, C., ed.), Vol. I, pp. 477-480, Martinus Nijhoff/Dr. Junk Publishers, The Hague

85. Crofts, A.R., Robinson, H.H. and Snozzi, M. (1984) in *Advances in Photosynthesis Research* (Sybesma, C., ed.), Vol. I, pp. 461-468, Martinus Nijhoff/Dr. Junk Publishers, The Hague
86. Vermaas, W.F.J., Renger, G. and Dohnt, G. (1984) *Biochim. Biophys. Acta* 764, 194-202
87. Stemler, A. and Murphy, J.B. (1983) *Photochem. Photobiol.* 38, 701-707
88. Blubaugh, D.J. and Govindjee (1984) *Z. Naturforsch.* 39C, 378-381
89. Vermaas, W.F.J. and Govindjee (1982) *Biochim. Biophys. Acta* 680, 202-209
90. Govindjee, Nakatani, H.Y., Rutherford, A.W. and Inoue, Y. (1984) *Biochim. Biophys. Acta*, 766, 416-423
91. Hesketh, J.E., Wolley, J.T. and Peters, D.B. (1982) in *Photosynthesis: Development, Carbon Metabolism and Plant Productivity* (Govindjee, ed.) Vol. II, pp. 387-418, Academic Press, New York
92. Ireland, C.R., Baker, N.R. and Long, S.P. (1987) in *Progress in Photosynthesis Research* (Biggins, J., ed.), Vol. II, pp. 557-560, Martinus Nijhoff, Dordrecht
93. Fischer, K. and Metzner, H. (1981) *Photobiochem. Photobiophys.* 2, 133-140

## II. THE SITE OF ACTION OF $\text{HCO}_3^-$ REVERSIBLE ANIONIC INHIBITION

### A. Introduction

Bicarbonate ( $\text{HCO}_3^-$ ) is believed to be an activator of photosystem II (PS II) [1,2]. A site of  $\text{HCO}_3^-$  action has been established at the level of reoxidation of  $\text{Q}_\text{A}^-$  [3,4], where  $\text{Q}_\text{A}$  is the primary quinone electron acceptor of PS II. However, a major effect of  $\text{HCO}_3^-$ -depletion (*i.e.*, the effect that limits the electron flow) may be to inhibit the plastoquinone/plastoquinol exchange reactions at the two-electron gate involving a secondary quinone electron acceptor  $\text{Q}_\text{B}$  [5-8].

Measurements of ferricyanide-supported oxygen evolution, in formate-containing thylakoid membranes, have been used routinely to observe an eight to ten-fold stimulation of electron transport rates following the addition of millimolar amounts of  $\text{HCO}_3^-$  to previously  $\text{HCO}_3^-$ -depleted thylakoids (see, *e.g.*, [9,10]). Using methyl viologen as the electron acceptor in an anaerobic system, it was, however, reported [10] that the addition of  $\text{HCO}_3^-$  to  $\text{HCO}_3^-$ -depleted thylakoids was able to produce only a two-fold stimulation. This observation, coupled with other similar observations using artificial electron donors, has been used as evidence for an additional PS II donor side site of action for  $\text{HCO}_3^-$  [10]. Given the possibility of an involvement of  $\text{HCO}_3^-$  in the chemistry of oxygen evolution [11] and that such measurements are quite incompatible with the existing  $\text{HCO}_3^-$  literature [1,2], a further study of the stimulation of the  $\text{H}_2\text{O}$  to methyl viologen reaction by  $\text{HCO}_3^-$  was undertaken.

The site of action of the inhibitory anion, nitrite, and the inhibition resulting from a  $\text{HCO}_3^-$ -depletion procedure in the absence of formate and nitrite are also investigated in this chapter.

## B. Materials and Methods

### 1. Preparation of $\text{HCO}_3^-$ -depleted Samples

Thylakoid membranes were isolated from fresh spinach leaves by first grinding leaf segments in a medium containing 400 mM sorbitol, 50 mM NaCl, 1 mM EDTA (ethylenediaminetetraacetic acid) and 50 mM Tricine (pH 7.8) for 10 s in a Waring blender. The resultant homogenate was filtered through 4 and then 12 layers of cheesecloth. The filtrate was then spun at 5000 x g for 45 s and the supernatant collected and spun at 5000 x g for 10 min. After discarding the last supernatant, the pellet was resuspended and osmotically shocked in a medium containing 50 mM NaCl, 5 mM  $\text{MgCl}_2$  and 10 mM Tricine (pH 7.8). The thylakoids were then again spun at 5000 x g for 10 min and the pellet resuspended in 300 M sorbitol, 10 mM NaCl, 5 mM  $\text{MgCl}_2$  and 10 mM Tricine (pH 7.8) at a concentration of 2.0 mg Chl/ml. Chlorophyll (Chl) concentrations were determined as described by Arnon [12]. Where used, pea thylakoid suspensions were prepared as in [13]

$\text{HCO}_3^-$ -depletion was performed by a method developed by W.F.J. Vermaas in our laboratory and later in collaboration with J.F.H. Snel, and J.J.S. van Rensen in the Netherlands (personal communication). Thylakoids were suspended in 300 mM sorbitol, 25 mM sodium formate, 10 mM NaCl, 5 mM  $\text{MgCl}_2$ , 10 mM sodium phosphate (pH 5.8) and at a Chl concentration of 250  $\mu\text{g}/\text{ml}$ . The thylakoids were then immediately collected by centrifugation at 2500 x g for 10 min and depleted of  $\text{HCO}_3^-$  by resuspension, at a [Chl] of 250  $\mu\text{g}/\text{ml}$ , in the above medium under a constant stream of  $\text{N}_2$  gas. The gas was passed over the solution for 60-90 min. The above medium, called the depletion medium, was boiled and allowed to cool for at least 30 min before each experiment while being

constantly bubbled with  $N_2$  gas to remove  $HCO_3^-$ .

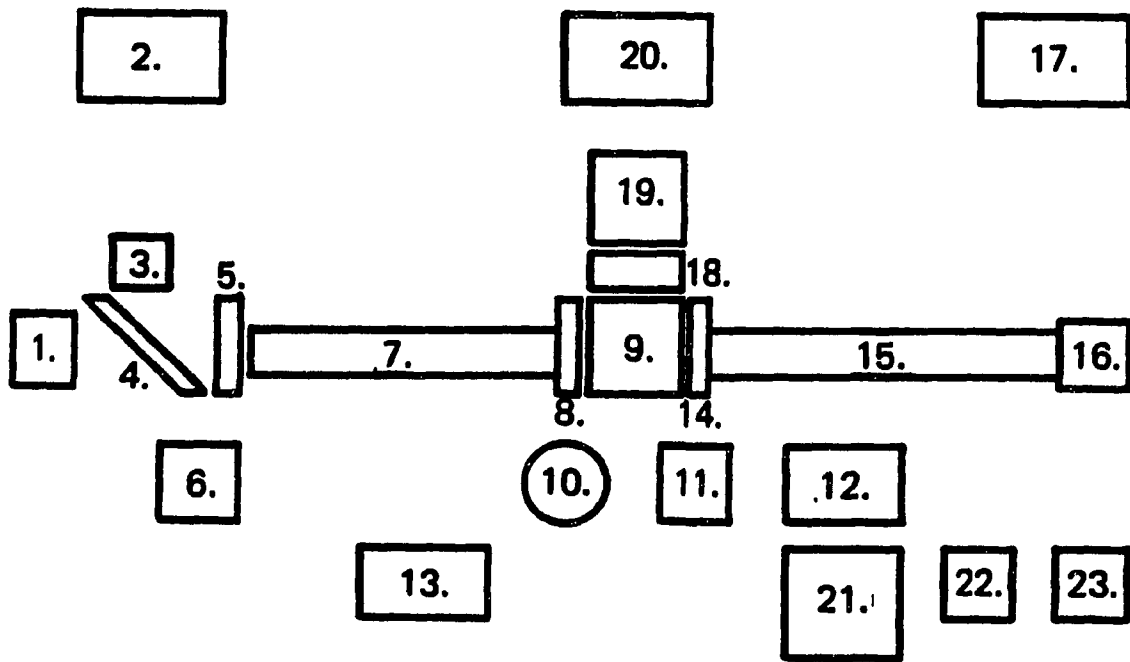
The reaction medium contained 300 mM sorbitol, 10 mM NaCl, 5 mM  $MgCl_2$ , 25 mM sodium phosphate (pH 6.5), 0.25 mM methyl viologen, 1 mM sodium azide and 200 units/ml of superoxide dismutase. To obtain maximum rates of electron flow and to avoid complications due to the possible effects of  $HCO_3^-$  on photophosphorylation [14], 10 mM ammonium chloride and 0.01  $\mu$ M gramicidin D were also present to uncouple the electron flow from photophosphorylation (see [15]).  $HCO_3^-$  was removed from the assay medium by bubbling with either  $N_2$  gas or a mixture of  $N_2$  (80%) and  $O_2$  (20%) for 45 min prior to any measurement. All gasses for the removal of  $HCO_3^-$  were passed through a column of soda-lime and ascarite to facilitate the removal of any trace of  $CO_2$ , and through a water column to prevent evaporation of the sample.

When experiments were conducted on the  $HCO_3^-$  effect in the absence of formate, the latter was omitted from both the depletion and reaction media. When experiments were conducted on the  $HCO_3^-$  effect in the presence of  $NO_2^-$ , formate was replaced with equal amounts of this anion in both the depletion and reaction media.

## 2. Steady-state Measurements of Electron Transport

Steady-state measurements were made with a Clark-type oxygen electrode (Hansatech, U.K.). Saturating orange light was obtained from white light supplied by a high-intensity slide projector (Kodak Carousel 4200 projector) which was passed through a 2 mm thick Corning colored glass filter, CS3-68, and a 2-inch water filter containing 1%  $CuSO_4$ . The intensity of the visible light (400-700 nm) on the surface of the temperature-controlled, water-jacketed electrode assembly was 225  $mW\ cm^{-2}$  as measured by a Lambda Instruments LI-185 radiometer. The

Figure 6. Schematic diagram of the kinetic fluorimeter for monitoring  $Q_A^-$  reoxidation as a function of variable Chl  $a$  fluorescence. Identification of components: (1) actinic saturating flash lamp (FX-124, EG and G); (2) 1.5 Kv power supply for actinic flash lamp; (3) measuring flash (Stroboslave 1539A, General Radio); (4) beam splitter; (5) shutter (Uniblitz 225 LOAOT54); (6) shutter drive unit (Uniblitz 100-2B/B); (7) plexiglas light guide; (8) Corning CS 4-96 filter; (9) sample cuvette (Helma cells 175.50-OS); (10) sample vat connected to cuvette in a flow-system. The cuvette (illumination volume 0.6 ml) is filled by gas pressure on top of the liquid in the vat. Reversing the pressure empties the cuvette back into the vat at the end of each measurement. The gas pressure is varied under computer control by switching a set of solenoid valves. (11) magnetic stir-bar unit. The contents of the vat are stirred via computer control. The stirrer is switched off during a measurement. (12) Flow-system control unit; (13) Neslab (Exacel 100 B) water bath/circulator for temperature regulation of the vat; (14) Corning CS 4-96 filter; (15) plexiglas light guide; (16) additional actinic flash lamp (EG and G) enabling two flashes to be given at very short time intervals ( $< 1$  ms dark-time); (17) 1.5 Kv power supply for additional flashlamp; (18) 685 nm Schott interference filter; (19) EMI 9558A photomultiplier tube; (20) high voltage regulated power supply for photomultiplier tube; (21) Zenith 110 computer with S-100 interface electronics; (22) Houston DMP 40 digital plotter; (23) Mannesman Tally MT 160 printer.



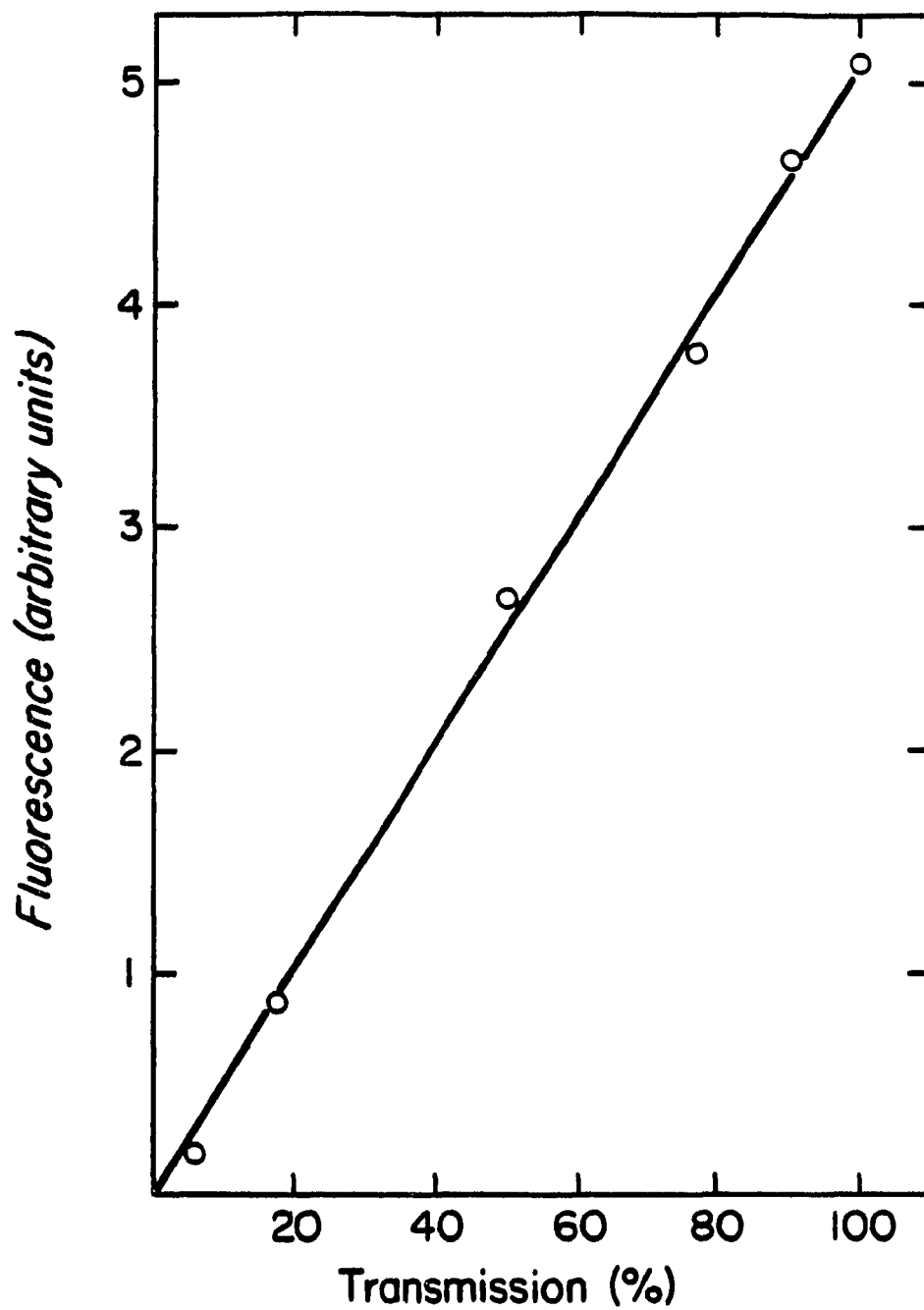
reaction volume (1.25 ml) was comprised of 100  $\mu$ l of  $\text{HCO}_3^-$ -depleted thylakoids added to 1.15 ml of the reaction medium. Thus, the thylakoid suspension in the reaction chamber was at a Chl concentration of 20  $\mu$ g/ml. The  $\text{O}_2$  evolution was recorded on an Esterline-Angus recorder (model E1101S). This apparatus was calibrated by adding sodium dithionite crystals to stirred water in the reaction chamber as described in [16]. The reaction chamber was flushed with  $\text{N}_2$  or the 80%  $\text{N}_2$ /20%  $\text{O}_2$  mixture before each measurement.

Addition of 10 mM  $\text{HCO}_3^-$  to depleted thylakoids was made in the dark and followed by an incubation for 2 min as described earlier [9]. Hydroxylamine [17-19] and benzidine [20,21] were used as electron donors to PS II. Details regarding the electron donor systems are given in the appropriate legends.

### 3. Fluorescence Instrumentation

Measurements of the decay of  $Q_A^-$  were made using the double-flash method monitoring the decay of Chl a variable fluorescence. A schematic diagram of the instrument assembled by the author for this research is presented in Fig. 6. (The help of Prof. A.R. Crofts and Dr. H. Robinson is greatly appreciated.) The kinetics of the decay of variable Chl a fluorescence were measured at 685 nm (10 nm bandwidth) by a weak measuring flash which could be fired at variable times after each of a series of actinic flashes. The measuring flash (Stroboslave 1593A, General Radio) sampled approximately 1% of the PS II centers present. Both the actinic flash (FX-124, EG and G) and the measuring flash were blocked by Corning CS4-96 filters and were of 2.5  $\mu$ s duration at half-maximal peak height [13]. All measurements were made on a sample diluted to contain 5  $\mu$ g/ml Chl in a final volume of 100 ml in a dark stirred vat. A flow

Figure 7. The linear response of the kinetic fluorimeter. The experiment shown presents the fluorescence emitted when the measuring flash was fired using a sample of chlorophyll in ethanol. The different percentage transmissions were obtained using neutral density filters.



cuvette was filled from the vat by computer control.

To insure that the actinic flash was saturating, the variable Chl  $a$  fluorescence yield was measured in the presence of 5  $\mu\text{M}$  DCMU (3-(3,4-dichlorophenyl)1,1-dimethylurea) as a function of light intensity. The tangent to the initial slope was then extrapolated to intercept the determined maximum level of fluorescence ( $F_{\text{max}}$ ). The light intensity indicated by a perpendicular line, from the intercept of  $F_{\text{max}}$  with the tangential slope, to the abscissa was noted. The actinic flash intensity was then set to be approximately three times this level.

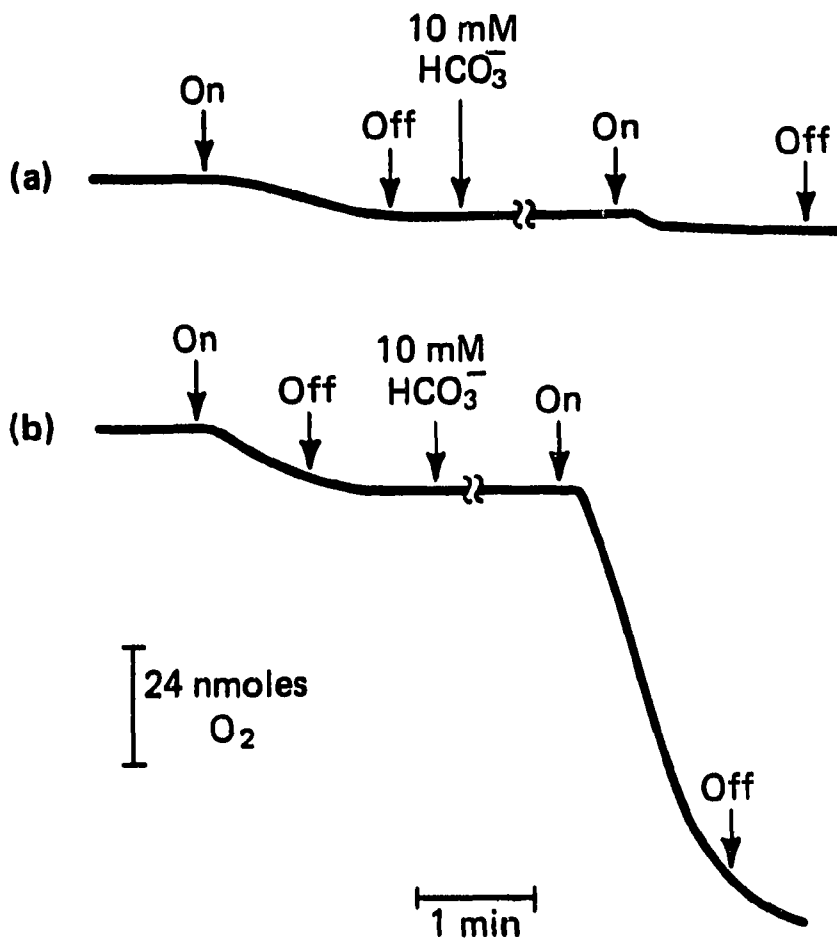
The linear response of the instrument is shown in Fig. 7. For this experiment 10  $\mu\text{l}$  of a 2.0 mg/ml Chl suspension were diluted in 100 ml of ethanol in the dark stirred vat. The measuring flash was then fired with various neutral density filters positioned between the beam splitter and the shutter as shown in Fig. 6. The tail of the actinic flash was determined to be of 70  $\mu\text{s}$  duration by measuring the fluorescence during the actinic flash for a solution of Chl extracted in ethanol.

### C. Results and Discussion

#### 1. Steady-state Electron Transport from Water to Methyl Viologen

Electron flow from  $\text{H}_2\text{O}$  to methyl viologen was measured as  $\text{O}_2$  uptake, by the Clark electrode. The stimulation of electron transport rates in  $\text{HCO}_3^-$ -depleted thylakoids containing 25 mM formate, following an addition of 10 mM  $\text{HCO}_3^-$ , is depicted in Fig. 8. These data were obtained under both anaerobic (Fig. 8a) and aerobic (Fig. 8b) conditions. When  $\text{HCO}_3^-$  had been removed in the reaction medium by bubbling only with  $\text{N}_2$  gas, regeneration of the  $\text{H}_2\text{O}$  to methyl viologen reaction was severely inhibited. This is in agreement with the report of Fischer

Figure 8. Bicarbonate stimulation of photosynthetic electron transport supported by methyl viologen. (a) anaerobic conditions (initial rate, in  $\mu\text{equiv.}(\text{mg Chl})^{-1}.\text{hr}^{-1}$ , is 100, and after the addition of 10 mM  $\text{HCO}_3^-$  it cannot be measured); (b) aerobic conditions (initial rate, in  $\mu\text{equiv.}(\text{mg Chl})^{-1}.\text{hr}^{-1}$ , is 145 and after the addition of 10 mM  $\text{HCO}_3^-$ , 1074). The spinach thylakoids used in this experiment had been stored in liquid nitrogen. For other details see Materials and Methods.



and Metzner [10] where argon gas was used to keep the reaction medium  $\text{HCO}_3^-$ -free. It was under these conditions that the low (i.e., only two-fold) maximal stimulation of electron flow by  $\text{HCO}_3^-$  was inferred from a plot of the methyl viologen Hill reaction as a function of the concentration of added  $\text{HCO}_3^-$ . Under anaerobic conditions, it was possible to reproduce the published observations (data not shown). However, a quite different result was obtained when  $\text{HCO}_3^-$  was removed from the reaction medium using a mixture of 80%  $\text{N}_2$  and 20%  $\text{O}_2$ . Under these aerobic conditions, regeneration of electron transport rates following the addition of 10 mM  $\text{HCO}_3^-$  resulted in a seven-fold stimulation. In fact, as can be seen from Table I, the  $\text{HCO}_3^-$ -restored rate in the presence of methyl viologen was identical to that observed for non-depleted thylakoids measured in the same reaction medium. Thus, when there is no rate-limitation due to the experimental conditions used, a normal  $\text{HCO}_3^-$  effect is indeed observed in the  $\text{H}_2\text{O}$  to methyl viologen electron flow. Thus, the argument [10] for a  $\text{HCO}_3^-$  effect on the electron donor side of PS II, based on a comparison of this effect with ferricyanide from that with methyl viologen as electron acceptor, cannot be sustained.

## 2. Steady-state Electron Transport to Methyl Viologen from Artificial Electron Donors

As noted in the Introduction, there is now considerable evidence that  $\text{HCO}_3^-$ -depletion in the presence of formate results in a rate-limiting step at the level of the plastoquinone/plastoquinol exchange reactions with the plastoquinone pool [5-8]. However, there exists considerable interest in a possible site of  $\text{HCO}_3^-$  action on the donor side of PS II [11]. Fischer and Metzner [10] found that in the presence of artificial electron donors (notably, hydroxylamine), addition of  $\text{HCO}_3^-$

to  $\text{HCO}_3^-$ -depleted samples produced only a slight stimulation of photosynthetic electron transport. This observation was suggested to support the claim that the major site of  $\text{HCO}_3^-$  action was before the site of hydroxylamine donation.

Table 1 shows the results obtained for three artificial electron donor systems under aerobic conditions. Although it is clear in the cases of hydroxylamine and benzidine (both PS II donors) that the addition of  $\text{HCO}_3^-$  produces little or no stimulation in electron transport rates, the key observation is contained in the electron transport rates for the non-depleted controls. Using artificial electron donors to PS II, the electron transport rates in non-depleted controls are not significantly different from those obtained in  $\text{HCO}_3^-$ -depleted samples. An identical result was also obtained when catechol was used as an electron donor (data not shown). Thus, the rate-limiting step in electron transport systems employing artificial donors to PS II is of the order of the rate-limiting step introduced by  $\text{HCO}_3^-$ -depletion, and therefore no further conclusions can be drawn regarding the site of  $\text{HCO}_3^-$  action from this approach.

On the other hand, Fig. 9 demonstrates the existence of the  $\text{HCO}_3^-$ -dependent site on the acceptor side of PS II when electrons are supplied by the artificial donor hydroxylamine. These data show the decay of  $Q_A^-$ , as monitored by the decay of chlorophyll *a* variable fluorescence yield, after the third of a series of actinic flashes spaced 1 s apart. The half-time for the  $\text{HCO}_3^-$ -depleted sample is approximately 10 ms and for the  $\text{HCO}_3^-$ -resupplied sample the half-time is approximately 350  $\mu\text{s}$ , which is the same as for the non-depleted control thylakoids. The half-time for this decay with the intact oxygen-evolving system (with water acting as the natural donor), under the experimental conditions used

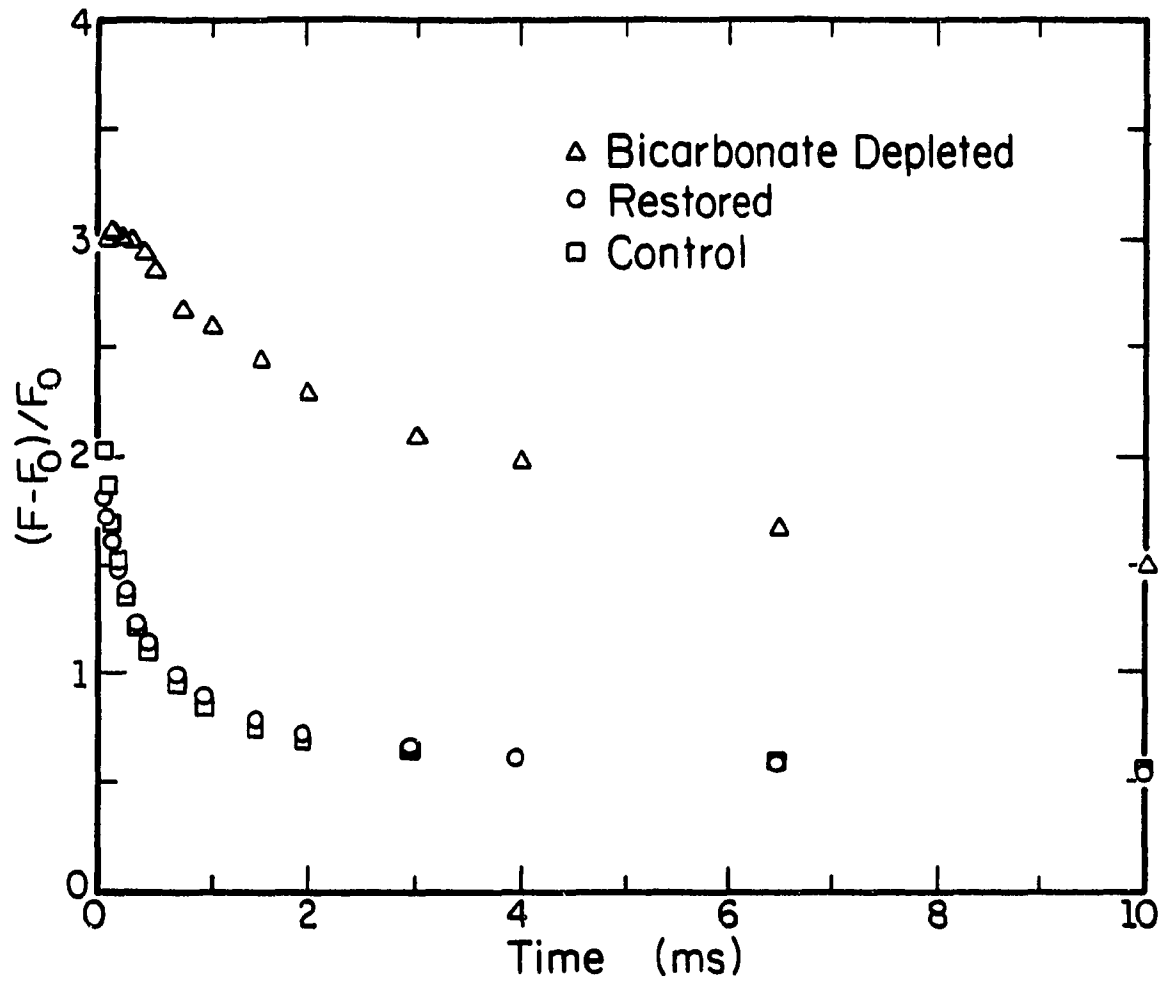
TABLE 1

EFFECT OF BICARBONATE ON VARIOUS ELECTRON TRANSPORT SYSTEMS SUPPORTED BY  
METHYL VIOLOGEN

In (2) 15 mM hydroxylamine was used. In (3) the thylakoids were treated in 0.8 M Tris (pH 8.0) at 250  $\mu$ g chlorophyll/ml for 30 min on ice in diffuse room light; the donor system had 1 mM benzidine and 1 mM ascorbate. In (4) 1 mM duroquinol, prepared as in [22], and 5  $\mu$ M DCMU (3-(3,4-dichlorophenyl)1,1-dimethylurea) were also present. Data are average values of three measurements. Other experimental conditions are as described in Materials and Methods.

System	Electron Transport ( $\mu$ equiv./mg chlorophyll per h)		
	-HCO <sub>3</sub> <sup>-</sup>	+10 mM HCO <sub>3</sub> <sup>-</sup>	Control
1) H <sub>2</sub> O $\longrightarrow$ MV	202 $\pm$ 15	1351 $\pm$ 104	1382 $\pm$ 66
2) Hydroxylamine $\longrightarrow$ MV	122 $\pm$ 13	121 $\pm$ 6	129 $\pm$ 8
3) Benzidine $\longrightarrow$ MV	116 $\pm$ 9	195 $\pm$ 22	195 $\pm$ 26
4) Duroquinol $\longrightarrow$ MV	2176 $\pm$ 45	2091 $\pm$ 69	2108 $\pm$ 148

**Figure 9.** Decay of the variable Chl a fluorescence after the third actinic flash in a series of flashes spaced 1 s apart with 15 mM hydroxylamine acting as the electron donor to PS II.  $F_0$  is the chlorophyll a fluorescence yield from the measuring flash when all  $Q_A$  is oxidized, and  $F$  is the yield at the indicated time after the actinic flash. The reaction medium (containing formate; see Materials and Methods) was supplemented with 0.1 mM methyl viologen, and 0.1  $\mu$ M gramicidin D. Half-times were determined as in [8].



here, has recently been reported to be approximately 350  $\mu\text{s}$  ([8] and see Fig. 5 in Chapter I). Thus, there is complete agreement for these decays whether  $\text{H}_2\text{O}$  or hydroxylamine is the electron donor to PS II.

Table 1 also shows that the partial reaction of duroquinol (tetramethyl-p-hydroquinol) to methyl viologen is insensitive to  $\text{HCO}_3^-$ . Here, there is no rate-limitation in the electron donation by duroquinol. This result has been obtained independently by S. Izawa (personal communication). It has already been shown, using reduced diaminodurene, that PS I is unaffected by  $\text{HCO}_3^-$ -depletion [23]. However, duroquinol donates at the level of the plastoquinone pool and in a dibromothymoquinone (DBMIB)-sensitive fashion [22]. Therefore, the insensitivity of this reaction to  $\text{HCO}_3^-$ -depletion suggests that the site of  $\text{HCO}_3^-$  action is before the plastoquinol oxidation on the plastoquinol-plastocyanin oxidoreductase. It has already been shown that the  $\text{H}_2\text{O}$  to silicomolybdate partial reaction and the  $\text{H}_2\text{O}$  to ferricyanide reaction, following a treatment with trypsin that enables ferricyanide to accept electrons directly from  $\text{Q}_\text{A}^-$ , are both unaffected by  $\text{HCO}_3^-$ -depletion [23,24]. However, caution should be exercised in the interpretation of these results, since the electron acceptance rates may have been rate-limiting. Even so, Chl  $\text{a}$  fluorescence decays [6,8] and the results with duroquinol strongly support the notion that the site of  $\text{HCO}_3^-$  action is at the level of the plastoquinone/plastoquinol exchange reactions on the quinone acceptor complex.

### 3. The $\text{HCO}_3^-$ Effect in the Presence of $\text{NO}_2^-$

A dissociation constant of 80  $\mu\text{M}$  has been determined for the binding of  $\text{HCO}_3^-$  to PS II [25,26]. In addition, formate has been shown to be competitive with the  $\text{HCO}_3^-$  binding site (e.g., [8,25,27]). This

conclusion can now be extended to a number of anions which inhibit the Hill reaction and which also increase the dissociation constant for  $\text{HCO}_3^-$ . The most effective anion that has been tested is nitrite ( $\text{NO}_2^-$ ) [28]. Stemler and Murphy [28] were able to obtain a 3.6-fold stimulation of the Hill reaction by the addition of 5 mM  $\text{HCO}_3^-$  to preparations that had been incubated with 20 mM nitrite. Replacing formate with nitrite in the depletion and reaction media employed in this study resulted in a seven-fold  $\text{HCO}_3^-$  effect. The electron transport rates ( $\text{H}_2\text{O}$  to methyl viologen) were: for  $\text{HCO}_3^-$ -depleted, 75  $\mu\text{equiv. (mg Chl)}^{-1}\cdot\text{hr}^{-1}$ ; for  $\text{HCO}_3^-$ -resupplied, 539  $\mu\text{equiv (mg Chl)}^{-1}\cdot\text{hr}^{-1}$ .

To answer the question as to whether or not the 80  $\mu\text{M}$  dissociation constant was characteristic of the  $\text{HCO}_3^-$  binding that facilitated electron transfer through the two-electron gate (see Fig. 3 in Chapter I), the effect of nitrite incubation on  $\text{Q}_\text{A}^-$  reoxidation was studied. This experiment differs somewhat from the other experiments discussed in this chapter. In the protocol used here 25 mM nitrite was added to the reaction media, but the system was equilibrated with air containing 390  $\mu\text{l/l CO}_2$ . This experiment had previously been performed with formate ([8] and Chapter I, Figs. 4 and 5) and found to produce identical results to those seen in  $\text{HCO}_3^-$ -depleted samples.

Unlike formate, nitrite is found in the stroma of the chloroplast and participates in the pathway for the assimilation of nitrite into glutamate (e.g., see [29]). It is therefore of direct physiological significance to the plant if nitrite can inhibit PS II in the presence of atmospheric levels of  $\text{CO}_2$ . As in the presence of formate [8], an inhibition of  $\text{Q}_\text{A}^-$  oxidation was observed with the maximum inhibition occurring after the third actinic flash. The half-time for  $\text{Q}_\text{A}^-$  oxida-

Figure 10. Decay of the variable Chl a fluorescence after the third actinic flash in a series of flashes spaced 1 s apart in nitrite incubated thylakoids.  $F_0$  is the chlorophyll a fluorescence yield from the measuring flash when all  $Q_A$  is oxidized, and  $F$  is the yield at the indicated time after the actinic flash. The reaction medium (containing nitrite; see Materials and Methods) was supplemented with 0.1 mM methyl viologen and 0.1  $\mu$ M gramicidin D. Half-times were determined as in [8].

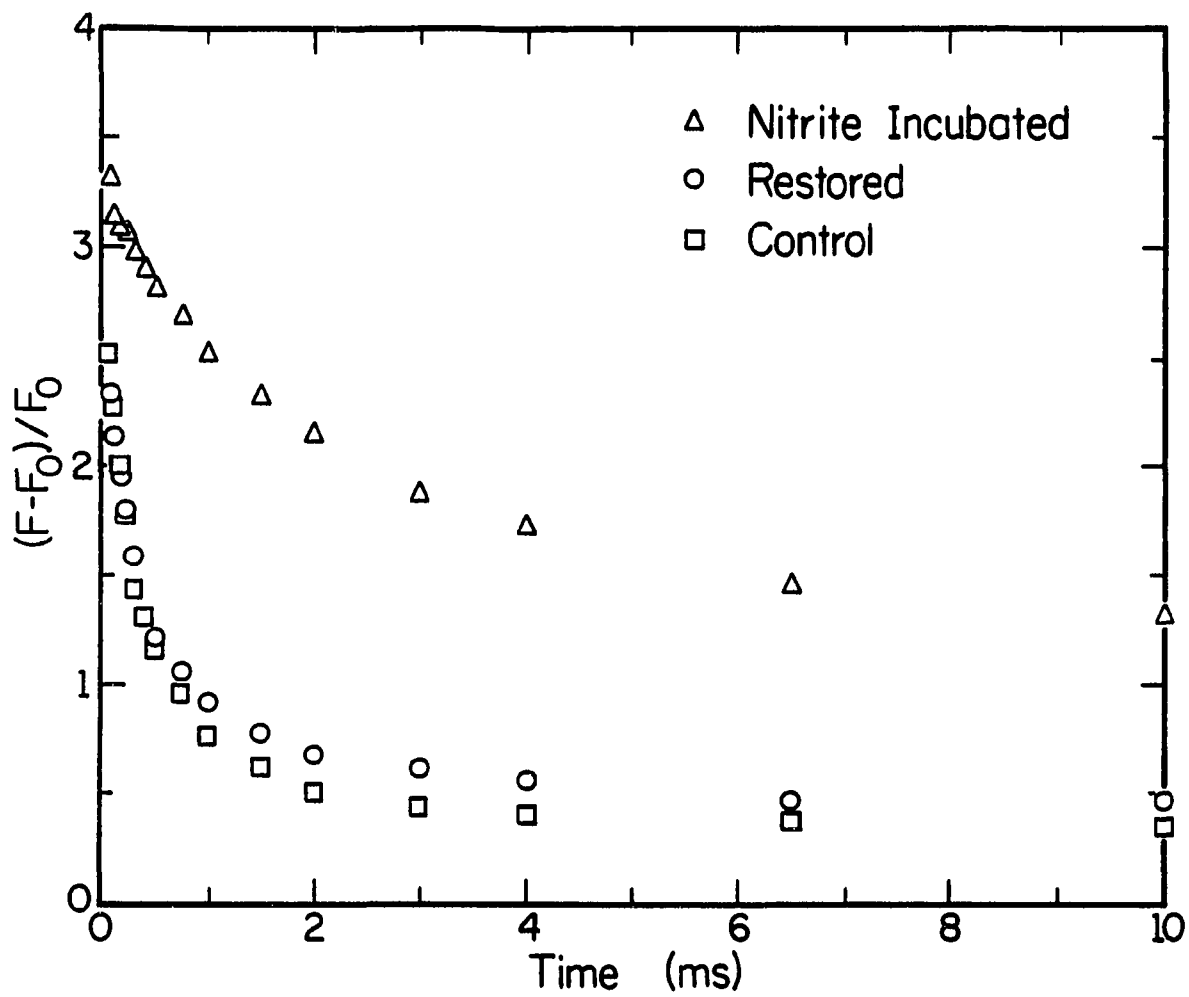
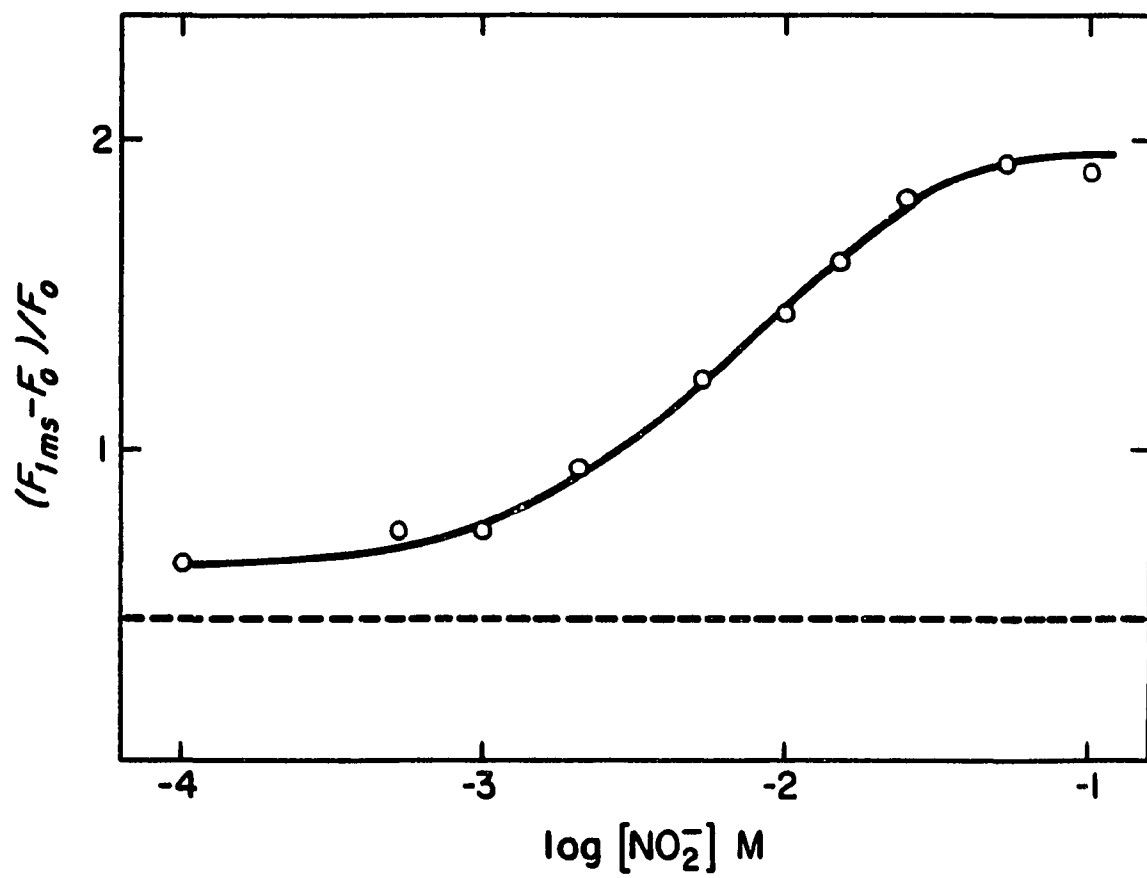


Figure 11. The variable Chl *a* fluorescence at 1 ms after an actinic flash plotted against the nitrite concentration on a logarithmic scale. The reaction medium contained 100 mM sorbitol, 10 mM NaCl, 5 mM MgCl<sub>2</sub>, 20 mM buffer (MES, pH 6.5), 0.1 mM methyl viologen and 0.1 μM gramicidin D. The chlorophyll concentration was 5 μg/ml. The broken line indicates the fluorescence level in control or restored membranes.



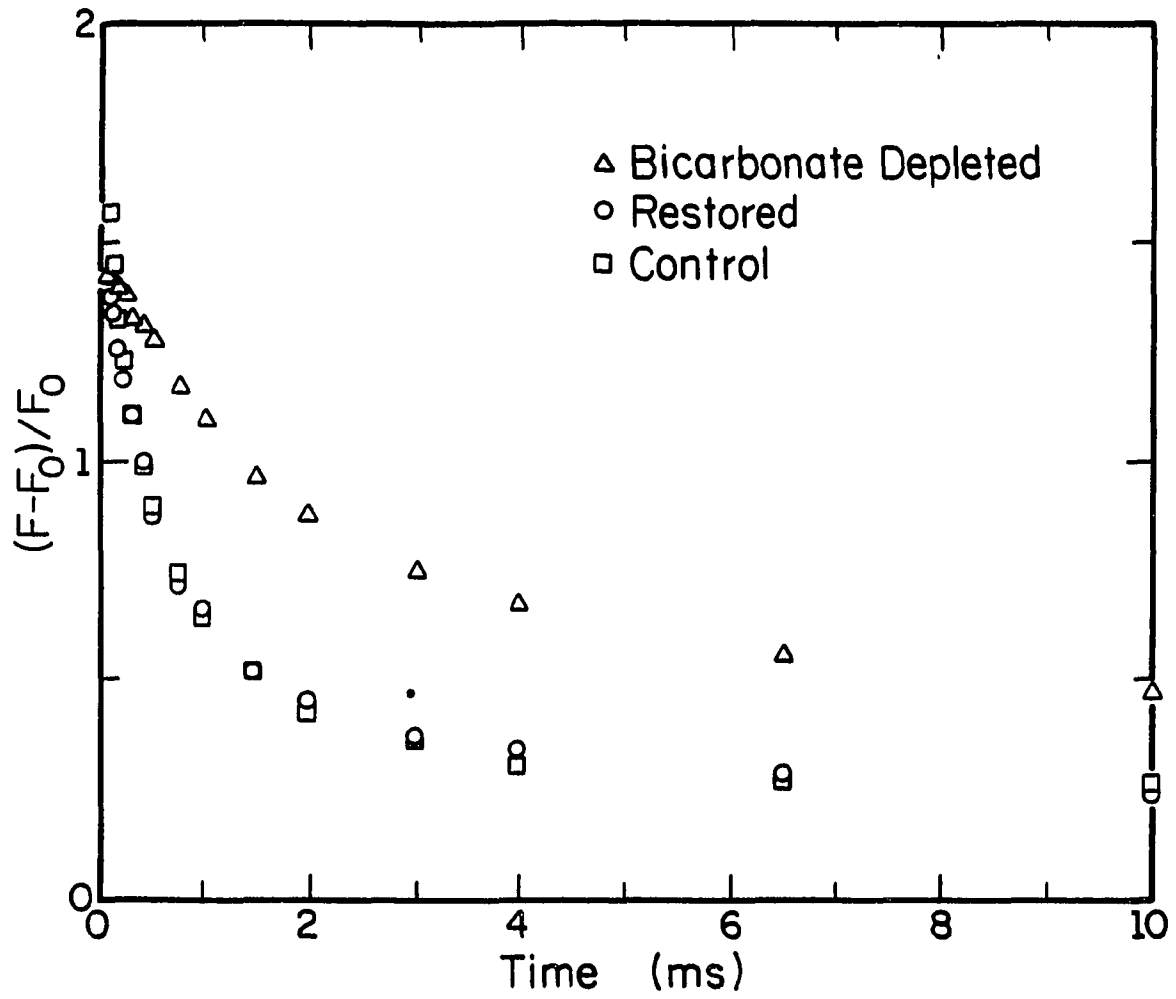
tion in the  $\text{NO}_2^-$ -incubated sample was approximately 15 ms and the half-time for the restored and control membranes was approximately 400  $\mu\text{s}$ . These data are presented in Fig. 10. A similar result was also obtained for  $\text{NO}_2^-$ -incubated samples in the presence of 10 mM hydroxylamine (data not shown). This result therefore supports the conclusion that the 80  $\mu\text{M}$  dissociation constant for  $\text{HCO}_3^-$  does represent a  $\text{HCO}_3^-$  binding site that facilitates electron transfer through the two-electron gate. This finding has previously been published by the author in a preliminary form [30] and has also recently received independent confirmation [31,32].

To probe further any possible physiological significance of nitrite, a dissociation constant for nitrite binding to PS II was determined in  $\text{NO}_2^-$ -incubated samples. The result of this experiment is given in Fig. 11. The assay chosen measured the variable Chl a fluorescence level 1 ms after a single actinic flash. This parameter was then plotted as a function of  $\text{NO}_2^-$  concentration. The broken line in Fig. 6 represents the Chl a fluorescence level in restored or control membranes. To insure that binding equilibrium was achieved in this experiment, a time course was measured for the lowest  $\text{NO}_2^-$  concentration used. Binding equilibrium was attained in 60 min and therefore all data points were collected following a 1 hour incubation. The experimental result indicates that the dissociation constant for nitrite is of the order of 5 mM. Consequently it would appear that the plant would need to be exposed to quite high levels of  $\text{NO}_2^-$  before this anion would become toxic to PS II.

#### 4. The $\text{HCO}_3^-$ Effect in the Absence of Inhibitory Anions

It has recently been claimed [25,26,33,34] that the  $\text{HCO}_3^-$  effect in

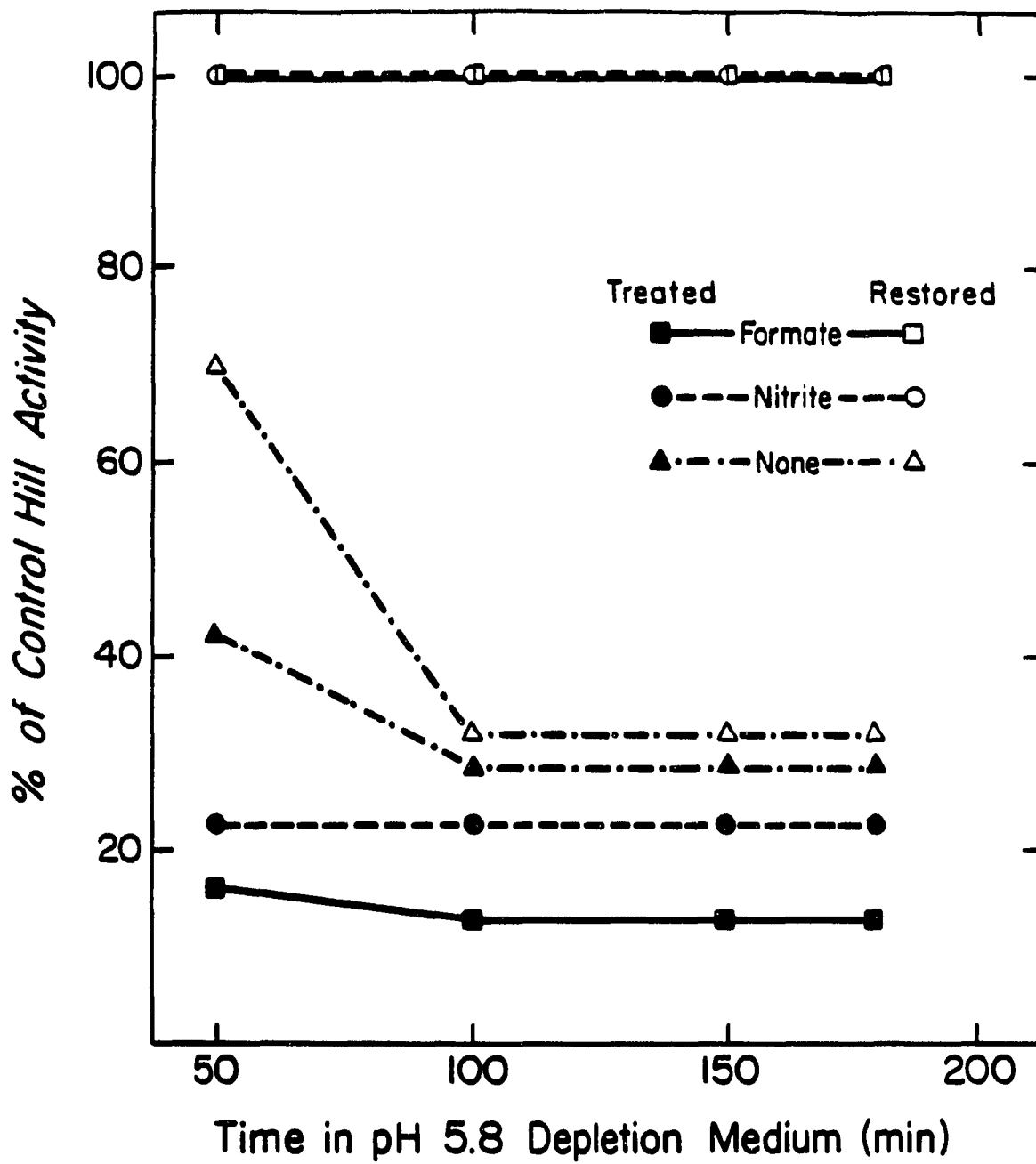
Figure 12. Decay of variable Chl a fluorescence, in formate-free samples, after the third actinic flash in a series of flashes spaced 1 s apart with water acting as the natural electron donor to PS II.  $F_0$  is the chlorophyll a fluorescence yield from the measuring flash when all  $Q_A$  is oxidized, and  $F$  is the yield at the indicated time after the actinic flash. Pea thylakoids were used in this experiment and prepared as described in [13]. Inhibitory anions were omitted from both the depletion and reaction media (see Materials and Methods). The reaction medium was supplemented with 0.1 mM methyl viologen, and 0.1  $\mu$ M gramicidin D. Half-times were determined as in [8].



formate-containing thylakoids does not result from the removal of  $\text{HCO}_3^-$  from the system, but only from the presence of the formate anion. That is, the restoration of control levels of electron transport in  $\text{HCO}_3^-$ -resupplied thylakoids only arises from  $\text{HCO}_3^-$  displacing the inhibitory formate from an anion binding site. This hypothesis could readily be extended to include  $\text{NO}_2^-$  (see section 3 above). Fig. 12 demonstrates that this is not the case. Here, the decay of Chl *a* variable fluorescence after the third of a series of actinic flashes spaced 1 s apart is again shown, but both formate and nitrite were omitted from the depletion and reaction media. A fully reversible  $\text{HCO}_3^-$  effect is demonstrated. The possibility that other anions in our experimental media may have produced this inhibition can be discounted. The chloride concentration used here is optimal for PS II activity [35,36], and a study of the effects of various buffer systems found that no inhibition could be attributed to the phosphate buffer (H. Robinson and the author, unpublished observations). As in the formate-containing system [6,8] maximal inhibition was obtained after the third flash. However, in the absence of inhibitory anions the overall half-time of  $Q_A^-$  reoxidation after the third and subsequent actinic flashes remained in the range of 2.0-2.5 ms. This should be compared with an overall half-time of approximately 10-15 ms in the formate or nitrite containing systems ([8] and section 3 above).

However, continued incubation beyond 90 min in the pH 5.8 depletion medium resulted in the kinetics of  $Q_A^-$  reoxidation becoming progressively slower. This additional inhibition was found to be irreversible. The results of a further investigation of this phenomenon are presented in Fig. 13. Here the  $\text{H}_2\text{O}$  to methyl viologen reaction was used to monitor the activity in treated and restored membranes over a period of

Figure 13. The influence of inhibitory anions in the  $\text{HCO}_3^-$ -depletion medium. The conditions were identical to Fig. 3 with the exception that the depletion and reaction media contained either 25 mM nitrite or formate or both anions were omitted. The restored rates were obtained by adding 5 mM  $\text{HCO}_3^-$ . For other details, see Materials and Methods.



3 hours. The rates are compared to those observed in control thylakoids incubated at pH 6.5 in the absence of any inhibitory anions and equilibrated with air. In samples containing both 25 mM formate or 25 mM nitrite a fully reversible  $\text{HCO}_3^-$  effect was observed. However, when both formate and nitrite were omitted the thylakoids failed to respond to added  $\text{HCO}_3^-$  beyond a 100 min incubation. In fact,  $\text{HCO}_3^-$ -restored membranes following a depletion treatment that had omitted inhibitory anions only exhibited electron transport rates that were 70% of the control after 50 min in the depletion medium. It can be concluded therefore that the removal of bound  $\text{HCO}_3^-$  in the absence of inhibitory anions results in irreversible damage to PS II reflected both in the kinetics of  $\text{Q}_\text{A}^-$  reoxidation and in linear electron transport between  $\text{H}_2\text{O}$  and methyl viologen.

##### 5. Rate-limitation in $\text{HCO}_3^-$ -depleted and Restored Samples

If we assume a molecular weight of 1000 for Chl, a photosynthetic unit size of 400 Chl molecules per PS II reaction center [13], and an average value of  $1366 \mu\text{equiv.}(\text{mg chl})^{-1}.\text{hr}^{-1}$  for our steady-state rates of electron transport in non-depleted and  $\text{HCO}_3^-$ -resupplied thylakoids (Table 1), then we obtain an average rate of transport of 150 electrons per reaction center per second for our methyl viologen system. This suggests that the rate-limiting step in our  $\text{HCO}_3^-$ -resupplied samples and controls is of the order of 6 or 7 ms per electron which is in agreement with the data of Whitmarsh and Cramer [37] on control thylakoids. These calculations do not, however, take into account any heterogeneity in PS II (e.g., [38]). However, accepting an average rate of  $200 \mu\text{equiv.}(\text{mg chl})^{-1}.\text{hr}^{-1}$  (Table 1) as the rate of electron transport in depleted thylakoids, the above assumptions would predict that the rate-limiting

step as a result of  $\text{HCO}_3^-$ -depletion is of the order of 45 ms per electron.

These calculations should not cause earlier measurements of the decay of Chl a variable fluorescence [6] and of plastoquinol oxidation [5], indicating a  $t_{1/2}$  of the order of 200 ms for plastoquinol oxidation in  $\text{HCO}_3^-$ -depleted samples, to be discounted. As noted in [8] the overall half-times for the oxidation of  $\text{Q}_\text{A}^-$  reported here yield several exponential decay components upon analysis. Previous experimental conditions may have resulted in changes being measured for a component with a half-time of the order of 200 ms (see [8]). Additionally, control measurements for the ferricyanide-supported Hill reaction in earlier studies (see e.g., [9,23]) resulted in rates seven to ten-fold lower than reported here. Thus, a  $t_{1/2}$  of approximately 200 ms [5] and of approximately 120-160 ms [6] for the rate-limiting step in  $\text{HCO}_3^-$ -depleted thylakoids reported under different experimental conditions (such as [5,6,9,23]), is qualitatively very similar to a half-time of approximately 10-15 ms for the oxidation of  $\text{Q}_\text{A}^-$  and a value of approximately 45 ms per electron in steady-state measurements of oxygen evolution. Therefore, the kinetics of  $\text{Q}_\text{A}^-$  oxidation and the estimated rate-limiting step for steady-state electron transfer in this chapter reflect the milder experimental conditions employed (using the method of W.F.J. Vermaas, personal communication) in comparison to earlier studies of the  $\text{HCO}_3^-$  effect.

The Chl a fluorescence decays presented here (Figs. 9,10 and 12) and in [8] are apparently biphasic. The observed large slow component in  $\text{HCO}_3^-$ -depleted samples may result from an altered equilibrium of  $\text{Q}_\text{A}^-$  with plastoquinone and/or plastoquinol at the  $\text{Q}_\text{B}$  binding site on the quinone acceptor complex of PS II. This conclusion is consistent with

the hypothesis that removal of  $\text{HCO}_3^-$  results in a slowing down of the plastoquinone/plastoquinol exchange reactions of the two-electron gate. This may be a consequence of alterations in the association constants for one or more of the plastoquinone/plastoquinol species and/or of effects on the protonation reactions of the partially reduced plastoquinone anion or the doubly reduced plastoquinol. These interpretations are investigated further in Chapters III and IV.

In addition to the biphasic decays discussed above, additional Chl *a* fluorescence decay components exist in the 0.1-10 s range [4,8]. These components may reflect the population of longer-lived  $Q_A^-$  reducing as yet unspecified chemical species in the membrane, or particularly in the case of components in the  $> 1$  s range, centers undergoing a back reaction. A possible contribution to these components from protonation reactions associated with  $Q_B$  reduction is discussed in Chapter III.

#### D. Summary and Conclusions

In this chapter the following key observations are presented: (1) there is no  $\text{HCO}_3^-$  effect in the electron flow from duroquinol to methyl viologen, but there is a large effect in the electron flow from  $\text{H}_2\text{O}$  to methyl viologen. Thus  $\text{HCO}_3^-$  affects electron transport at a site which precedes the step involving the reoxidation of plastoquinol (see Table 1 and Fig. 8); (2) no conclusion could be made about the site of  $\text{HCO}_3^-$  action from electron flow measurements from artificial electron donors to PS II. In control samples with the electron donors, hydroxylamine, benzidine and catechol, the electron transport rates to methyl viologen were not significantly different from the rates observed in  $\text{HCO}_3^-$ -depleted samples for the  $\text{H}_2\text{O}$  to methyl viologen reaction. However, measurements on chlorophyll *a* fluorescence decays (with hydroxylamine as

the electron donor) show an effect on the electron acceptor side of PS II (see Table 1 and Fig. 9); (3) nitrite can easily substitute for formate in replacing  $\text{HCO}_3^-$  from the membrane as demonstrated by the slowing of the decay of chlorophyll *a* fluorescence and thus  $\text{Q}_\text{A}^-$  oxidation (see Figs. 10 and 11). The dissociation constant for nitrite was found to be 5 mM (Fig. 11); (4) a six-fold  $\text{HCO}_3^-$  effect can be observed on the half-time of  $\text{Q}_\text{A}^-$  reoxidation in the absence of formate or nitrite, and this compares to a > thirty-fold effect in the presence of inhibitory anions (Figs. 9, 10 and 12). A  $\text{HCO}_3^-$  effect of approximately two-fold, instead of six to ten-fold, can be observed in the  $\text{H}_2\text{O}$  to methyl viologen reaction in the absence of formate or nitrite. However, removal of bound  $\text{HCO}_3^-$  in the absence of other anions causes irreversible inhibition of electron flow (Figs. 12 and 13).

#### References

1. Govindjee and J.J.S. van Rensen (1978) *Biochim. Biophys. Acta* 505, 183-213
2. Vermaas, W.F.J. and Govindjee (1981) *Proc. Indian Natl. Sci. Acad. Biol. Sci. Ser. B*47, 581-605
3. Jursinic, P., Warden, J. and Govindjee (1976) *Biochim. Biophys. Acta* 440, 322-330
4. Jursinic, P. and Stemler, A. (1982) *Biochim. Biophys. Acta* 681, 419-428
5. Siggel, U., Khanna, R., Renger, G. and Govindjee (1977) *Biochim. Biophys. Acta* 462, 196-207
6. Govindjee, Pulles, M.P.J., Govindjee, R., van Gorkom, H.J. and Duysens, L.N.M. (1976) *Biochim. Biophys. Acta* 449, 602-605
7. Govindjee, Nakatani, H.Y., Rutherford, A.W. and Inoue, Y. (1984)

- Biochim. Biophys. Acta 766, 416-423
8. Robinson, H.H., Eaton-Rye, J.J., van Rensen, J.J.S. and Govindjee (1984) Z. Naturforsch. 39C, 382-385
  9. Vermaas, W.F.J. and van Rensen, J.J.S. (1981) Biochim. Biophys. Acta 636, 168-174
  10. Fischer, K. and Metzner, H. (1981) Photobiochem. Photobiophys. 2, 133-140
  11. Stemler, A. (1982) in Photosynthesis: Development, Carbon Metabolism, and Plant Productivity (Govindjee, ed.), Vol. II, pp. 513-539, Academic Press, New York
  12. Arnon, D.I. (1949) Plant Physiol. 24, 1-15
  13. Robinson, H.H. and Crofts, A R. (1983) FEBS Lett. 153, 221-226
  14. Batra, P.P. and Jagendorf, A.T. (1965) Plant Physiol. 40, 1074-1079
  15. McCarty, R.E. (1980) in Methods in Enzymology 69, part C (San Pietro, A., ed.), pp 719-728, Academic Press, New York
  16. Delieu, T. and Walker, D.A. (1972) New Phytol. 71, 201-225
  17. Izawa, S., Heath, R.L. and Hind, G. (1969) Biochim. Biophys. Acta 180, 388-398
  18. Bennoun, P. and Joliot, A. (1969) Biochim. Biophys. Acta 189, 85-94
  19. Mohanty, P., Mar, T. and Govindjee (1971) Biochim. Biophys. Acta 253, 213-221
  20. Babcock, G.T. and Sauer, K. (1975) Biochim. Biophys. Acta 396, 48-62
  21. Jursinic, P. and Govindjee (1977) Biochim. Biophys. Acta 461, 253-267
  22. Izawa, S. and Pan, R.L. (1978) Biochem. Biophys. Res. Commun. 83, 1171-1177
  23. Khanna, R., Govindjee and Wydrzynski, T.J. (1977) Biochim. Bio-

phys. Acta 462, 208-214

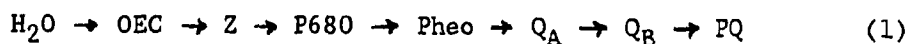
24. van Rensen, J.J.S. and Vermaas, W.F.J. (1981) *Physiol. Plant.* 51, 106-110
25. Stemler, A. and Murphy, J. (1983) *Photochem. Photobiol.* 38, 701-707
26. Snel, J.F.H. and van Rensen, J.J.S. (1984) *Plant Physiol.* 75, 146-150
27. Snel, J.F.H. and van Rensen, J.J.S. (1983) *Physiol. Plant.* 57, 422-427
28. Stemler, A. and Murphy, J.B. (1985) *Plant Physiol.* 77, 974-977
29. Anderson, J.W. (1981) in *The Biochemistry of Plants, Photosynthesis* (Hatch, M.D. and Boardman, N.K., eds.), Vol. 8, pp. 473-500, Academic Press, New York
30. Eaton-Rye, J.J., Blubaugh, D.J. and Govindjee (1986) in *Ion Interactions in Energy Transfer Biomembranes* (Papageorgiou, G.C., Barber, J. and Papa, S., eds.), pp. 263-278, Plenum Publishing Corporation, New York
31. Sinclair, J. (1987) *Photosynthesis Res.*, in the press
32. Jursinic, P. and Stemler, A. (1987) *Photosynthesis Res.*, in the press
33. Stemler, A. and Jursinic, P. (1983) *Arch. Biochem. Biophys.* 221, 227-237
34. Snel, J.F.H., Groot-Schaursberg, A. and van Rensen, J.J.S. (1984) in *Advances in Photosynthesis Research* (Sybesma, C., ed.), Vol. I, pp. 557-560, Martinus Nijhoff/Dr. Junk Publishers, The Hague
35. Hind, G., Nakatani, H.Y. and Izawa, S. (1969) *Biochim. Biophys. Acta* 183, 361-373
36. Kelley, P.M. and Izawa, S. (1978) *Biochim. Biophys. Acta* 502, 198-

37. Whitmarsh, J. and Cramer, W.A. (1979) *Biophys. J.* 26, 223-234
38. Vermaas, W.F.J. and Govindjee (1981) *Photochem. Photobiol.* 34, 775-793
39. Stemler, A. and Govindjee (1973) *Plant Physiol.* 52, 119-123

### III. ELECTRON TRANSFER THROUGH THE QUINONE ACCEPTOR COMPLEX OF PS II IN BICARBONATE-DEPLETED OR ANION INHIBITED THYLAKOID MEMBRANES AS A FUNCTION OF ACTINIC FLASH NUMBER AND FREQUENCY

#### A. Introduction

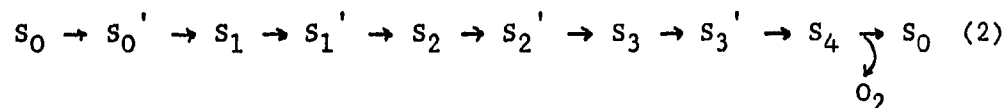
Bicarbonate (or  $\text{CO}_2$ ) was shown by Warburg and Krippahl [1] to stimulate electron transport during the Hill reaction (see Chapter I for details). This phenomenon has been referred to as the bicarbonate ( $\text{HCO}_3^-$ ) effect, and it has recently been shown that  $\text{HCO}_3^-$  and not  $\text{CO}_2$  or  $\text{CO}_3^{2-}$  is the active species involved [2]. It has been established that the site of action of  $\text{HCO}_3^-$  is on the acceptor side of photosystem II (see Chapter II). Photosystem II (PS II) is summarized in scheme (1) (see Figs. 1 and 2 in Chapter I).



The electron donor side of PS II contains the oxygen-evolving complex (OEC) and a bound plastoquinol, Z, that supplies the electrons to the reaction center chlorophyll (Chl) a P680. The electron acceptor side contains a pheophytin (Pheo) molecule and two plastoquinones,  $\text{Q}_A$  and  $\text{Q}_B$ . Electrons are transferred from Pheo<sup>-</sup> to  $\text{Q}_A$ , that can only be reduced to the semiquinone form. After two such events,  $\text{Q}_B$  is reduced to plastoquinol (see Fig. 3 in Chapter I). The plastoquinol,  $\text{Q}_B\text{H}_2$ , is then able to exchange with the plastoquinone (PQ) pool to provide a second  $\text{Q}_B$  molecule for subsequent reduction. This two-electron transfer step at the  $\text{Q}_B$  level is known as the two-electron gate (see e.g., [3,4]). Stoichiometrically, two  $\text{PQH}_2$  molecules are formed and two water molecules oxidized for each  $\text{O}_2$  evolved. The resultant  $\text{PQH}_2$  molecules are oxidized at the plastoquinol-plastocyanin oxidoreductase or cytochrome  $b_6/f$  complex [5]. The oxidation of  $\text{H}_2\text{O}$  and  $\text{PQH}_2$  supply protons

to the internal thylakoid space for chemiosmotic coupling [6].

The oxygen-evolving mechanism has been described by a kinetic model which recognizes 5 separate oxidation states or S-states [7]:



A single photoact advances an S-state from  $S_n$  to  $S_n'$  while the transition from  $S_n'$  to  $S_{n+1}$  represents a recovery reaction before a center is able to utilize a second photon. Molecular  $O_2$  is released during the  $S_4$  to  $S_0$  transition. For a review of PS II the reader is referred to [8] and of the OEC to [9,10].

A number of  $HCO_3^-$ -reversible inhibitory phenomena have been associated with the donor side of PS II. These include the modulation of binding affinity of  $HCO_3^-$  by different S-states [11] and an effect on the re-reduction of  $P680^+$  [12]. However, the major rate-limiting step in  $HCO_3^-$ -depleted or treated membranes is at the level of the passage of electrons through the two-electron gate (see Chapters I and II).

In addition to the conclusions of Chapter II, the principal arguments to support the site of action of  $HCO_3^-$  are: (1) the reoxidation of  $Q_A^-$ , as measured by the Chl *a* fluorescence yield decay [13,14] or by the absorbance change at 320 nm [15,16], is stimulated ten to twenty-fold by  $HCO_3^-$  in  $HCO_3^-$ -depleted membranes; (2) in PS II particles, a light- and chemically-induced EPR signal ( $g = 1.82$ ), attributed to the  $Q_A^-$ - $Fe^{2+}$  complex, is reversibly increased in amplitude by a factor of about 10 by  $HCO_3^-$ -depletion [17]; (3) the Chl *a* fluorescence yield [18] and thermoluminescence [19] after a series of single flashes of light suggest a dramatic slowing down of electron flow after the third and subsequent flashes following  $HCO_3^-$ -depletion, which is totally reversed upon  $HCO_3^-$ -

addition; this suggests that there is a large  $\text{HCO}_3^-$  effect on the exchange of  $\text{Q}_\text{B}^{2-}$  with PQ at the  $\text{Q}_\text{B}$ -apoprotein and (4)  $\text{HCO}_3^-$ -depletion causes a several-fold change in the affinity of the binding of  $^{14}\text{C}$ -atrazine or  $^{14}\text{C}$ -ioxynil, which bind in the  $\text{Q}_\text{B}$ -apoprotein region [17,18]. We have suggested that the ability of  $\text{HCO}_3^-$  to facilitate electron flow may involve participation in the protonation reactions of the two-electron gate [19]. To test this hypothesis, the kinetics of  $\text{Q}_\text{A}^-$  reoxidation in control, anion inhibited/ $\text{HCO}_3^-$ -depleted and  $\text{HCO}_3^-$ -restored samples have been studied as a function of flash number and flash frequency at pH 6.5 or pH 7.5.

#### B. Materials and Methods

Thylakoid membranes were isolated from spinach leaves by first grinding leaf segments in a medium containing 400 mM sorbitol, 50 mM NaCl, 1 mM EDTA (ethylenediaminetetraacetic acid) and 50 mM Tricine (pH 7.8) for 5 s in a Waring blender. The resultant homogenate was filtered through 6 and then 12 layers of cheesecloth. The filtrate was then spun at 5000 X g for 10 min. After discarding the last supernatant, the pellet was resuspended and osmotically shocked in a medium containing 50 mM NaCl, 5 mM  $\text{MgCl}_2$  and 10 mM Tricine (pH 7.8). Chlorophyll (Chl) concentrations were determined in micromolar units as described by Graan and Ort [23].

Bicarbonate-depleted samples and/or anion inhibited membranes (hereafter referred to as treated membranes) were obtained by a dark incubation for 60 min in  $\text{CO}_2$ -free buffer under a stream of  $\text{N}_2$ (80%) and  $\text{O}_2$ (20%). The gas was passed through a column of soda-lime and ascarite to facilitate the removal of any trace of  $\text{CO}_2$ , and through a water column to prevent evaporation of the sample.

The treatment buffer contained 300 mM sorbitol, 25 mM sodium formate, 10 mM NaCl, 5 mM MgCl<sub>2</sub> and 10 mM sodium phosphate (pH 6.0). The Chl concentration was 250 μM. The reaction medium contained 100 mM sorbitol, 10 mM sodium formate, 10 mM NaCl, 5 mM MgCl<sub>2</sub>, 20 mM buffer (MES, pH 6.5; HEPES, pH 7.5-7.6), 100 μM methyl viologen and 0.1 μM gramicidin. All measurements were made on a sample diluted to contain 5 μM Chl in a final volume of 100 ml in a dark stirred vat. A flow cuvette was filled from the vat by computer control.

Restored membranes were obtained by adding 5 mM HCO<sub>3</sub><sup>-</sup> to a 2 ml aliquot of the treated stock. After a 2 min dark incubation these membranes were transferred to the reaction medium which also contained 5 mM HCO<sub>3</sub><sup>-</sup>. Control membranes were obtained by omitting formate from the treatment and reaction media and not CO<sub>2</sub>-depleting these buffers. In the case of the control the incubation pH was also raised to pH 7.5. Following isolation, the thylakoid membranes were maintained at 20° C in all cases.

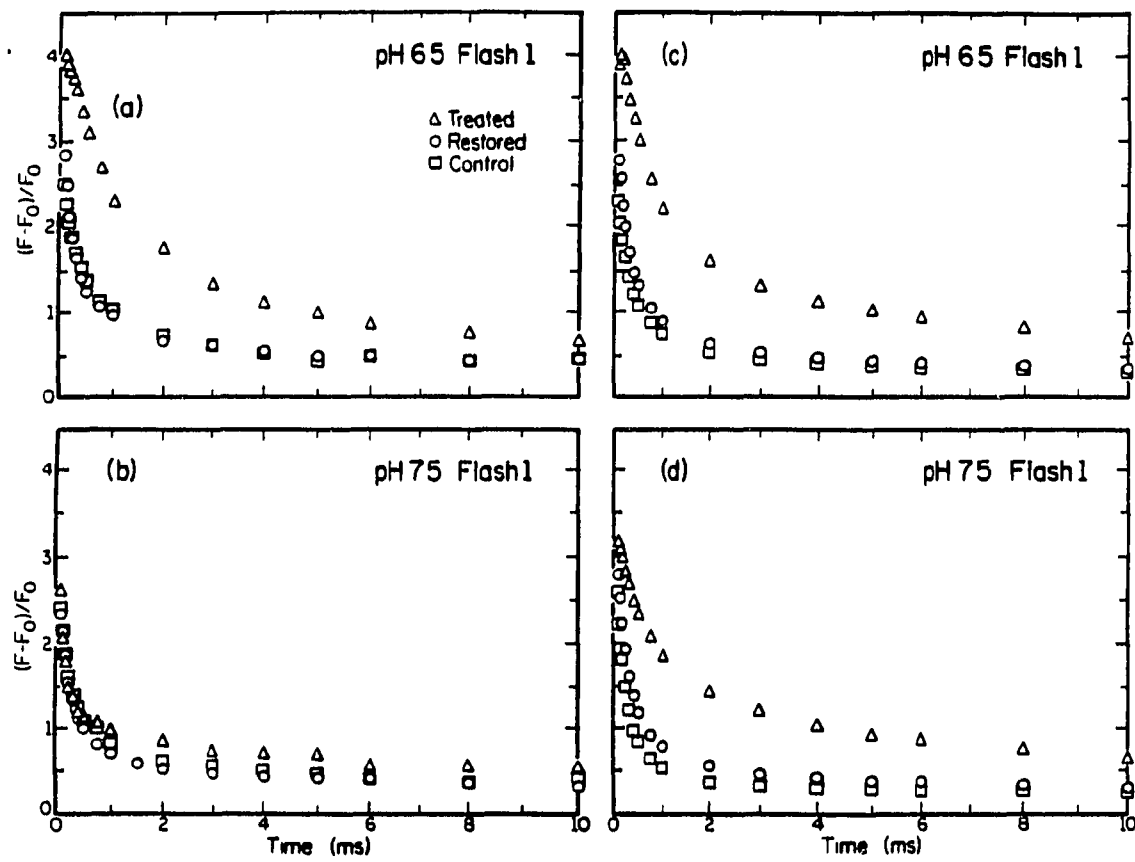
The kinetics of the decay of variable Chl a fluorescence were measured at 685 nm (10 nm bandwidth) by a weak measuring flash which could be fired at variable times after each of a series of actinic flashes. The measuring flash (Stroboslave 1593A, General Radio) sampled approximately 1% of the PS II centers present [24]. Both the actinic flash (FX-124, EG and G) and the measuring flash were blocked by Corning CS4-96 filters, and were of 2.5 μs duration at half-maximal peak height ([25] and see also in Chapter II Figs. 6 and 7 and section B 3.).

## C. Results

### 1. The Effect of pH on Flash 1 in Treated Membranes

Chlorophyll a fluorescence decays, monitoring the oxidation of Q<sub>A</sub><sup>-</sup>,

**Figure 14.** Decay of variable Chl a fluorescence after a single actinic flash at pH 6.5 and pH 7.5.  $F_0$  is the Chl a fluorescence yield from the measuring flash with all  $Q_A$  oxidized and  $F$  is the yield at the indicated time after actinic flash. Two experiments are shown with measurements at pH 6.5 and measurements at pH 7.5. In (a) and (b) the results are typical of those obtained from market spinach obtained between January and March 1986. In (c) and (d) the results are typical of spinach obtained between April 1986 and February 1987. The approximate half-times are: (a) for treated membranes, 2.2 ms; for restored membranes, 520  $\mu$ s; for control membranes, 550  $\mu$ s; (b) treated, 360  $\mu$ s; restored, 340  $\mu$ s; control, 320  $\mu$ s; (c) treated, 2.4 ms; restored, 390  $\mu$ s; control, 280  $\mu$ s and (d) treated, 1.7 ms, restored, 350  $\mu$ s; control, 230  $\mu$ s.



following a single actinic flash are presented in Fig. 14. The data for two experiments at pH 6.5 and at pH 7.5 are shown.

The relationship between variable Chl *a* fluorescence and  $[Q_A^-]$  is non-linear [26]. To derive half-times for  $Q_A^-$  oxidation from Fig. 14 it is first necessary to correct for inter-system energy or exciton migration. Forbush and Kok [27] ascertained that the probability for this transfer was 0.5 in spinach thylakoid membranes. The half-times for  $Q_A^-$  oxidation given in the legend of Fig. 14, and elsewhere in this thesis, were therefore determined employing the equations derived by Joliot and Joliot [26] relating variable Chl *a* fluorescence to  $[Q_A^-]$  assuming a probability of energy transfer of 0.5 as noted above

$$\frac{F - F_0}{F_m - F_0} = \frac{(1 - p)q}{1 - pq} \quad (3)$$

where  $F$  is the fluorescence yield at time  $t$ ,  $F_0$  is the fluorescence yield when all  $Q_A$  is in the oxidized state,  $F_m$  is the maximum fluorescence yield when all  $Q_A$  is in the reduced state,  $p$ , the connection parameter, is taken as the probability of the intersystem energy transfer, and  $q$  is the fraction of the closed reaction centers (*i. e.*,  $q = 1$  when  $Q_A^-$  is maximum). Our analysis does not include further refinement discussed by Paillotin [28].

At pH 6.5 the two experiments in Fig. 14 yield practically identical results. The overall half-times for the treated membranes being 2.2 ms in Fig. 14(a) and 2.4 ms in Fig. 14(c). At pH 7.5 a clear difference can be observed in the treated case. In Fig. 14(b) the  $t_{1/2}$  is 360  $\mu$ s while in Fig. 14(d), also at pH 7.5, the  $t_{1/2}$  is 1.7 ms. These results do not represent isolated cases. The spinach for this study was obtained from a commercial source originating from widely different locations over a period of 18 months. All data shown are typical results

obtained from at least three separate bushels of spinach obtained on an approximately weekly basis. It is also interesting to note that PS II particles obtained from the same spinach represented in Fig. 14(a) and (b) exhibited oxygen evolution rates of approximately  $400 \mu\text{moles O}_2 \cdot (\text{mg Chl})^{-1} \cdot \text{hr}^{-1}$  while PS II particles from the same spinach represented by Fig. 14(c) and (d) exhibited rates of approximately  $250 \mu\text{moles O}_2 \cdot (\text{mg Chl})^{-1} \cdot \text{hr}^{-1}$  (see Fig. 2 in Chapter II of Ref. [29]). However, the data seen in Fig. 14(a) and (b) were reproducible over a 3 month period from January to March 1986. A preliminary report on this data has been published previously [30]. The kinetic data from Fig. 14(c) and (d) have routinely been observed over the remaining 15 month period, although variation in the total variable fluorescence is common and typically ranges between 3 and 4 units.

The results for the treated membranes at pH 7.5 in Fig. 14 do show in common a faster rate of  $Q_A^-$  oxidation than seen for the pH 6.5 cases.  $F_{\text{max}}$  for Fig. 14 is 4.50. The apparent differences seen in the intersection of the ordinate by the decay curves, particularly obvious in the treated cases, arises in part from the limitation of our instrument to collect data until 70  $\mu\text{s}$  has elapsed after the actinic flash has been fired. This is due to the tail from the xenon flash lamp. Additionally, fluorescence quenching arises as a consequence of the equilibration of an electron between Z, the primary putative plastoquinol donor to the PS II reaction center, and P680, the reaction center pigment chlorophyll. This results in the presence of a significant amount of  $P680^+$  after an actinic flash which behaves as a fluorescence quencher [31, 32]. The relative contributions of differential rates of  $Q_A^-$  oxidation and fluorescence quenching to the apparent intersection with the ordin-

ate for the treated cases cannot be resolved from this data, but such a study is possible and may prove helpful in extending recent observations that indicate that the re-reduction of  $P680^+$  by Z is sensitive to an inhibitory anion treatment [12].

The increase in the apparent forward rate constant observed at pH 7.5 with respect to pH 6.5 in treated membranes in Fig. 14 is possibly due to changes in the association constant for  $Q_B$  at the  $Q_B$  binding site on the quinone acceptor complex. The association constant appears to be decreased in treated membranes in a pH dependent manner with approximately 25% of the PS II centers with a bound  $Q_B$  in dark adapted samples at pH 6.5 and 50% at pH 7.5 (see Chapter IV). The oxidation of  $Q_A^-$  can be seen to be biphasic in Fig 14, and it has been suggested that the amplitude of the fast phase corresponds to centers that have  $Q_B$  bound before the actinic flash. The slower phase in turn reflects a second order process involving binding of  $Q_B$  from the PQ pool [33]. Therefore, in treated membranes at pH 6.5 there is a larger contribution from the second order process than seen at pH 7.5. In addition, a slight pH effect on the overall half-time for  $Q_A^-$  oxidation is observed in restored and control membranes when no effect is seen on the association constant (see Chapter IV). For example, the overall half-time for control membranes was 550  $\mu$ s (pH 6.5; Fig. 14(a)), and 320  $\mu$ s (pH 7.6; Fig. 14(b)). A similar result is seen in Fig. 14(c) and (d). This indicates that not all of the pH effect observed for the treated membranes is specifically related to the anion treatment.

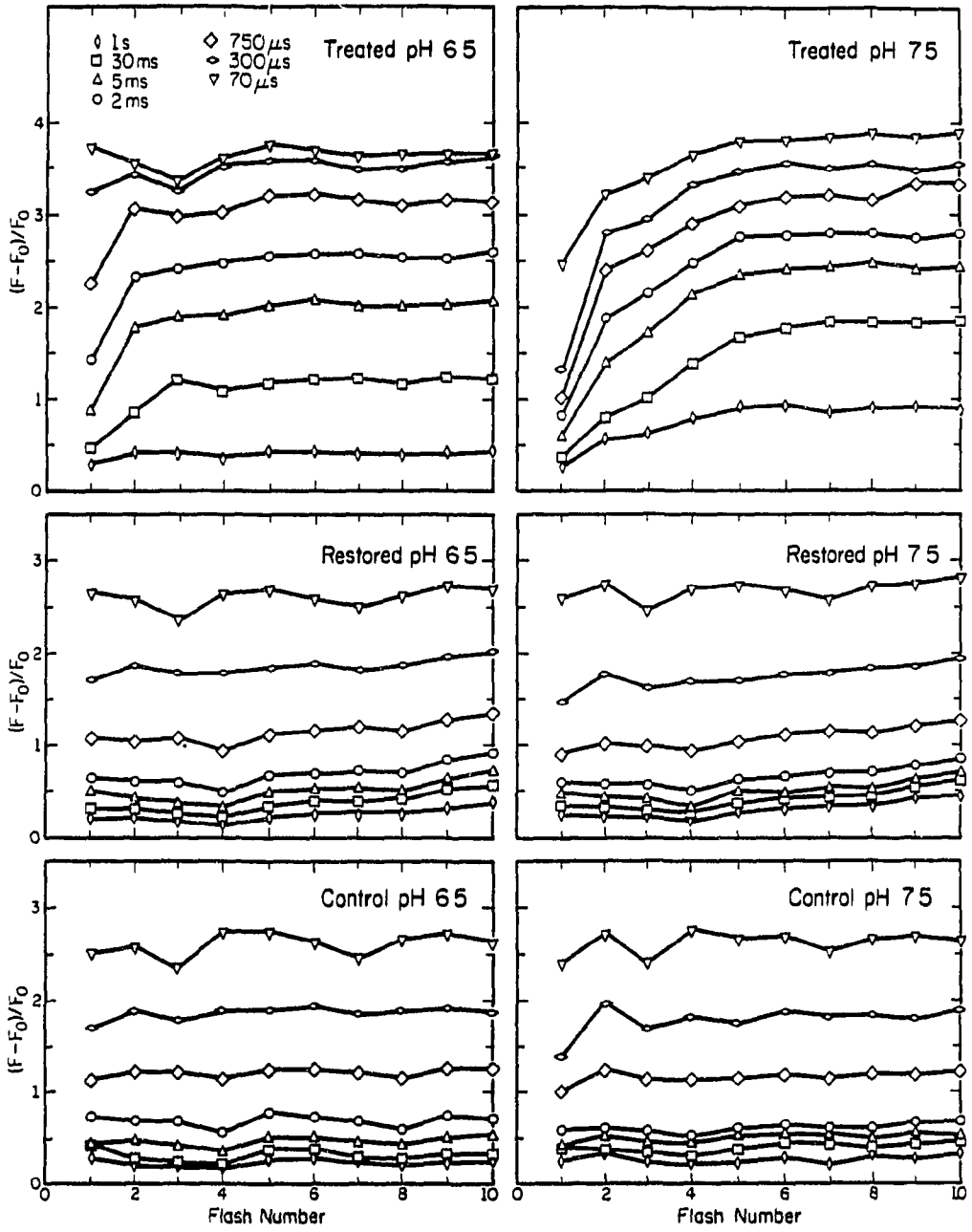
A second possibility, also discussed in Chapter IV, is that the amplitude of the fast phase in treated membranes reflects the equilibration of a proton with  $Q_B^-$  (see Fig. 3, Chapter I). This interpretation implies that the increase in the apparent forward rate constant observed

at pH 7.5 with respect to pH 6.5 in treated membranes in Fig. 14 may be attributed to treated membranes behaving as unprotonated control membranes. The pK for the protonation of  $Q_B^-$  in control membranes has been estimated to be approximately 7.9 [33]. At alkaline pH neither the control nor the treated membranes have a proton associated with  $Q_B^-$ . At acidic pH  $Q_B^-(H^+)$  is formed readily in the control but not in the treated case. This suggests that at least one role for the  $HCO_3^-$  anion is associated with the mechanism of  $Q_B^-$  protonation.

## 2. The Effect of pH and Flash Number in Treated Membranes

In Fig. 15 the variable Chl a fluorescence yield as a function of flash number is presented for treated, restored and control membranes at both pH 6.5 and pH 7.5. The flash 1 data in Fig. 15 are the data plotted in Figs. 14(a) and (b). The oscillations observed in the control and restored data arise from at least two causes. A binary oscillation, seen here most clearly at 300  $\mu$ s after the actinic flashes, arises from the differential rates of  $Q_A^-$  oxidation by either  $Q_B$  after an odd number of flashes or  $Q_B^-$  after an even number [25]. Superimposed upon this binary oscillation, and seen here in the 70  $\mu$ s data point in Fig. 15, is a period-of-four oscillation arising from the cycling of the S-states associated with the water oxidation process [7,34]. The different S-states re-reduce Z at different rates and different equilibria are involved. In turn, this affects the re-reduction of  $P680^+$  by Z after an actinic flash and the associated equilibrium between these two species [31]. The resulting changes in the  $P680^+$  population then impose the period-of-four oscillation. The oscillations, although clearly seen, are considerably damped when compared with samples that have not been subjected to the incubation required in these studies (e.g., see [25]).

Figure 15. Variable Chl a fluorescence as a function of flash number. The figure shows the  $\text{HCO}_3^-$ -reversible effect in treated membranes at pH 6.5 and pH 7.5. The flash frequency was 1 Hz. The times indicated are when the measuring flash was fired.



Furthermore, these oscillations are seen to be completely lost in the treated thylakoids.

Fig. 15 demonstrates that at both pH 6.5 and pH 7.5 the two-electron gate turnover proceeds without obvious impediment in the restored and control membranes. However, the flash pattern for the treated membranes at these pH values indicates that successive turnovers of the two-electron gate in these centers proceed more slowly at the alkaline pH than at the acidic pH. It can be seen, for example, that the maximum fluorescence yield at 2 ms after the actinic flash is higher at pH 7.5 (> flash 5) than at pH 6.5 (> flash 3). Therefore, the oxidation of  $Q_A^-$  in treated samples, after two turnovers of the reaction center, exhibits a pH dependence where the inhibited rate of  $Q_A^-$  oxidation is slowed further when changing the pH from 6.5 to 7.5.

In Fig. 16, we present additional data for the variable Chl a fluorescence yield as a function of flash number in treated membranes. Comparison of this data with Fig. 15 shows the largest variation observed throughout the duration of this study. The flash data from samples used in Fig. 16 appear not to confirm the pH dependence described for the treated membranes in Fig. 15. However, in Fig. 17, a plot of the overall half-time of  $Q_A^-$  oxidation as a function of actinic flash number taken from the same data as Fig. 16, establishes this point. Here it can be seen that after 5 actinic flashes, given at 1 Hz, the overall  $t_{1/2}$  measured at pH 7.5 is approximately double that obtained at pH 6.5. That is, the half-time at pH 6.5 is 8 ms and at pH 7.5 it is 14 ms. Figure 17 also presents the half-times ( $t_{1/2}$ ) for the control and restored data. Careful inspection of these data reveals a binary oscillation and some indication of a period-of-four oscillation as well. Interestingly, the binary oscillation is reversed in the two

Figure 16. Variable Chl a fluorescence yield as a function of flash number in different samples from those used for Fig. 15. The flash frequency was 1 Hz. The times indicated are when the measuring flash was fired.

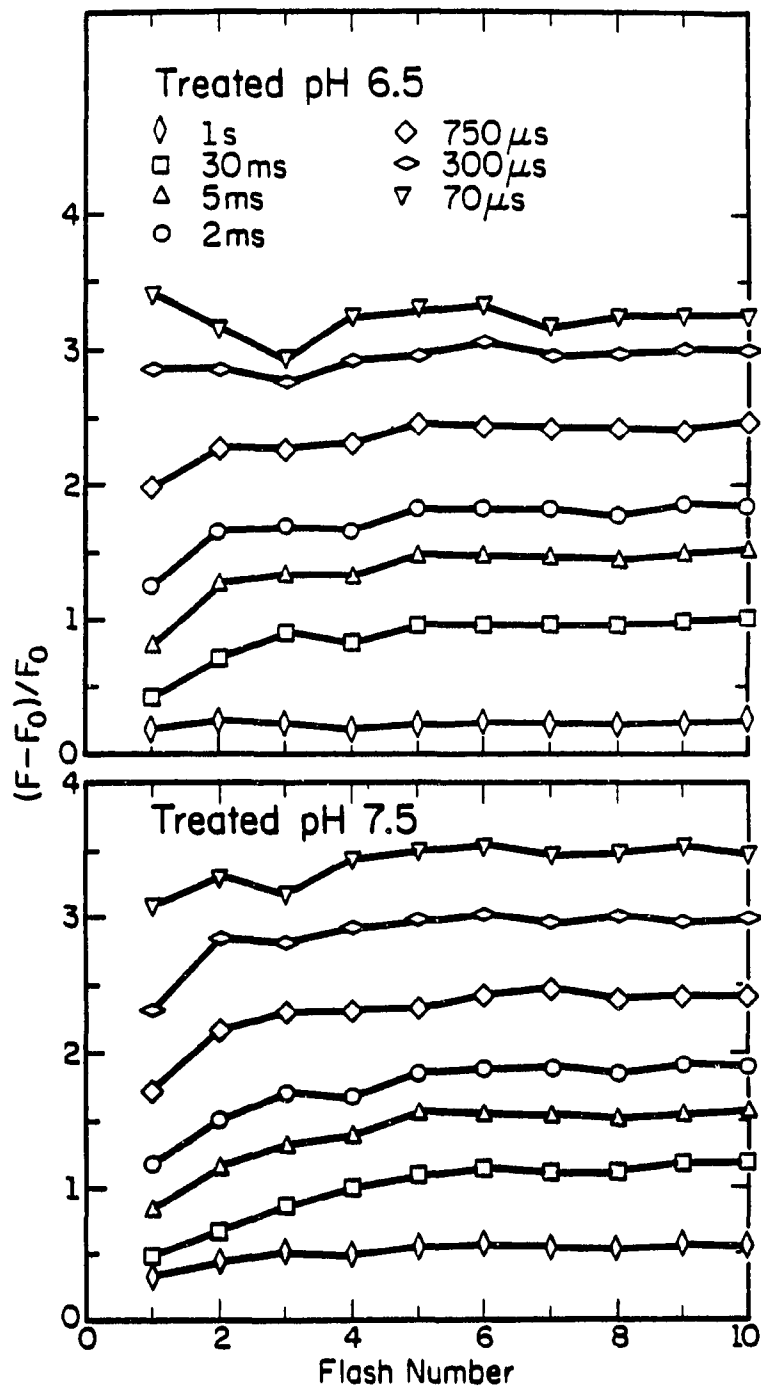
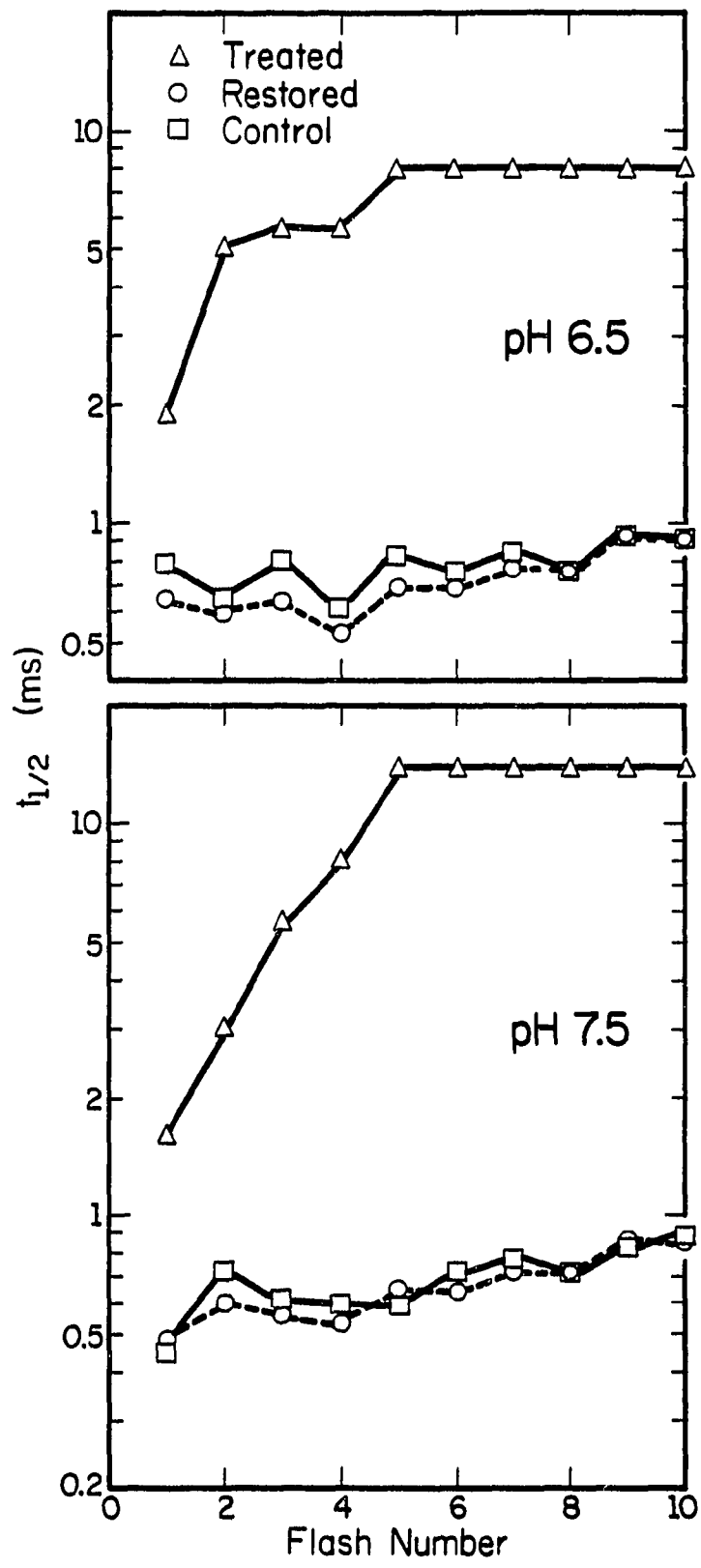


Figure 17. Plot of the overall half-time of  $Q_A^-$  oxidation as a function of flash number in treated, restored and control membranes. The flash frequency was 1 Hz.



cases. The control  $t_{1/2}$  at pH 6.5 is slower for flash 1 than for flash 2 in agreement with the data in Fig. 14 and the flash pattern in Fig. 15. In Fig. 17, however, the control and restored data for flash 2 are seen to be essentially pH independent, and thus the differential effect observed for the treated membranes does indeed appear to be a consequence of the  $\text{HCO}_3^-$ -depletion or the anion inhibitory treatment. A parallel study of the pH effect in treated membranes after 1 or 2 actinic flashes has confirmed this result (Chapter IV).

The data for treated membranes in Fig. 15 and an intermediate example between Figs. 15 and 16 (see Fig. 19(c) and (d)) are shown as the overall half-time of  $\text{Q}_A^-$  oxidation as a function of flash number in Fig. 18. The slower  $\text{Q}_A^-$  oxidation rate at pH 7.5 after two turnovers (4 flashes) of the two-electron gate is evident in both these examples when compared with that seen at pH 6.5. In addition, the rate of  $\text{Q}_A^-$  oxidation after the first two flashes is again faster at pH 7.5 than at pH 6.5. The data for flash 3 in Fig. 17 and Fig. 18(b) show that the  $t_{1/2}$  at pH 6.5 and pH 7.5 is essentially the same. These data reflect the more typical result for flash 3. The data for Fig. 18(a) are representative of spinach supplied over an approximately 3 month period (January-March, 1986), as noted above, out of the 18 month period from which this work is drawn.

The kinetics of  $\text{Q}_A^-$  oxidation in treated membranes have been analyzed for discrete exponential components [13,35]. Caution, however, must be exercised when interpreting such data, as it is uncertain whether the processes reflected in the resulting components are first order or not. This approach to the data yields an apparent biphasic decay with a component in the 0.3-1.0 ms range and a second component in the 5-20 ms range with additional components in the 0.1-10 s range. The

Figure 18. Plot of the overall half-time of  $Q_A^-$  oxidation in treated membranes with measurements at pH 6.5 and pH 7.5. Two experiments are shown. The flash frequency was 1 Hz.

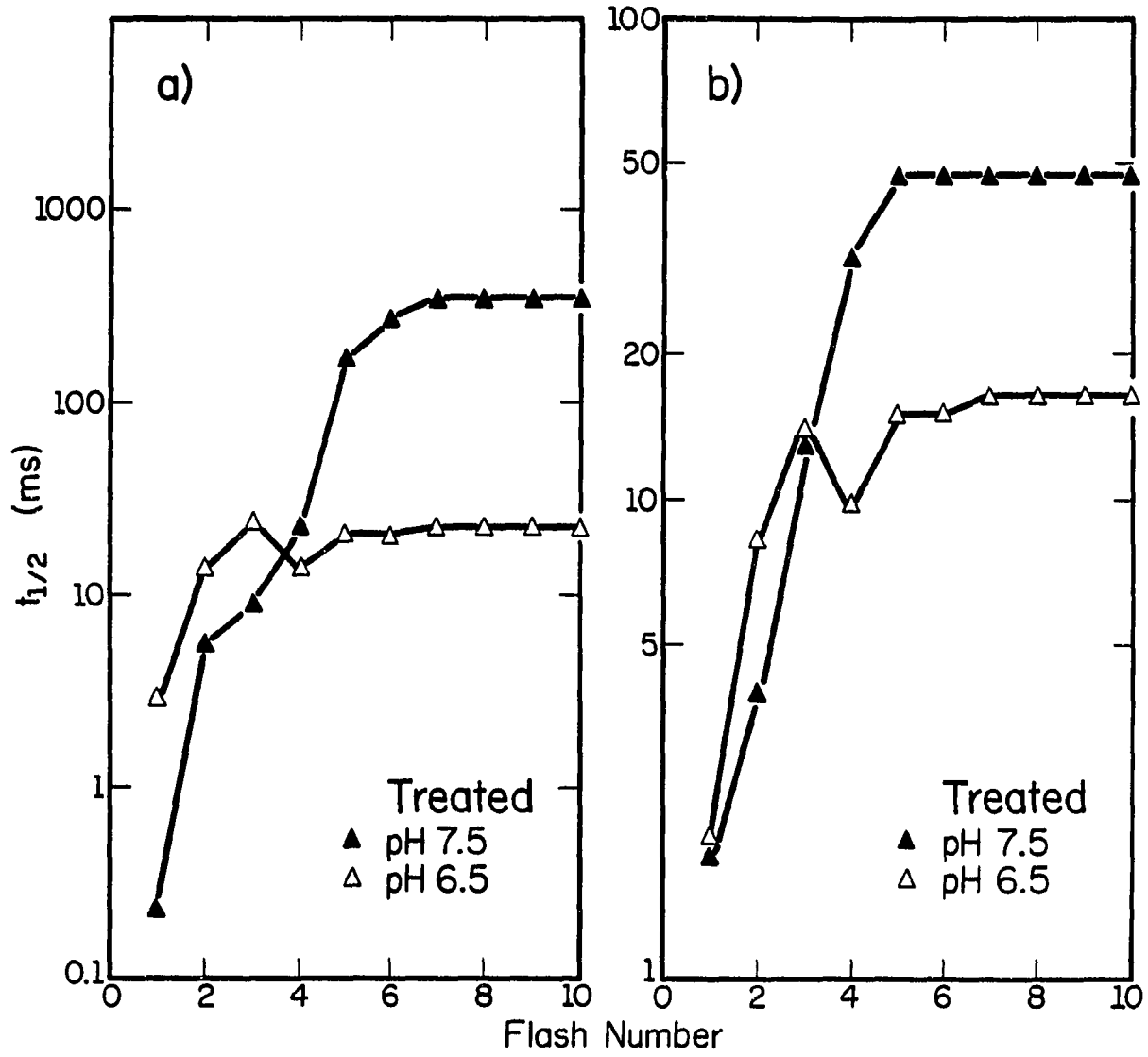


Figure 19. Variable Chl a fluorescence yield as a function of flash number at two frequencies (1 or 5 Hz) and at pH 6.5 and pH 7.5

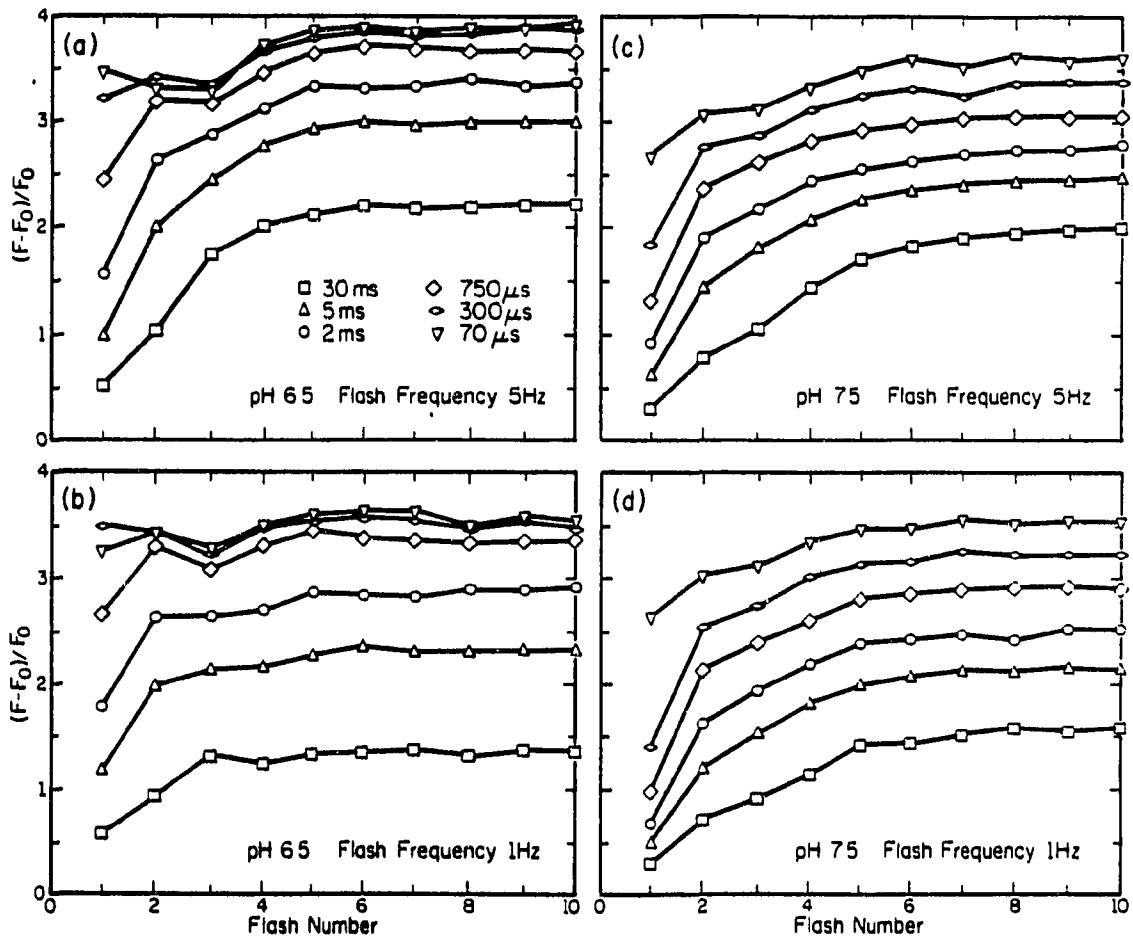
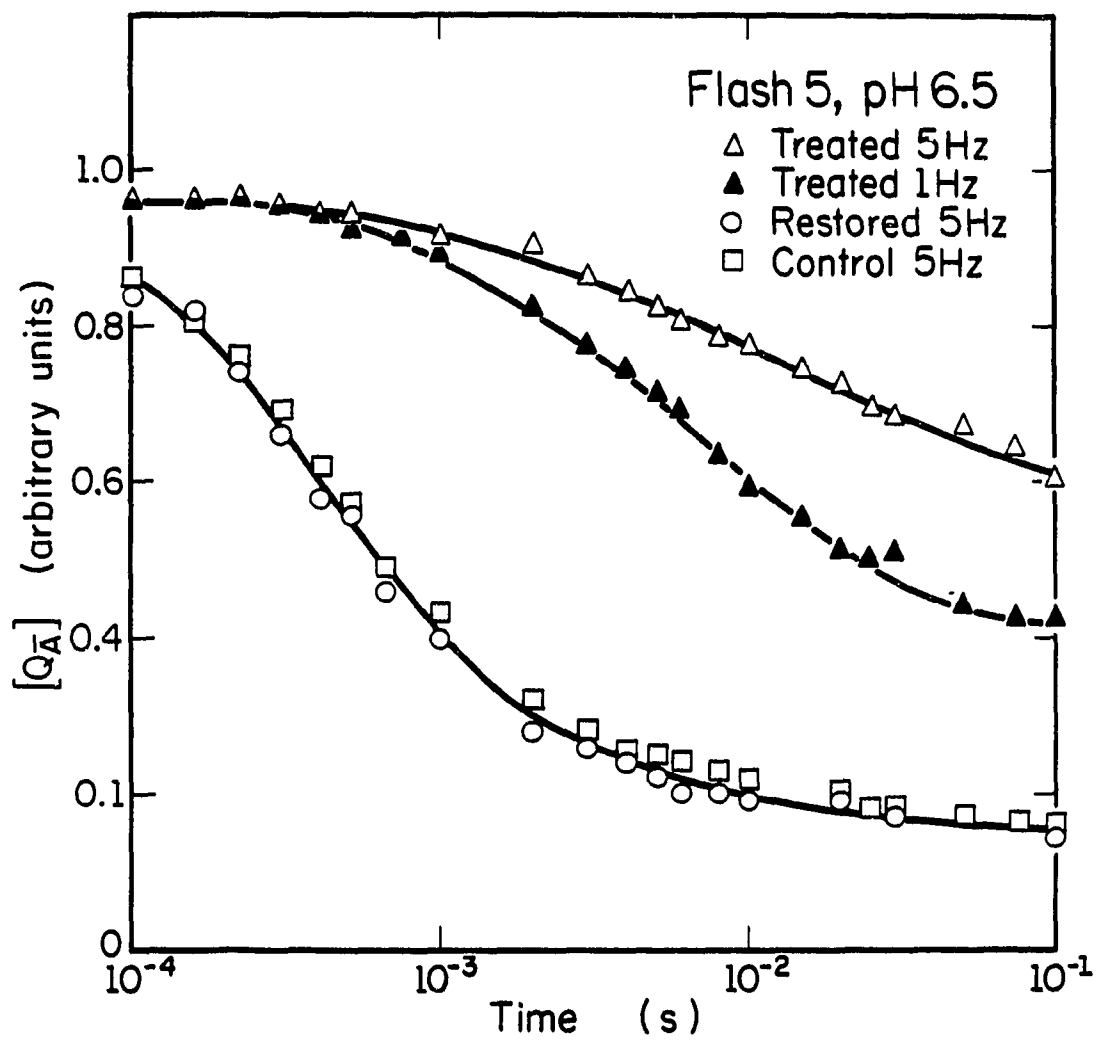


Figure 20. Oxidation of  $Q_A^-$  after the fifth actinic flash in a train of five flashes spaced at 5 Hz or 1 Hz. Open symbols are for the data collected at 5 Hz and solid triangles are for the data collected at 1 Hz. The data are expressed as  $[Q_A^-]$  against time plotted on a logarithmic scale. A value of 1.0 on the ordinate is equivalent to all centers being in the state  $Q_A^-$ . The pH was 6.5.



variation in the overall  $t_{1/2}$  shown for the treated membranes in Figs. 17 and 18 appears in large part to be correlated with the relative contribution of these additional slow components. Similarly, the variation observed for the overall half-time between Fig. 18(a) and (b) at pH 7.5 may have the same explanation. In Fig. 18(a) the overall  $t_{1/2}$  for  $Q_A^-$  oxidation at pH 7.5 after the fifth actinic flash is 135 ms and in Fig. 18(b) the corresponding  $t_{1/2}$  is 47 ms.

In both Fig. 18(a) and (b) we observed a slight dip corresponding to an accelerated decay of  $Q_A^-$  for flash 4 relative to flash 3 at pH 6.5. It is possible that this phenomenon is related to the relative ratio of centers undergoing oxidation by either  $Q_B$  or  $Q_B^-$ . If the fraction of centers experiencing  $Q_A^-$  oxidation by  $Q_B$  is greater after flash 4 than after flash 3, a decrease in overall half-time, as seen here, would be expected. This would seem to be quite possible since  $HCO_3^-$ -depletion in the presence of formate may alter both the association constant for  $Q_B$  and the kinetic stability of the bound  $Q_B^-$  species (Chapter IV). The association constant parameter is pH dependent and decreases with the lowering of pH in an acidic direction. This may explain the absence of a similar dip in the flash pattern at pH 7.5 here. Presumably this phenomenon is not observed at higher flash numbers due to the damping of the relative levels of  $Q_B$  and  $Q_B^-$  to approximately 1:1 following successive turnovers. The phenomenon may also be related to protonation since it is seen to correlate with a similar dip in the control samples in Fig. 17(a).

### 3. The Effect of pH and Flash Frequency in Treated Membranes

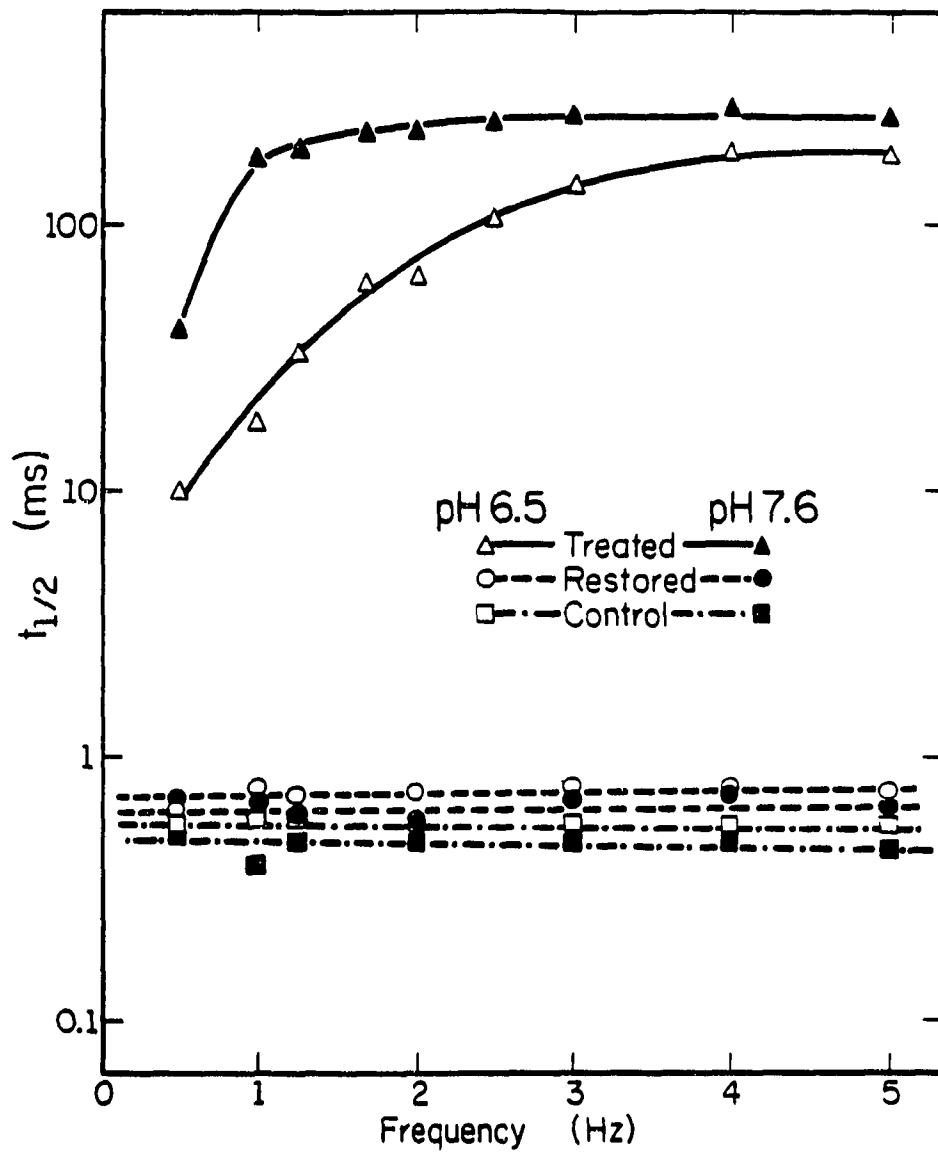
The results of the preceding section are extended in Fig. 19 by altering the actinic flash frequency. It can be seen that at 30 ms

after the actinic flash in a train of flashes given at 1 Hz (Figs. 15,16 and Fig. 19(b) and (d)) the fluorescence yield, proportional to  $[Q_A^-]$ , reaches its maximum after flash 5 at pH 7.5 and after flash 3 at pH 6.5. Fig. 19(a) demonstrates that even at pH 6.5 the number of turnovers necessary before maximal  $[Q_A^-]$  is reached is extended to flash 5 if the flash frequency is increased to 5 Hz. It is therefore possible that a dark-time of 200 ms (at 5 Hz) is insufficient for an equal amount of protonation to occur at the electron acceptor side of PS II than when 1 s (1 Hz) is allowed to elapse between flashes.

The  $Q_A^-$  oxidation data for the treated samples after flash 5 at pH 6.5 and two flash frequencies, 1 or 5 Hz, are shown as a function of time in Fig. 20. The reversibility of the treatment at 5 Hz is clearly shown. The half-time for the restored and control decays was approximately 600  $\mu$ s which was quite similar to that measured for flash 1 in Fig. 14(a) and (c) and suggests that no obvious inhibition is caused at this frequency in these membranes. The treated membranes at 1 Hz exhibited a half-time for  $Q_A^-$  oxidation of 22 ms and approximately 170-180 ms at 5 Hz. Similar data were obtained at pH 7.5. The half-time in control or restored membranes being 540  $\mu$ s and for the treated membranes at 1 Hz, 25 ms and at 5 Hz, 180-200 ms. The data at 5 Hz is not as precise as that at 1 Hz due to the fact that our instrument collects data after each actinic flash in a train of actinic flashes with the limitation that the measuring flash cannot be fired after  $f-50$  ms, where  $f$  is the dark time between actinic flashes.

To investigate the combined effect of actinic flash frequency and pH the experiment in Fig. 21 was performed. Here pH 6.5 and 7.6 were used and the data after flash 5 are presented as the overall half-time as a function of flash frequency between 0.5 and 5 Hz.

Figure 21. Plot of the overall half-time of  $Q_A^-$  oxidation in treated, restored and control membranes after the fifth actinic flash in a train of five flashes. The data are shown as a function of flash frequency and at both pH 6.5 and pH 7.6.



The dependence on frequency is clearly seen at pH 6.5 with the  $t_{1/2}$  parameter increasing from 10 ms at 0.5 Hz to 175 ms at 4 Hz. At pH 7.6 the half-time at 0.5 Hz was 42 ms and it reached a maximum of approximately 250 ms by 2.5 Hz. The differential pH effect is clearly evident in a comparison between the two sets of treated data at 1 Hz and 5 Hz. At pH 6.5 and 1 Hz, the  $t_{1/2}$  is 18 ms while at pH 7.6 and 1 Hz it is 182 ms. The decay components in the 0.1-10 s range had an amplitude of 55% at pH 6.5 and 70% at pH 7.6. Therefore a 15% increase in the amplitude of these slow components corresponds to a ten-fold increase in the overall half-time. At 5 Hz the half-time at pH 7.6 is seen to be approximately 240 ms and that at pH 6.5, 182 ms. This represents only a 1.3-fold increase in  $t_{1/2}$  and in both cases the contribution from the slow components in the 0.1-1 s range was estimated to be 72%.

No dependence of overall  $t_{1/2}$  on flash frequency was observed in the control and restored data for flash 5 in Fig. 21. A slight pH effect however was seen. The approximate half-times at pH 6.5 were: for restored membranes, 660  $\mu$ s; for control membranes, 550  $\mu$ s; and at pH 7.6: for restored membranes, 630  $\mu$ s, for control membranes, 480  $\mu$ s. The restoration at both pH 6.5 and 7.6 is seen to be almost complete. However, a small difference can be seen between control and restored samples here; this is also seen with increasing flash number at pH 6.5 and pH 7.5 in Fig. 15.

#### D. Discussion

The results presented in this paper establish four major points with respect to the  $\text{HCO}_3^-$ -reversible inhibition seen in treated membranes: (1) the oxidation of  $\text{Q}_A^-$  by  $\text{Q}_B$  or  $\text{Q}_B^-$ , following 1 or 2 actinic flashes respectively, exhibits a smaller overall half-time at pH 7.5

than at pH 6.5 (Figs. 14,15,17, and 18); (2) the characteristic oscillations observed in the fluorescence flash pattern, generated by assaying the Chl *a* variable fluorescence at specific times after an actinic flash and plotting these data as a function of flash number, are entirely lost (Figs. 15 and 16); (3) the slowest oxidation of  $Q_A^-$ , as indicated by the overall half-time parameter, depends on both pH and flash number (Figs. 15,16,17 and 18) and (4) the overall half-time parameter also depends on the actinic flash frequency (Figs. 19-21).

Two principal mechanisms have been proposed to explain the action of  $HCO_3^-$  on electron transport through the plastoquinone acceptor of PS II. These are: (1) that bound  $HCO_3^-$  brings about a conformational change in the quinone acceptor complex facilitating electron transfer (e.g., [19,20,36]) and (2) that  $HCO_3^-$  is involved in the protonation steps associated with  $Q_B$  reduction to  $Q_B^{2-}(2H^+)$  [22,37]. Both of these hypotheses have been advanced to explain the result that the inhibition due to  $HCO_3^-$ -depletion, in the presence of formate or nitrite ([38,39] and see Chapter II), attains a maximum level after two turnovers of the reaction center [13,15,18,19]. The pH of these experiments was either 6.5 or 6.8. Since the inhibited state after three actinic flashes was characterized by a high level of Chl *a* variable fluorescence, the inhibited reaction center was suggested to be locked in the state  $Q_A^-Q_B^{2-}$  [18,35]. The conformational hypothesis then required that the rearrangement of the quinone acceptor complex prevented the release of  $Q_B^{2-}$  to the plastoquinol pool. The protonation hypothesis implied that the  $Q_B^{2-}$  could not be released to the plastoquinone pool until the state  $Q_B^{2-}(2H^+)$  was formed. While it can be seen that the two hypotheses need not be mutually exclusive, the findings of this study do allow for revision of our understanding of the rate-limiting step introduced in

treated membranes.

An unusual pH dependence is evident in the above results. In a train of actinic flashes given at 1 Hz following 1 or 2 flashes, the oxidation of  $Q_A^-$  in treated membranes is characterized by a smaller overall half-time at pH 7.5 than at pH 6.5, a transition occurs with the measurement following flash 3 and the dependence is reversed for the remaining flash numbers. That is, the oxidation of  $Q_A^-$  after 4 successive turnovers of the PS II reaction center proceeds more slowly at pH 7.5 than at pH 6.5.

The pH dependence seen for  $Q_A^-$  oxidation after 1 or 2 actinic flashes can be understood from the perspective of both the conformational hypothesis and the protonation hypothesis. The amplitude of the initial linear component observed in semi-logarithmic plots of  $Q_A^-$  oxidation after a single actinic flash in treated membranes is reduced with respect to control and restored samples (Chapter IV). This amplitude has been suggested to reflect the fraction of centers that have  $Q_B$  bound before the actinic flash in control samples (see *e.g.*, [33]). This would suggest that the association constant ( $K_0$ ) for  $Q_B$  at the  $Q_B$ -site is decreased in treated membranes. Alternatively, the reduction seen in the amplitude may reflect a decrease in the equilibration of a proton with  $Q_B^-$  in the treated case.

Considering first the apparent effect on  $K_0$ , then it appears that the association constant ( $K_0$ ) for  $Q_B$  at the quinone acceptor complex is decreased from  $420 \text{ M}^{-1}$  to  $80 \text{ M}^{-1}$  at pH 6.5 and from  $420 \text{ M}^{-1}$  to  $230 \text{ M}^{-1}$  at pH 7.5 in treated membranes. The data here are in agreement with this finding with the exception of Fig. 14(b) from which we found that the  $K_0$  at pH 7.5 in these membranes was essentially identical to that

measured for the restored and control samples. The pH dependence seen for  $K_0$  in treated membranes does, however, demonstrate that this parameter does approach that observed for the restored and control membranes (Chapter IV). In addition, the pH dependence and the kinetic components seen for  $Q_A^-$  oxidation after two actinic flashes given with an interval of 1 s, are indicative of a large fraction of centers, perhaps as large as 50%, undergoing oxidation by  $Q_B$  rather than  $Q_B^-$  (Chapter IV). To explain this it is suggested in Chapter IV that the kinetic stability of  $Q_B^-$  is decreased in treated membranes.

The above inhibitory effects associated with  $Q_A^-$  oxidation after 1 or 2 actinic flashes in treated membranes would not appear to be associated with  $HCO_3^-$  acting as a proton donor. If this were the case, then the pH dependence would be expected to be the opposite of that observed, since increasing the bulk proton concentration by lowering the pH would be expected to substitute, at least in part, for the normal native proton donor

A different conclusion is reached if it is assumed that the truncated amplitude of the initial linear component for the decay of  $Q_A^-$  in treated membranes arises as a consequence of a decrease in the equilibrium constant for protons in association with  $Q_B^-$  (see  $K_3$  in Fig. 3, Chapter I). As stated in Results above, this interpretation implies that the increase in the apparent forward rate constant observed at pH 7.5 with respect to pH 6.5 in treated membranes in Fig. 14 may be attributed to treated membranes behaving as unprotonated control membranes. The  $pK$  for the protonation of  $Q_B^-$  in control membranes has been estimated to be approximately 7.9 (see e.g., [33]). At alkaline pH neither the control nor the treated membranes have a proton associated with  $Q_B^-$ . At acidic pH  $Q_B^-(H^+)$  is formed readily in the control but not

in the treated case. This suggests that at least one role for the  $\text{HCO}_3^-$  anion is associated with the mechanism of  $\text{Q}_\text{B}^-$  protonation.

The notion that the inhibited centers become locked in the state of  $\text{Q}_\text{A}^- \text{Q}_\text{B}^{2-}$  is not supported by this study. While the results obtained at pH 6.5 when an actinic flash frequency of 1 Hz is used are in reasonable agreement with earlier reports that the observed inhibition reaches a maximum after 3 flashes, this number is clearly extended to 5 flashes at pH 7.5 (Figs. 17 and 18). Furthermore, a dependency on actinic flash frequency is clearly observed. In Fig. 20 the half-time of  $\text{Q}_\text{A}^-$  oxidation after the fifth actinic flash, even at pH 6.5, is slower when the actinic flash frequency is given at 5 Hz than at 1 Hz. In addition, the overall half-time for  $\text{Q}_\text{A}^-$  oxidation at pH 6.5 is faster after 4 actinic flashes than following 3 actinic flashes, in a train of actinic flashes given at 1 Hz (Fig. 18).

Two conclusions are evident from the combined effect of actinic flash frequency (0.5 to 5 Hz) and pH (6.5 and 7.6) on  $\text{Q}_\text{A}^-$  oxidation after the fifth actinic flash: (1) a relatively small change in the fraction of centers undergoing oxidation by processes with components in the 0.1-10 s range results in very large changes in the apparent overall half-time and (2) at low frequencies (e.g., 1 Hz) the amplitude of these components is sensitive to pH. The first point may explain the large variations observed during the course of this study and which is clearly seen by comparing Figs. 17 and 18. The second point may indicate that the slow component is associated with protonation reactions accompanying  $\text{Q}_\text{B}$  reduction.

Jursinic and and Stemler [35] were the first to report the existence of a significant fraction of PS II centers remaining closed to

photochemistry after a single actinic flash in treated membranes. In our samples, approximately 20% of the corrected variable Chl  $a$  fluorescence, proportional to  $[Q_A^-]$ , decays in a 0.1-10 s range. In the control and restored samples a value of about 10-15% is typical and appears to be fairly independent of flash number. This fraction of inactive centers is probably related to inactive centers associated with PS II heterogeneity (see e.g., [40]). However, at pH 6.5 for flash 5, from a train of actinic flashes given at 1 Hz, the 20% amplitude is increased to 55% in treated membranes and the corresponding value at pH 7.6 is 70%. At an actinic flash frequency of 5 Hz the amplitude of the slow components (0.1-10 s) is approximately 72% at both pH 6.5 and pH 7.6 in treated membranes.

At 1 Hz the results for the treated membranes in Fig. 21 only suggest a 15% increase in the slow component for an approximate ten-fold drop in proton concentration. However, the existence of a 20% amplitude corresponding to  $Q_A^-$  oxidation processes in the 0.1-10 s range, even after a single flash in treated membranes, suggests that this fraction, present at both pH 6.5 and pH 7.6, is not associated with protonation. In addition, a pH dependence on the association constant for  $Q_B$  will also be a contributing factor to the inhibition seen at pH 6.5. Therefore, an increase in the slow components corresponding to protonation associated with  $Q_B$  reduction, following a ten-fold reduction in proton concentration, as seen here, may in fact be considerably larger than the 15% observed at 1 Hz.

The equal amplitude in treated membranes at 5 Hz for the slow oxidation kinetics of  $Q_A^-$ , at both pH 6.5 and pH 7.6, suggests that the kinetics of protonation are such that even at pH 6.5 a dark-time of 200 ms (at 5 Hz) is insufficient for an equal amount of protonation to

occur, in conjunction with  $Q_B$  reduction, than when 1 s (1 Hz) is allowed to elapse between flashes. This interpretation also implies that even a five-fold increase in dark time from 200 ms to 1 s does not allow a significant increase in protonation to be observed at pH 7.6.

#### E. Summary

The results in this chapter demonstrate the existence of two pH dependencies associated with  $Q_A^-$  oxidation in treated membranes. After 1 or 2 actinic flashes spaced at 1 s (Figs. 14-18) or 200 ms (Fig. 19) the oxidation of  $Q_A^-$  by  $Q_B$  or  $Q_B^-$  exhibits a smaller overall half-time at pH 7.5 than pH 6.5. Following three turnovers of the reaction center the observed pH dependency is reversed. After the third actinic flash in a train of actinic flashes given at 1 Hz the kinetics of  $Q_A^-$  oxidation are slower at pH 7.5 than pH 6.5. That is, the overall  $t_{1/2}$  of  $Q_A^-$  oxidation is sensitive to the external proton concentration (Figs. 15-18). The rate of  $Q_A^-$  oxidation at pH 6.5 after the fifth actinic flash in a train of actinic flashes is slowed to that observed at pH 7.6 as the flash frequency is increased from 0.5 Hz to 1 Hz (Fig. 21).

#### References

1. Warburg, O. and Krippahl, G. (1958) Z. Naturforsch. 13B, 509-514
2. Blubaugh, D.J. and Govindjee (1986) Biochim. Biophys. Acta 848, 147-151
3. Velthuys, B.R. (1981) FEBS Lett. 126, 277-281
4. Crofts, A.R. and Wraight, C.A. (1983) Biochim. Biophys. Acta 726, 149-185
5. Joliot, P. and Joliot, A. (1986) Photosynth. Res. 9, 113-124
6. Ort, D. (1986) Encyclopedia of Plant Physiology New Series 19, 143-

7. Wydrzynski, T.J. (1982) in *Photosynthesis: Energy Conversion by Plants and Bacteria* (Govindjee, ed.), Vol. I, pp. 469-506, Academic Press, New York
8. van Gorkom, H.J. (1985) *Photosynthesis Res.* 6, 97-112
9. Govindjee, Kambara, T. and Coleman, W. (1985) *Photochem. Photobiol.* 42, 187-210
10. Renger, G. (1987) *Photosynthetica*, in the press
11. Stemler, A., Murphy, J. and Jursinic, P. (1984) *Photobiochem. Photobiophys.* 8, 289-304
12. Saygin, O., Gerken, S., Meyer, B. and Witt, H.T. (1986) *Photosynthesis Res.* 9, 71-78
13. Robinson, H.H., Eaton-Rye, J.J., van Rensen, J.J.S. and Govindjee (1984) *Z. Naturforsch.* 39C, 382-385
14. Jursinic, P., Warden, J. and Govindjee (1976) *Biochim. Biophys. Acta* 440, 322-330
15. Siggel, U., Khanna, R., Renger, G. and Govindjee (1977) *Biochim. Biophys. Acta* 462, 196-207
16. Farineau, J. and Mathis, P. (1983) in the *Oxygen Evolving System of Photosynthesis* (Inoue, I., Crofts, A.R., Govindjee, Murata, N., Renger, G. and Satoh, K., eds.), pp. 317-325, Academic Press, Tokyo
17. Vermaas, W.F.J. and Rutherford, A.W. (1984) *FEBS Lett.* 175, 243-247
18. Govindjee, Pulles, M.P.J., Govindjee, R., van Gorkom, J.H. and Duysens, L.M.N. (1976) *Biochim. Biophys. Acta* 449, 602-605
19. Govindjee, Nakatani, H.Y., Rutherford, A.W. and Inoue, Y. (1984) *Biochim. Biophys. Acta* 766, 416-423
20. Khanna, R., Pfister, K., Keresztes, A., van Rensen, J.J.S. and Govindjee (1981) *Biochim. Biophys. Acta* 634, 105-116

21. Vermaas, W.F.J., van Rensen, J.J.S. and Govindjee (1982) *Biochim. Biophys. Acta* 681, 242-247
22. Govindjee, and Eaton-Rye, J.J. (1986) *Photosynthesis Res.* 10, 365-379
23. Graan, T. and Ort, D.R. (1984) *J. Biol. Chem* 259, 14003-14010
24. Joliot, A. (1974) in *Proceedings of the Third International Congress on Photosynthesis* (Avron, M., ed.), Vol I, pp. 315-322, Elsevier, Amsterdam
25. Robinson, H.H. and Crofts, A.R. (1983) *FEBS Lett.* 153, 221-226
26. Joliot, A. and Joliot, P. (1964) *Compt. Rend. Acad. Sci. Paris* 258D, 4622-4625
27. Forbush, B. and Kok, B. (1968) *Biochim. Biophys. Acta* 162, 243-253
28. Paillotin, G (1976) *J. Theoret. Biol.* 58, 219-252
29. Coleman, W. (1987) Ph.D. Thesis, University of Illinois, Urbana
30. Eaton-Rye, J.J. and Govindjee (1987) in *Progress in Photosynthesis Research* (Biggins, J., ed.), Vol. II, pp. 433-436, Martinus Nijhoff, Dordrecht
31. Robinson, H.H. and Crofts, A.R. (1987) in *Progress in Photosynthesis Research* (Biggins, J., ed.), Vol II, pp. 429-432, Martinus Nijhoff, Dordrecht
32. Jursinic, P. and Govindjee (1977) *Biochim. Biophys. Acta* 461, 253-267
33. Crofts, A.R., Robinson, H.H. and Snozzi, M. (1983) in *Advances in Photosynthesis Research* (Sybesma, C., ed.), Vol. I, pp. 461-468, Martinus Nijhoff/Dr.Junk Publishers, The Hague
34. Delosme, R. (1972) in *Proceedings of the II<sup>nd</sup> International Congress on Photosynthesis* (Forti, G., Avron, M. and Melandri, A.,

- eds.), Vol. I, pp. 187-195, Dr. W. Junk N.V. Publishers, The Hague
35. Jursinic, P. and Stemler, A. (1982) *Biochim. Biophys. Acta* 681, 419-428
  36. Vermaas, W.F.J. and Govindjee (1982) *Biochim. Biophys. Acta* 680, 202-209
  37. Eaton-Rye, J.J. and Govindjee (1984) *Photobiochem. Photobiophys.* 8, 279-288
  38. Eaton-Rye, J.J., Blubaugh, D J. and Govindjee (1986) in *Ion Interactions in Energy Transfer Biomembranes* (Papageorgiou, G.C., Barber, J. and Papa, S. eds.), pp. 263-278, Plenum Publishing Corporation, New York
  39. Jursinic, P. and Stemler, A. (1987) *Photosynthesis Res.*, in the press
  40. Chylla, R.G., Garab, G. and Whitmarsh, J. (1987) *Biochim. Biophys. Acta*, submitted

#### IV. THE EFFECT OF pH ON ELECTRON TRANSFER THROUGH THE QUINONE ACCEPTOR COMPLEX OF PS II AFTER 1 OR 2 ACTINIC FLASHES IN BICARBONATE-DEPLETED OR ANION INHIBITED THYLAKOIDS

##### A. Introduction

The quinone reductase of photosystem II (PS II) consists of two quinone molecules ( $Q_A$  and  $Q_B$ ) and an iron atom. Its structure is thought to be analogous to that of the Rhodospseudomonas viridis reaction centers [1,2]. X-ray analysis of the crystal structure of the R. viridis reaction center has revealed how the chromophores (2 bacteriochlorophyll b "special pair" molecules, 2 bacteriochlorophyll b monomer molecules, 2 bacteriopheophytin molecules and the above-mentioned  $Q_A$ ,  $Q_B$  and Fe atoms) are arranged in the midst of the L and M polypeptides. A cytochrome was attached on the side where the "special pair" was located, and the H-subunit was on the side where the quinones were located [1-3].

A homology exists between the L and M subunits and the D1 ( $Q_B$ -binding polypeptide) and D2 (another 34KD intrinsic polypeptide) subunits of photosystem II (see e.g., Trebst and Draber [4] and Chapter I, Fig. 2). This homology has been strengthened by the isolation and characterization of a PS II complex that contains D1, D2, the two subunits of cytochrome b<sub>559</sub> (see Chapter I, Fig. 2), 4-5 chlorophyll a molecules and 2 pheophytin molecules (it was assumed that  $Q_A$  and  $Q_B$  were lost during isolation) [5].

$Q_A$ , the primary quinone acceptor, is an obligate one electron accepting species and is stable on a microsecond to a millisecond time-scale in its reduced form.  $Q_B$ , the secondary quinone acceptor, is able to be doubly reduced to plastoquinol by two successive turnovers of the

reaction center and is therefore capable of oxidizing  $Q_A^-$  in its plastoquinone ( $Q_B$ ) and plastosemiquinone ( $Q_B^-$ ) form. This two-electron gating mechanism was first described in PS II by Bouges-Bocquet [6] and Velthuys and Amesz [7].

Velthuys [8] and Wraight [9] independently proposed, for thylakoids and purple bacteria respectively, that  $Q_B$  is readily exchangeable with the plastoquinone (PQ) pool when it is fully oxidized ( $Q_B$ ) or reduced ( $Q_B^{2-}$ ), and that the semiquinone form,  $Q_B^-$ , exists as a stable bound species. The  $Q_B$  binding site is located on the D1 reaction center protein which also binds urea (e.g., DCMU (3-(3,4-dichlorophenyl)-1, dimethylurea)) and triazine (e.g., atrazine) herbicides (see reviews [10-12]).

Both the forward rate constants for  $Q_A^-$  oxidation by  $Q_B$  or  $Q_B^-$  are decreased following the depletion of  $HCO_3^-$  in the presence of inhibitory anions such as formate or nitrite [13-17]. In addition, the exchange of plastoquinol with the PQ pool [13,18] and the binding of  $^{14}C$ -atrazine and  $^{14}C$ -ioxynil [19,20], both herbicides that bind to PS II [10], are inhibited in  $HCO_3^-$ -depleted membranes. Experiments employing single turnover actinic flashes indicated that the maximal inhibition of  $Q_A^-$  oxidation in  $HCO_3^-$ -depleted samples occurred after 3 successive turnovers [13,16,18], although the results presented in Chapter III show the dependency to be related to flash frequency and pH (see also [21]). As a result, little attention has been given to the effect of  $HCO_3^-$ -depletion after the second actinic flash.

In this chapter the effect of  $HCO_3^-$ -depletion on electron transfer through the quinone acceptor molecules after one or two actinic flashes is focused upon specifically. With this approach the effects of  $HCO_3^-$ -

depletion on the operation of the two-electron gate can be studied in a more exact manner than hitherto attempted.

Figure 3 in Chapter I is a self-explanatory scheme for the reactions associated with the two step reduction of  $Q_B$  to  $PQH_2$  by the quinone reductase, and the steps influenced by  $HCO_3^-$  are indicated. Detailed reviews treating the reactions of the two-electron gate may be found in references [11,22-24], and reviews on the  $HCO_3^-$  effect may be found in references [25-29].

## B. Materials and Methods

Thylakoid membranes were prepared from market spinach, and anion inhibited/ $HCO_3^-$ -depleted samples (hereafter referred to as treated membranes) were obtained by a dark incubation for 60 min in a  $CO_2$ -free buffer. Detailed methods for these procedures are given in Chapter III. The treatment buffer contained 300 mM sorbitol, 25 mM sodium formate, 10 mM NaCl, 5 mM  $MgCl_2$  and 10 mM sodium phosphate (pH 6.0). The chlorophyll (Chl) concentration was 250  $\mu M$ . The reaction medium contained 100 mM sorbitol, 10 mM sodium formate, 10 mM NaCl, 5 mM  $MgCl_2$ , 20 mM buffer (MES, pH 6.0-6.5; HEPES, pH 6.7-8.0), 100  $\mu M$  methyl viologen and 0.1  $\mu M$  gramicidin. All measurements were made on a sample diluted to contain 5  $\mu M$  Chl in a final volume of 100 ml in a dark stirred vat. A flow cuvette was filled from the vat by computer control.

Restored membranes were obtained by adding 5 mM  $HCO_3^-$  to a 2 ml aliquot of the treated stock. After a 2 min dark incubation these membranes were transferred to the reaction medium which also contained 5 mM  $HCO_3^-$ . Control membranes were obtained by omitting formate from the treatment and reaction media and not  $CO_2$ -depleting these buffers. In the case of the control, the incubation pH was also raised to pH 7.5.

Following isolation, the thylakoid membranes were maintained at 20° C in all cases.

The kinetics of decay of variable Chl a fluorescence at 685 nm (indicating oxidation of  $Q_A^-$  by either  $Q_B$  or  $Q_B^-$ ) were measured by a weak measuring flash after each actinic flash. The kinetic fluorimeter and the technique are described in detail in Chapter II.

### C. Results

#### 1. Oxidation of $Q_A^-$ in the Absence of an Inhibitor

Electron transfer through the plastoquinone acceptors of PS II may be followed in a stepwise manner by monitoring the decay of variable Chl a fluorescence over time as a function of the actinic flash number. To achieve this a second weak flash, sampling approximately 1% of the centers, is given at specified times after each actinic flash [30]. Figures 22 and 23 show the results obtained using this approach for one and two actinic flashes respectively. The reactions under consideration, together with the various equilibria and dissociation constants involved, were shown in Fig. 3 (Chapter I). A further complication is also introduced by the presence of some  $Q_B^-$  before the first flash. We determined the amount of  $Q_B^-$  in our samples before the flash by measuring the amount of DCMU-induced variable Chl a fluorescence yield [7]. No significant amount of  $Q_B^-$  was detected in our preparations following the incubation treatment (see Materials and Methods).

The rates of  $Q_A^-$  oxidation for both control and restored membranes after 1 or 2 actinic flashes, as given in the figure legends, are a factor of two slower than the earlier reported values (see e.g., [31]). This is due to the incubation period used to obtain appropriate controls. After a single flash the overall  $t_{1/2}$  for the treated membranes

Figure 22. Decay of variable Chl a fluorescence after a single actinic flash at pH 6.5 and pH 7.5. The data for pH 6.5 are in (a) and the data for pH 7.5 are in (b).  $F_0$  is the Chl a fluorescence yield from the measuring flash with all  $Q_A$  oxidized and  $F$  is the yield at the indicated time after the actinic flash. Time is plotted on a logarithmic scale. The inserts show the decays of Chl a fluorescence on a linear scale over the first 5 ms. The half-times are (a) for treated membranes, 2.8 ms; for restored and control membranes, 547  $\mu$ s and (b) treated, 1.5 ms; restored and control, 400  $\mu$ s. Half-times were determined as in Chapter III.

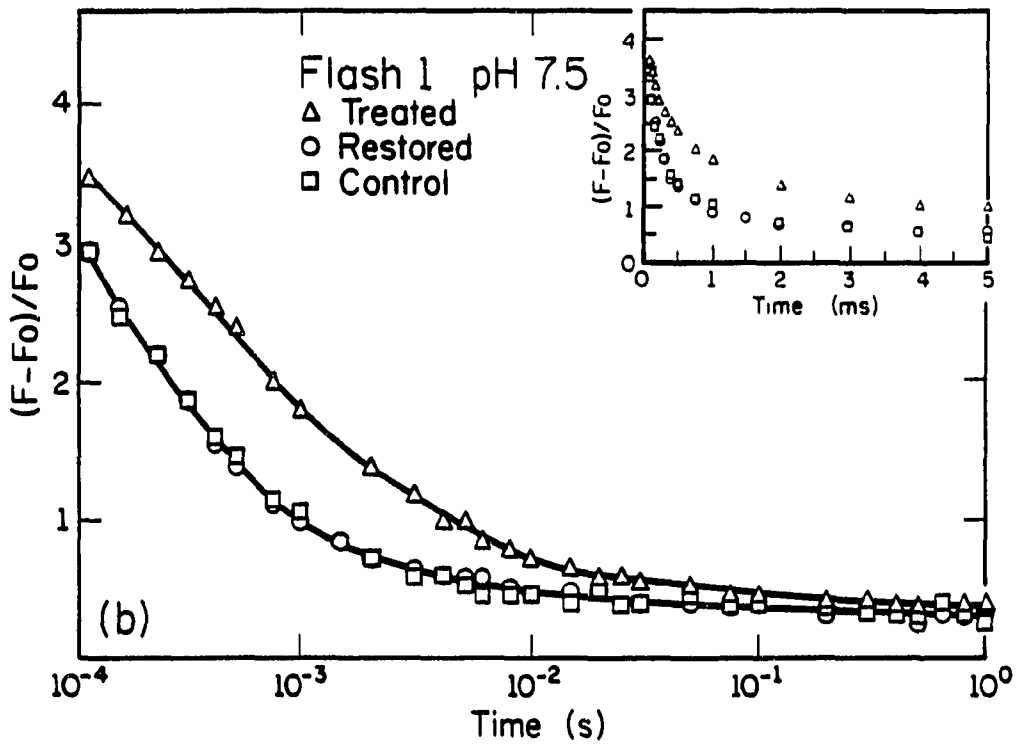
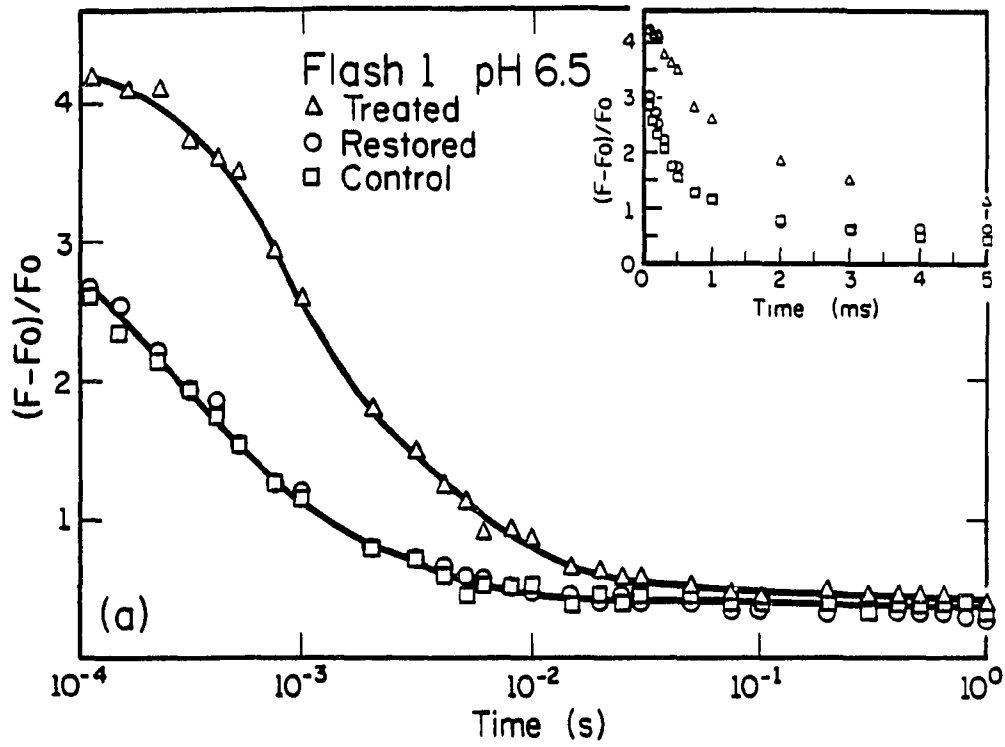
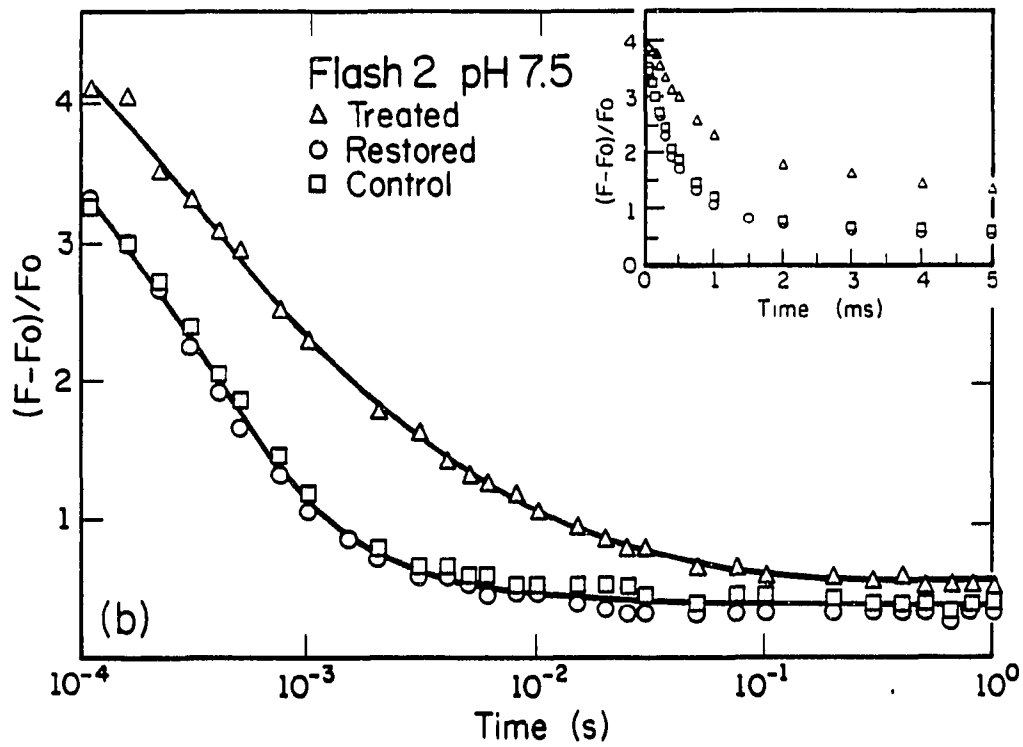
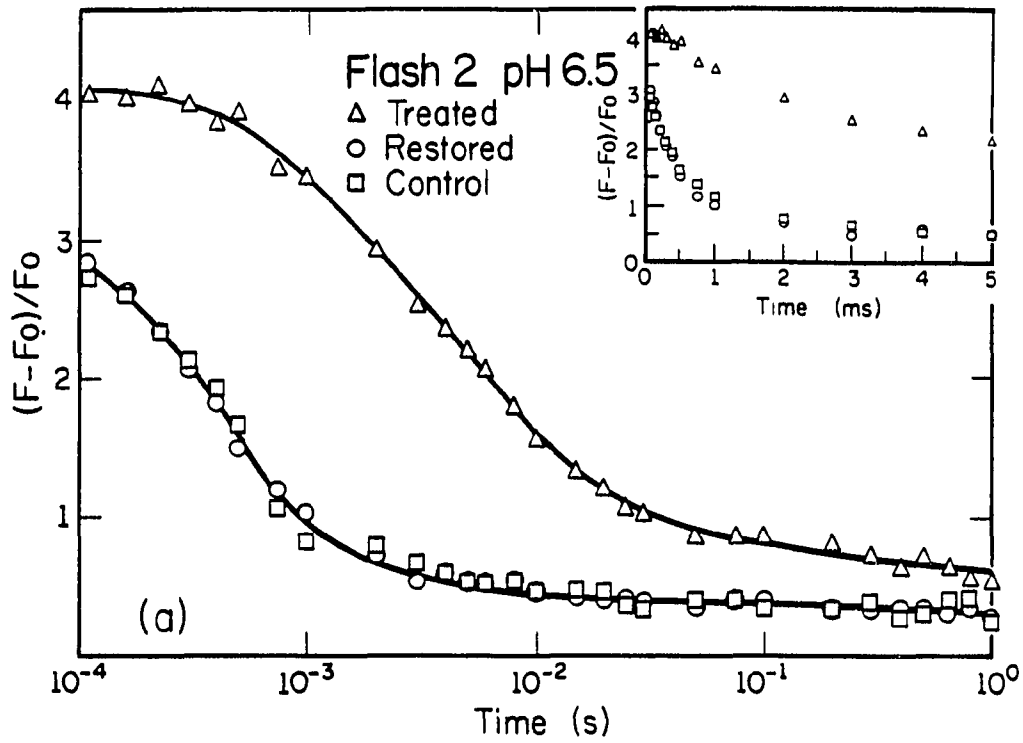


Figure 23. Decay of variable Chl a fluorescence at pH 6.5 and pH 7.5 after two actinic flashes spaced at 1 s. The data for pH 6.5 are in (a) and the data for pH 7.5 are in (b). Other details are as in Fig. 22. The half-times are: (a) for treated membranes, 11 ms; for restored and control membranes, 600  $\mu$ s, and (b) treated, 3.6 ms; restored and control, 633  $\mu$ s. Half-times were determined as in Chapter III.



is extended from 547  $\mu$ s to 2.8 ms at pH 6.5 and from 400  $\mu$ s to 1.5 ms at pH 7.5, but the oxidation reaction proceeds to the same apparent equilibrium of the restored and control membranes within 100 ms in each case. Therefore the fraction of  $Q_A Q_B^-$  centers in treated and restored or control membranes when the second flash is spaced 1 s after the first appears unchanged in each instance. Consequently, this protocol allows the specific effect of the  $HCO_3^-$ -reversible inhibitory treatment to be studied for  $Q_A^-$  oxidation by both  $Q_B$  (after a single flash) and  $Q_B^-$  (after a second flash). Figures. 22 and 23 also demonstrate that the rate of  $Q_A^-$  oxidation is faster at pH 7.5 than pH 6.5 in treated membranes. This is also true for control and restored membranes after a single flash but little or no effect of pH after a second flash was observed. This is in agreement with our earlier findings ([21] and see Chapter III). In treated membranes the effect on  $Q_A^-$  oxidation by  $Q_B^-$  is seen to be considerably larger than oxidation by  $Q_B$  at both pH values (Fig. 23). At pH 6.5 the overall half-time is extended from 600  $\mu$ s to 11 ms and at pH 7.5 from 633  $\mu$ s to 3.6 ms.

Both sets of data have been normalized to the same  $F_{max}$  level as determined by an addition of 5  $\mu$ M DCMU. We found that this level is pH independent in treated membranes. The observed intersections of the various fluorescence decays with the ordinate, therefore, do not depict the actual origin of the kinetic components. An artifactual contribution is introduced by the logarithmic time scale used. This may be seen in part by comparison with the variable Chl *a* fluorescence decay, plotted against linear time, in the insert in each case. In addition, the decays are also subject to fluorescence quenching by the oxidized form of the PS II reaction center Chl pigment, P680<sup>+</sup>. The degree of quenching attributable to this mechanism has been suggested to reflect the

differential kinetics of  $Z^+$  re-reduction (Z is a putative plastoquinol electron carrier between the OEC (oxygen evolving complex) and P680). This in turn affects the equilibrium between the charge on Z with that on P680 [32]. A reversible effect on the re-reduction of  $P680^+$  following an inhibitory anion treatment in the thermophilic cyanobacterium Synechococcus has recently been reported [33]. However, the contributions from this to the degree of fluorescence quenching, when measuring  $Q_A^-$  oxidation kinetics, and the pH dependence, if any, are not known.

The decays of the Chl a fluorescence in Figs. 22 and 23 can be corrected to be proportional to  $[Q_A^-]$  as described in Chapter III. Figures 24 and 25 present the semi-logarithmic plots of these data for flashes 1 and 2 respectively. Since the restored and control data are essentially the same in Figs. 22 and 23, only the treated and restored data are shown for clarity.

In the case of flash 1 the initial linear component is thought to reflect reaction centers which have  $Q_B$  bound before the flash while the remainder of the decay represents centers which had the  $Q_B$ -site unoccupied [24]. The initial linear component for the restored data in Fig. 5 (following 2 actinic flashes) is thought to reflect electron transfer between  $Q_A^-$  and  $Q_B^-(H^+)$  with the residual decay reflecting a second-order process involving the protonation reaction [24]. The treated membranes in Fig. 25, however, are clearly biphasic. For both flash 1 and flash 2 the points for the initial linear component deviate from the line, at short times after the actinic flash, as a result of the fluorescence quenching by  $P680^+$  discussed above. The half-times and respective amplitudes for these components are given in the appropriate figure legends.

Figure 24. Semi-logarithmic plots of the decay of  $[Q_A^-]$  after a single actinic flash calculated from the Chl *a* fluorescence decays in Fig. 22. The calculation was performed as described in Chapter III. The half-times for the initial linear components at pH 6.5 are: for treated membranes, 550  $\mu$ s with an amplitude of 30%; for restored membranes, 285  $\mu$ s with an amplitude of 70%. The half-times for the initial linear component at pH 7.5 are: treated, 460  $\mu$ s with an amplitude of 54%; restored, 252  $\mu$ s with an amplitude of 71%.

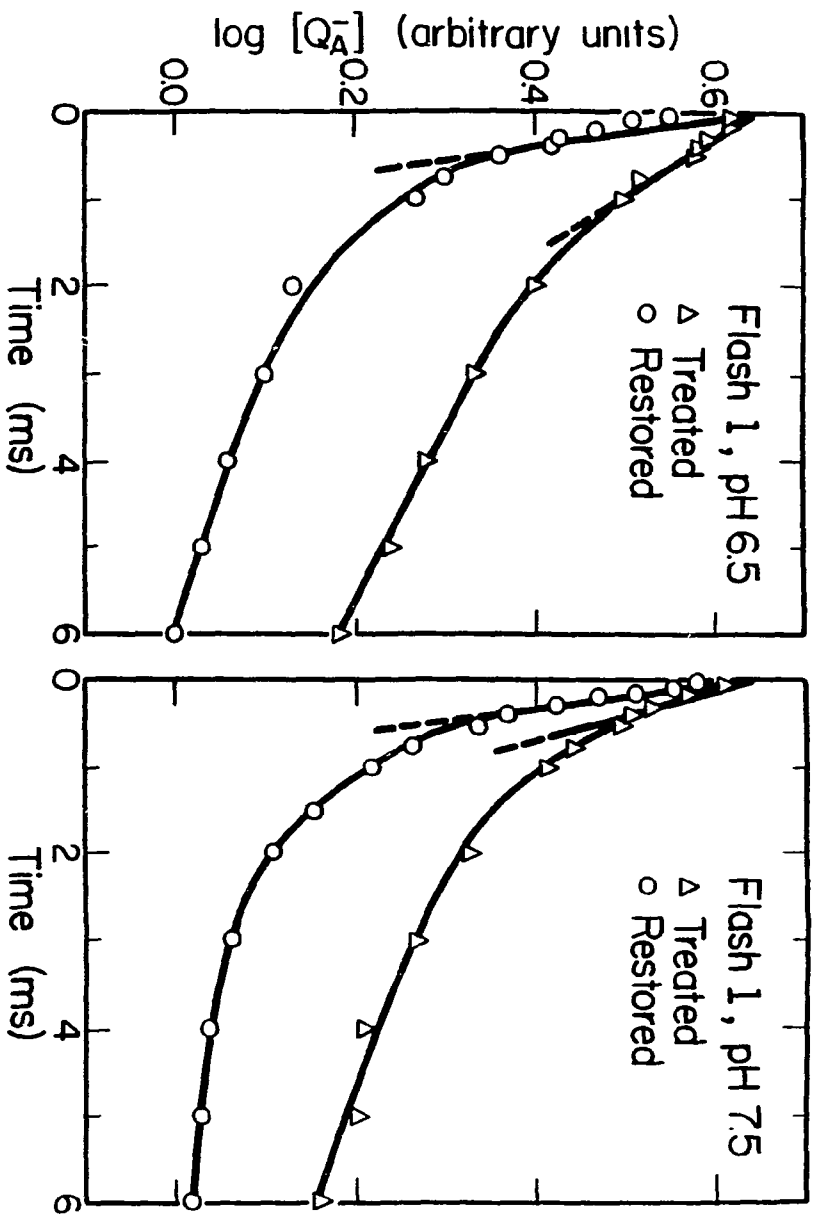


Figure 25. Semi-logarithmic plots of the decay of  $[Q_A^-]$  after two actinic flashes spaced 1 s apart calculated from the Chl a fluorescence decays in Fig. 23. The calculation was performed as described in Chapter III. The half-times for the initial linear components at pH 6.5 are: for treated membranes, 665  $\mu$ s with an amplitude of 21%, for restored membranes, 330  $\mu$ s with an amplitude of 75%. The half-times for the initial linear components at pH 7.5 are: treated, 464  $\mu$ s with an amplitude of 37%; restored, 332  $\mu$ s with an amplitude of 70%. The additional linear component for the treated membranes had an apparent half-time of 15 ms at pH 6.5 and 12 ms at pH 7.5.

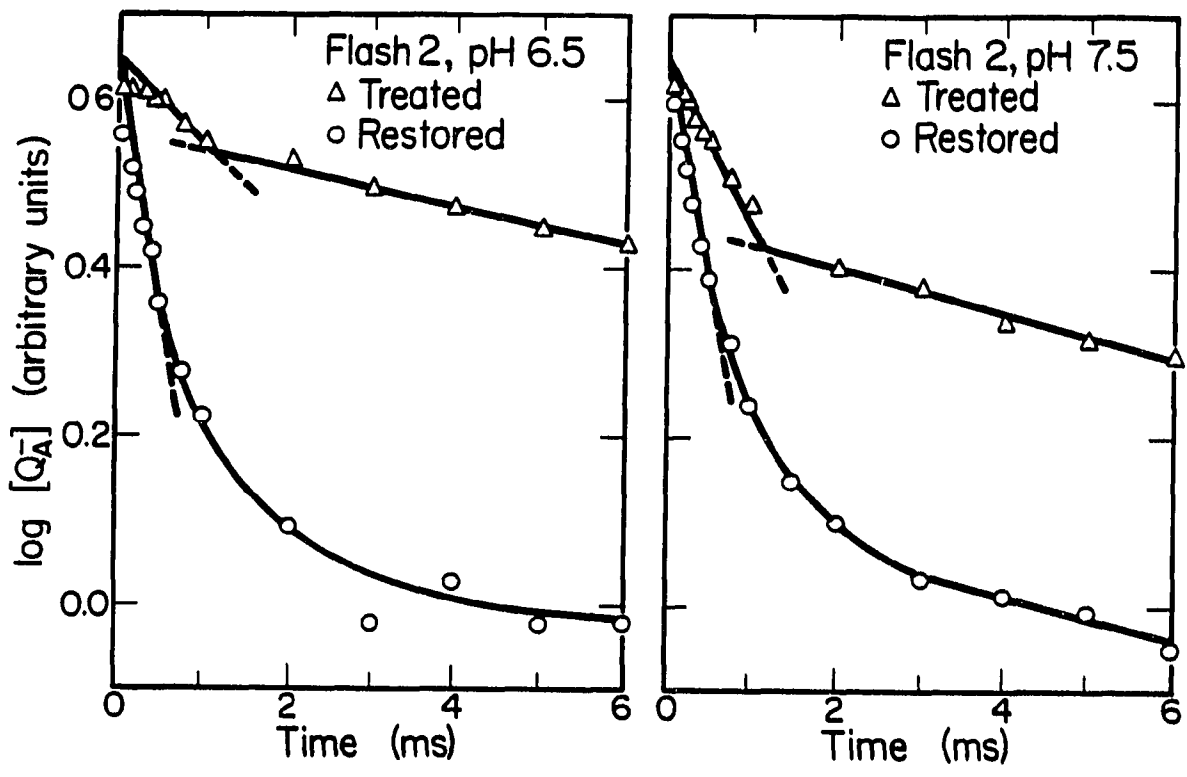


Figure 26. Plot of the overall half-time for  $Q_A^-$  oxidation as a function of pH after 1 and 2 flashes. In (a) the data are after a single actinic flash, and in (b) the data are after two actinic flashes spaced at 1 s. See text for additional details.

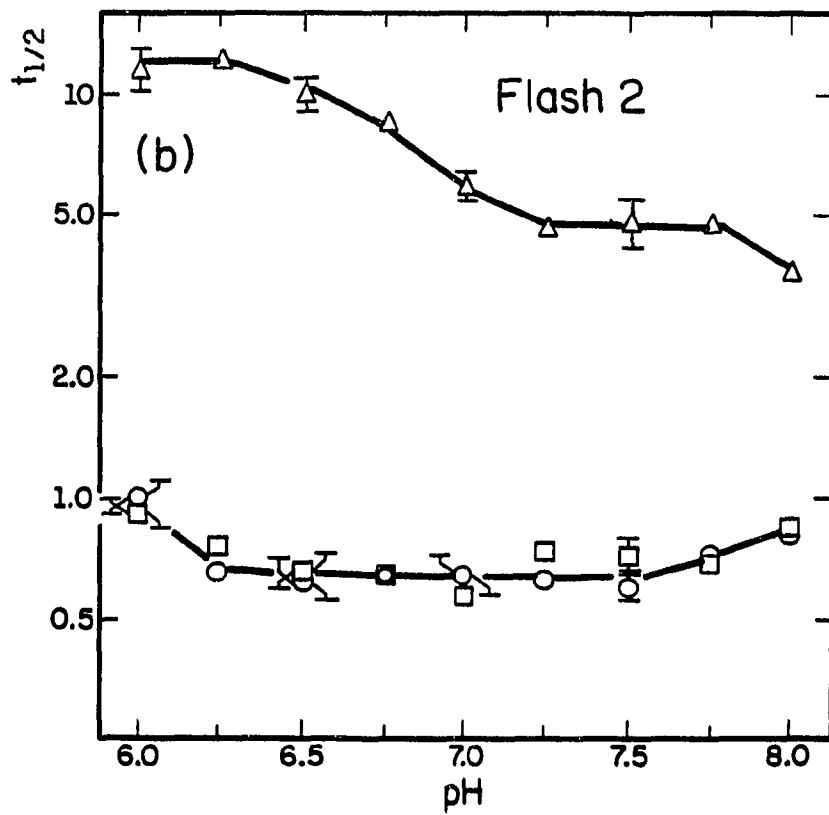
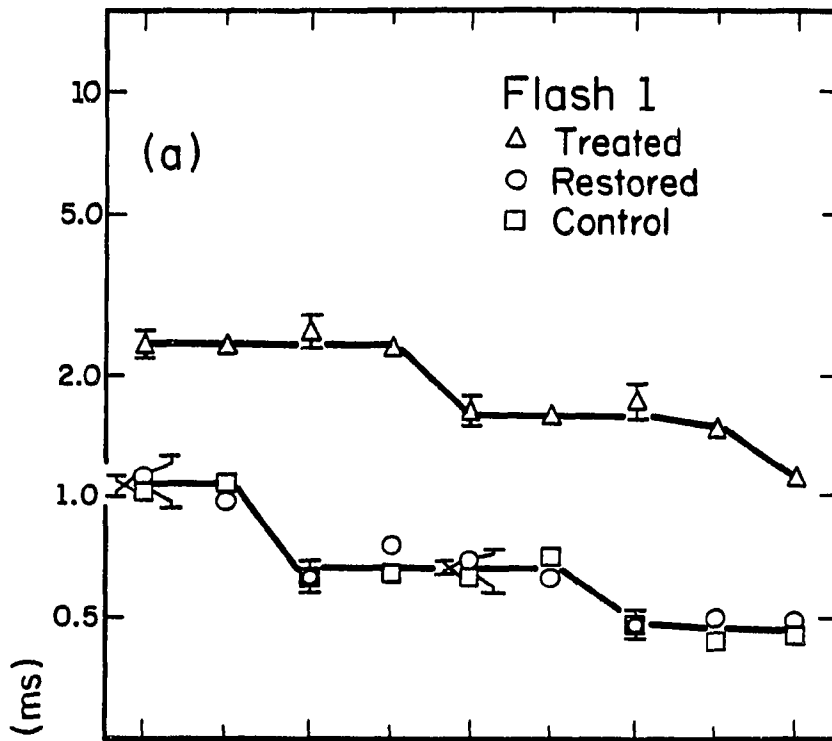


Figure 26(a) shows the overall half-time for  $Q_A^-$  oxidation, after a single flash, over a pH range from pH 6.0 to pH 8.0. The restored and control curve is staggered with transitions between pH 6.25 and pH 6.5 and between pH 7.25 and pH 7.5. At pH 6.0 and pH 6.25 the overall  $t_{1/2}$  is 1.1 ms, between pH 6.5 and pH 7.25, 660  $\mu$ s and between pH 7.5 and pH 8.0, 420  $\mu$ s. Semi-logarithmic plots of this data over 5 ms yielded an initial linear component, as seen in Fig. 24, from which approximate half-times and corresponding amplitudes could be estimated. These data are presented in Table 2

The two transitions observed in the control and restored data appear to be shifted 0.5 pH units in a basic direction in the treated case. Between pH 6.0 and pH 6.5 the overall  $t_{1/2}$  was 2.4 ms in these membranes. Between pH 7.0 and pH 7.5 the overall  $t_{1/2}$  was 1.6 ms and at pH 8.0, 1.1 ms. Semi-logarithmic plots produced an initial linear component as in the control and restored cases. These data are also presented in Table 2.

In Fig. 26(b) the overall  $t_{1/2}$  as a function of pH after two actinic flashes, spaced at 1 s, is presented. At pH 6.0 the control and restored membranes exhibit a  $t_{1/2}$  of approximately 950  $\mu$ s while from pH 6.25 to pH 7.5 they are pH independent with a  $t_{1/2}$  of approximately 645  $\mu$ s. Unlike the behavior seen for flash 1 the overall  $t_{1/2}$  then increases above pH 7.5 with a  $t_{1/2}$  of approximately 850  $\mu$ s at pH 8.0. Semi-logarithmic plots over 5-10 ms for Fig. 26(b) yielded an initial linear component in the control and restored samples and biphasic decays in the treated membranes. From these plots the approximate half-times and corresponding amplitudes for the initial linear components were estimated. These data are shown in Table 3.

TABLE 2

ESTIMATED HALF-TIMES AND AMPLITUDES FOR THE INITIAL LINEAR COMPONENT OF  
 $Q_A^-$  OXIDATION AFTER A SINGLE FLASH

Estimated half-times and corresponding amplitudes for the initial linear component of  $Q_A^-$  oxidation in treated, restored and control membranes after a single actinic flash. These data are taken from Fig. 26(a) and analyzed using semi-logarithmic plots of the decay of  $[Q_A^-]$  in an identical manner to that shown in Fig. 24. The data are tabulated as a function of pH.

pH	Treated		Restored and Control	
	$t_{1/2}$ ( $\mu$ s)	amplitude (%)	$t_{1/2}$ ( $\mu$ s)	amplitude (%)
6.00	560	23	370	53
6.50	630	29	310	64
7.00	470	45	320	63
7.50	410	51	230	65
7.75	240	62	230	66
8.00	200	48	250	63

An earlier report using unincubated pea thylakoids showed a  $t_{1/2}$  of 400  $\mu$ s at acidic pH and determined that the equilibrium for the sharing of an electron between  $Q_A$  and  $Q_B$  was pH dependent with a pK of 7.9 on the one-electron reduced complex [34]. Below this pK the rate of the  $Q_A^-$  oxidation reaction was found to be relatively independent of pH, but above the pK an increasingly slower reaction was observed. The reaction was therefore suggested to be limited by a second-order reaction between  $Q_B^-$  and a proton above the pK [24,34]. The results obtained for our overall half-times for  $Q_A^-$  after a second flash appear in reasonable agreement with this earlier report.

The data for the treated membranes illustrate, across the whole pH range studied, the strong inhibitory effect of  $HCO_3^-$ -depletion or anion inhibition on the oxidation of  $Q_A^-$  by  $Q_B^-$ . At pH 6.0 and pH 6.25 the overall  $t_{1/2}$  is approximately 12 ms.  $Q_A^-$  oxidation is pH dependent between pH 6.25 and pH 7.25. Between pH 7.25 and pH 7.75 the overall  $t_{1/2}$  is pH independent and is seen to be approximately 4.8 ms

In this instance the semi-logarithmic plots demonstrated an increase in both rate and amplitude for the initial fast component over the pH dependent portion of the curve. At pH 6.0 the  $t_{1/2}$  of the fast component was approximately 870  $\mu$ s with a amplitude of 20%. Between pH 7.25 and pH 7.75 the  $t_{1/2}$  decreased to approximately 470  $\mu$ s and the amplitude increased to 43% (see Table 3).

## 2. Oxidation of $Q_A^-$ in the Presence of DCMU

The back-reaction of  $Q_A^-$  with the  $S_2$  state (for a discussion of the S-states see [35]) of the OEC, in the presence of 5  $\mu$ M DCMU, is seen in Fig. 27 to exhibit a similar pH dependence to that seen for the forward reaction in Fig. 22. The approximate half-times for these reactions

TABLE 3

ESTIMATED HALF-TIMES AND AMPLITUDES FOR THE INITIAL LINEAR COMPONENT OF  
 $Q_A^-$  OXIDATION AFTER TWO ACTINIC FLASHES SPACED 1 S APART

Estimated half-times and corresponding amplitudes for the initial linear component of  $Q_A^-$  oxidation in treated, restored and control membranes after two actinic flashes spaced at 1 s. The data are taken from Fig. 26(b) and analyzed using semi-logarithmic plots of the decay of  $[Q_A^-]$  in an identical manner to that shown in Fig. 25. The data are tabulated as a function of pH.

pH	Treated		Restored and Control	
	$t_{1/2}$ ( $\mu$ s)	amplitude (%)	$t_{1/2}$ ( $\mu$ s)	amplitude (%)
6.00	870	20	400	64
6.50	670	21	330	67
7.00	560	36	350	64
7.50	460	37	330	66
7.75	470	43	370	64
8.00	550	45	400	58

Figure 27. Decay of variable Chl a fluorescence after a single actinic flash at pH 6.5 and pH 7.5 in the presence of 5  $\mu$ M DCMU. The data for pH 6.5 are shown in (a) and the data for pH 7.5 are shown in (b).  $F_0$  is the Chl a fluorescence yield from the measuring flash with all  $Q_A$  oxidized and  $F$  is the yield at the indicated time after the actinic flash. The half-times are: (a) for treated membranes, 5.3 s; for restored membranes, 1.3 s; for control membranes, 1.3 s and (b) treated, 2.9 s; restored, 2.3 s; control, 2.0 s. Half-times were determined as in Chapter III.

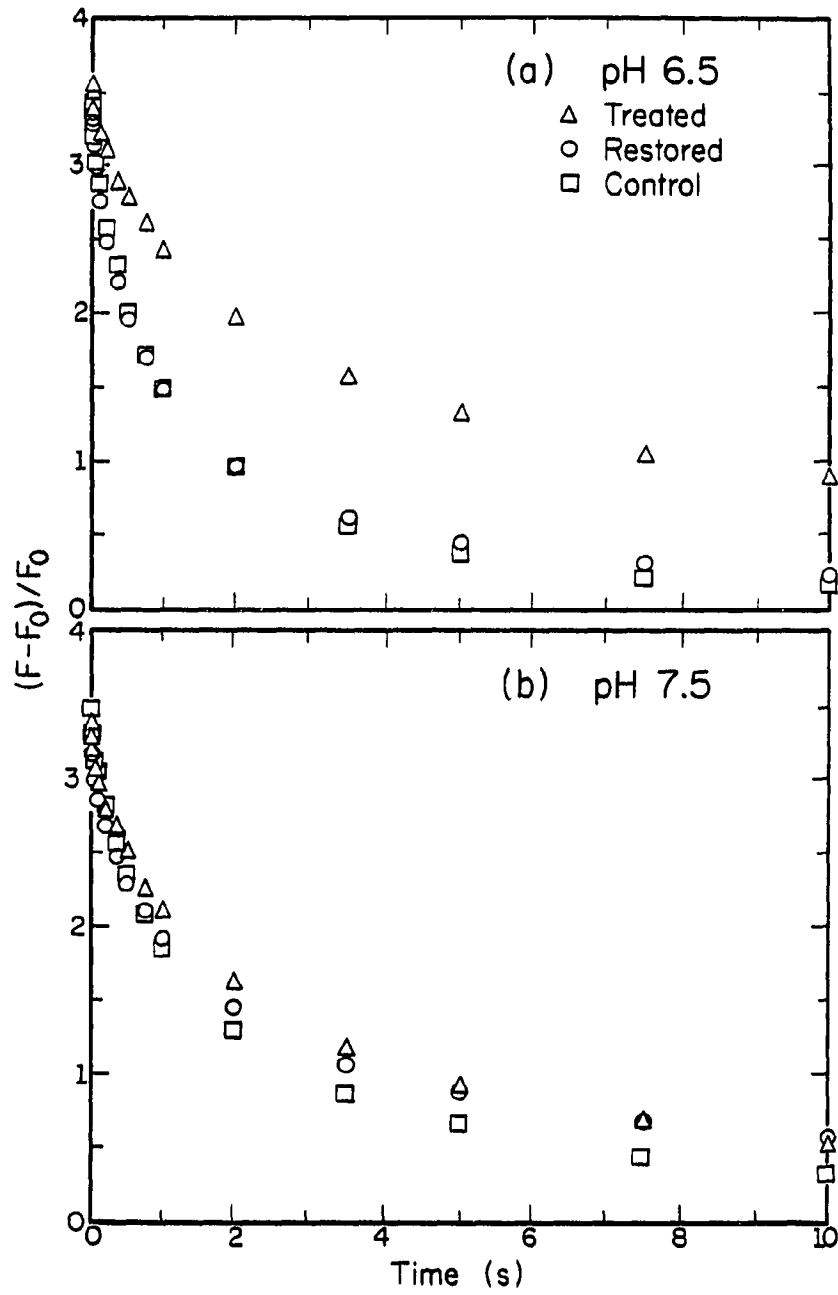
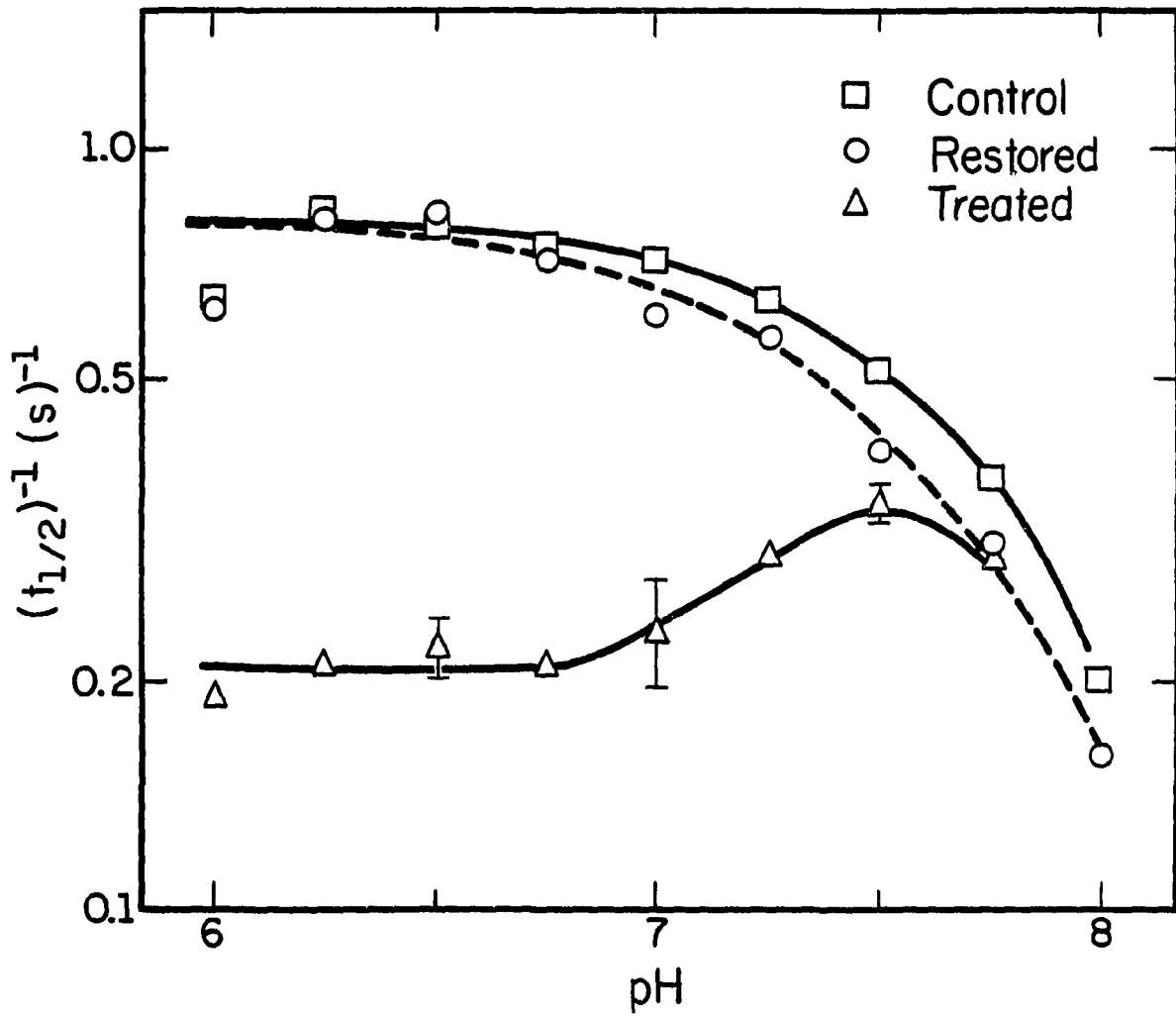


Figure 28. The reciprocal of the overall half-time of  $Q_A^-$  oxidation, in the presence of 5  $\mu\text{M}$  DCMU, plotted as a function of pH. For additional details see text.



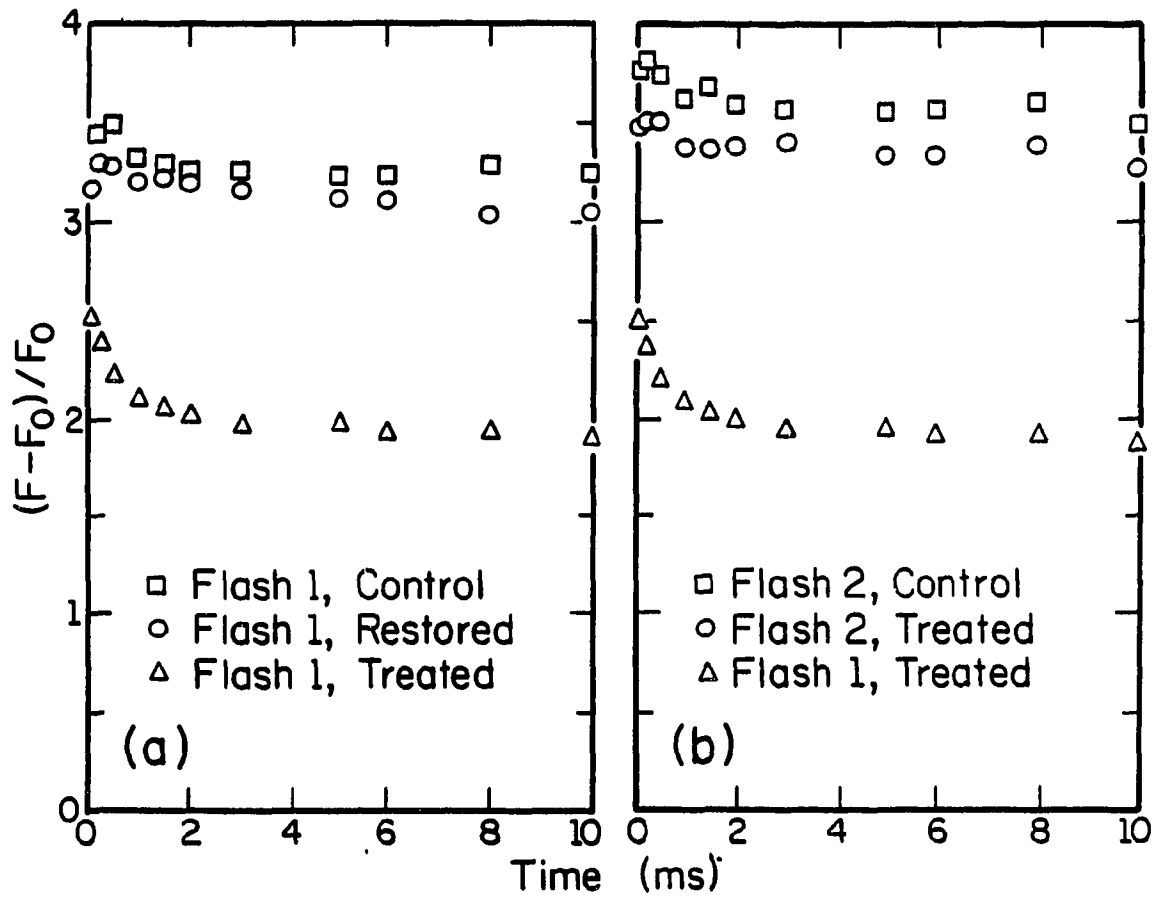
were 5.2 s for the treated membranes and 1.3 s for both restored and control membranes at pH 6.5. However, at pH 7.5 the back reaction has a half-time of 2.9 s in the treated membranes, 2.3 s for the restored membranes and 2.0 s for the control.

Extending the data of Fig. 27, the pH effect has been investigated across the pH range from pH 6.0 to pH 8.0 in Fig. 28. The plot of the reciprocal  $t_{1/2}$  against pH shows good agreement with that obtained in untreated pea thylakoids [34]. The  $t_{1/2}$  at pH 6.0 for the restored and control membranes (1.5 s) as compared to the  $t_{1/2}$  at pH 6.25 (1.2 s) is the only exception to this

From pH 6.0 to pH 6.75 the  $t_{1/2}$  in the treated membranes remains pH independent in agreement with the result obtained for the oxidation of  $Q_A^-$  after a single flash in the absence of DCMU in Fig. 26(a). The transition observed for the treated membranes between pH 6.75 and pH 7.0 in the latter case correlates with the onset of the pH dependent portion in the data for treated membranes here. The agreement of the treated and restored data at pH 7.75 and the slight deviation from the control curve at this point probably reflect the low pH treatment relative to the control treatment to achieve the  $HCO_3^-$ -reversible inhibition.

The explanation for the omission of a data point for the treated case at pH 8.0 in Fig. 28 is provided by Figs. 29(a) and (b). At pH 8.0 the treated membranes exhibit a rapid oxidation of  $Q_A^-$  with a  $t_{1/2}$  of less than 100  $\mu$ s which cannot be resolved with our instrumentation. Figure 29(a) shows that this can be reversed by the prior addition of  $HCO_3^-$ , and Fig. 29(b) demonstrates that this phenomenon is not seen when a second flash is given, in this instance, 1 s after the preceding flash. This pH 8.0 phenomenon also correlates with the second transition in Fig. 26(a) for the forward reaction in treated membranes.

Figure 29. Decay of variable Chl a fluorescence at pH 8.0 in the presence of 5  $\mu$ M DCMU. Other details are as in Fig. 27. In (a) the decay after a single flash is shown for treated, restored and control membranes. In (b) the decay after a single flash and after two actinic flashes, spaced at 1 s, is shown for treated membranes. The decay for a control sample after flash 2 is also shown.



## D. Discussion

### 1. $\text{HCO}_3^-$ -reversible Changes in Thermodynamic and Kinetic Parameters of the Two-electron Gate

Since the original discovery in 1975 [36] that the  $\text{HCO}_3^-$ -effect regulated the electron flow on the acceptor side of PS II our understanding of the problem has been advanced by timely developments in other areas of PS II research. The most noteworthy example of this has been the characterization of the two-electron gate in PS II by Velthuys and Amesz [7] and Velthuys [8], which led to the proposal that  $\text{HCO}_3^-$  action was involved in the protonation steps associated with the reduction of plastoquinone at the  $Q_B$ -site [24,37].

A separate hypothesis for the  $\text{HCO}_3^-$ -effect suggests a conformational role for the anion bound to the PS II acceptor side with the bound anion facilitating the electron transfer between  $Q_A$  and  $Q_B$  [38]. Further support for this idea has been provided by the observation of a ten-fold increase in the light-induced EPR (electron paramagnetic resonance) signal at  $g = 1.82$  attributed to the  $Q_A^- \cdot \text{Fe}^{2+}$  complex in PS II-enriched thylakoid membrane fragments or PS II particles [39]. The data from Fig. 26(a) provide additional evidence for a conformational change, in this case, associated with  $K_0$  for plastoquinone binding at the  $Q_B$ -site (see Fig. 3, Chapter I).

$$K_0 = [Q_A Q_B] / ([Q_A] \cdot [PQ_{(\text{pool})}]) \quad (1)$$

In equation (1) above,  $[Q_A Q_B] + [Q_A] = [\text{PS II}]$ . The concentration of PS II can be estimated from the ratio of non-chlorophyll lipids to Chl and the ratio of Chl molecules to PS II. This gives an approximate value of 0.7 mM [31]. The concentration of the PQ (plastoquinone) pool in the membrane has been estimated to be approximately 5 mM from the

ratio of PQ to PS II as determined by the area over the Chl a fluorescence transient from thylakoids inhibited with DCMU to the area with thylakoids inhibited with  $\text{Hg}^{2+}$  and  $\text{CN}^-$  [31,40]. As noted earlier, a measure of centers existing as  $\text{Q}_A\text{Q}_B$  is given by the amplitude of the initial linear component arising from semi-logarithmic plots of the data in Figs. 22 and 26(a) [24]. Values for  $K_0$  estimated from the data here are given in Table 4. Above pH 6.5 the control and restored data yield a value for  $K_0$  of  $420 \text{ M}^{-1}$  which compares with  $500 \text{ M}^{-1}$  obtained in unincubated pea thylakoids [24]. Below pH 6.5  $K_0$  is decreased to  $240 \text{ M}^{-1}$ . In contrast,  $K_0$  for the treated membranes exhibits a dependence on pH and ranges from  $60 \text{ M}^{-1}$  at pH 6.0 to  $350 \text{ M}^{-1}$  at pH 7.75. An increase in  $K_0$  following  $\text{HCO}_3^-$ -depletion or anion inhibition was anticipated since this treatment has been observed to produce a three-fold increase in the binding constant of the triazine herbicide, atrazine and the phenolic herbicide, ioxynil [19,20]. Both these herbicides have also been shown to display competitive characteristics with quinone binding at the  $\text{Q}_B$ -site [41].

Renger et al. [42] have suggested that electron transport between  $\text{Q}_A$  and  $\text{Q}_B$  proceeds through a channel established by a specific arrangement of functional amino acid residues in the quinone acceptor complex. It is therefore possible that the conformational change, indicated here by our data for  $K_0$ , may disrupt such a channel. The data also indicate that the inhibitory treatment introduces a change in the first order rate constant for electron transfer between  $\text{Q}_A$  and  $\text{Q}_B$  which is seen as an increase in  $t_{1/2}$  accompanying the decrease in  $K_0$  as the pH is lowered (see also Table 2).

TABLE 4

THE EFFECT OF  $\text{HCO}_3^-$ -DEPLETION OR ANION INHIBITION ON  $K_0$ ,  $K_{\text{app}}$  AND THE OPERATING REDOX POTENTIAL OF THE  $Q_B/Q_B^-$  COUPLE

The effect of  $\text{HCO}_3^-$  depletion or anion inhibition on  $K_0$ , the association constant for  $Q_B$ ,  $K_{\text{app}}$ , the apparent equilibrium constant for the sharing of an electron between  $Q_A$  and  $Q_B$ , and  $E_m$ , the operating redox potential of the  $Q_B/Q_B^-$  couple. T represents treated membranes, R represents restored membranes and C represents control membranes. The data are tabulated as a function of pH.

pH	$K_0 \text{ M}^{-1}$			$K_{\text{app}}$			$E_m \text{ } Q_B/Q_B^- \text{ mV}$		
	T	R	C	T	R	C	T	R	C
6.00	60	240	240	16	63	62	-60	-25	-25
6.50	80	420	420	17	69	69	-58	-23	-23
7.00	180	420	420	11	29	35	-70	-44	-40
7.50	230	420	420	12	14	19	-67	-63	-55
7.75	350	420	420	10	10	12	-72	-72	-67

The equilibrium constant for sharing an electron between  $Q_A$  and  $Q_B$  is given by equation (2) ([24] and see Fig. 3, Chapter I).

$$K_{app} = \frac{[Q_A Q_B^-] + [Q_A Q_B^-(H^+)]}{[Q_A^-] + [Q_A^- Q_B]} \quad (2)$$

$K_{app}$  can be measured from the ratio of the half-times for the back reaction with  $S_2$  in uninhibited compared to DCMU-inhibited centers [31]. Chlorophyll *a* fluorescence measurements to determine the back reaction in uninhibited centers requires quantitation of the characteristic flash pattern observed due to the differential kinetics of  $Q_A^-$  oxidation by either  $Q_B$  or  $Q_B^-$  [31]. This approach is not possible here since the treated membranes exhibit an extremely distorted flash pattern and the restored and control cases exhibit a damped oscillation due to the necessary incubation involved in these experiments (Chapter III). However, the back reaction in the presence of DCMU can be measured in this system and the results are presented in Fig. 28.

Vermaas *et al.* [43] have shown that the back reaction in the absence of DCMU at pH 6.0 is of the order of 100 s and insensitive to  $HCO_3^-$ -depletion or an anion inhibitory treatment. This was achieved by monitoring the decay of  $S_2$  with a Joliot type oxygen electrode [43,44]. This value for the uninhibited back reaction and the data in Fig. 28 allow us to calculate a value for  $K_{app}$  of 16 in the treated membranes and 63 in the restored and control samples. Robinson and Crofts [34] obtained a value of approximately 61 for  $K_{app}$  at pH 6.0 in unincubated pea thylakoids. Our data therefore indicate that the equilibrium for

the sharing of an electron between  $Q_A$  and  $Q_B$  experiences a four-fold shift toward  $Q_A^-$  at pH 6.0. This value is a factor of two larger than reported by Vermaas *et al.* [43].

If we assume that the uninhibited back reaction is unaffected by  $HCO_3^-$ -depletion/anion inhibition between pH 6.0 and pH 7.75, then at pH 7.75 the data in Fig. 28 and Ref. [34] give a value of 10 for  $K_{app}$  in both treated and restored membranes and a value of 12 in the control. Robinson and Crofts [34] obtained a value of 8 in their unincubated pea thylakoids. Since the midpoint potential of the  $Q_A/Q_A^-$  couple is unaffected by  $HCO_3^-$ -depletion [38], it is possible to calculate the operational redox potential for the  $Q_B/Q_B^-$  couple. Using the value of -130 mV (see [46]) for the working potential of  $Q_A/Q_A^-$  our data give a value of -25 mV for the  $Q_B/Q_B^-$  couple at pH 6.0 in restored and control membranes and -60 mV in the treated membranes. At pH 7.75 the corresponding values are -72 mV for restored and treated membranes and -67 mV in the control. These results are summarized in Table 4. The corresponding values from unincubated pea thylakoids in Ref. [34] were -25 mV at pH 6.0 and -77 mV at pH 7.75. There is therefore good agreement between our restored and control data and that obtained in pea thylakoids with the operating redox potential of the  $Q_B/Q_B^-$  couple depending upon the protonation at the  $Q_B$  site. In contrast, the operating redox potential of the  $Q_B/Q_B^-$  couple in the treated membranes demonstrates a very limited dependence on pH. This would appear to be due to the pH-dependent decrease of  $K_0$ .

Figure 26(b) presents the effect of  $HCO_3^-$ -depletion or anion inhibition on the reduction of  $Q_B^-$  to  $Q_BH_2$ , following a second actinic flash, as a function of pH. The values in Table 4 allow us to estimate the redox midpoint potential for the  $Q_B^-/Q_B^{2-}$  couple, although the values

obtained depend upon the value chosen for the midpoint potential of the plastoquinone pool. Taking a value of 110 mV, varying by -60 mv/pH for the PQ/PQH<sub>2</sub> couple [24] and assuming no HCO<sub>3</sub><sup>-</sup> effect on this value, a calculated value of approximately 200 mV is obtained for the Q<sub>B</sub><sup>-</sup>/Q<sub>B</sub><sup>2-</sup> couple in control, restored or treated membranes at pH 7.75. At pH 6.0 an estimated value of 365 mV is obtained in the restored and control and 400 mV in the treated case. It is concluded, therefore, that there is little effect on this couple in treated membranes. Following Ref. [24], it was also possible to estimate an equilibrium constant for the Q<sub>A</sub><sup>-</sup>Q<sub>B</sub><sup>-</sup> ⇌ Q<sub>A</sub>Q<sub>B</sub><sup>2-</sup> reaction. As noted in Ref. [15], the calculated values will depend on the pH, and on the protonation state of the couples, but even at pH 7.75 the equilibrium constant is of the order of 10<sup>5</sup> in the treated, control and restored membranes. Therefore there does not appear to be an appreciable effect of HCO<sub>3</sub><sup>-</sup>-depletion or anion inhibition of this parameter.

In addition, it is also possible to calculate the stability constant (K<sub>S</sub>) for the bound semiquinone at the Q<sub>B</sub>-site following a single flash using the relationship  $E_m(Q_B/Q_B^-) - E_m(Q_B^-/Q_B^{2-}) = 60 \log K_S$ . The data in Table 4 and the above calculated values give a K<sub>S</sub> at pH 6.0 of 2.15 x 10<sup>-7</sup> for control and restored membranes and 1.40 x 10<sup>-8</sup> for treated membranes; and at pH 7.75: 3.06 x 10<sup>-5</sup> for control membranes and 2.07 x 10<sup>-5</sup> for restored and treated membranes. These values are to be compared with K<sub>S</sub> of approximately 10<sup>-10</sup> estimated for the stability constant of semiquinone free in the membrane [46]. At pH 7.75, we see no appreciable difference on K<sub>S</sub> in treated or control and restored membranes, but a ten-fold decrease in the stability constant is evident in treated membranes at pH 6.0. However, these values suggest that Q<sub>B</sub><sup>-</sup> is

thermodynamically unstable in control, restored and treated membranes. This indicates that the characteristic long lifetime of the bound  $Q_B^-$  arises from kinetic stability (see [11]).

The data of Figs. 25, 26(b), 27 and 28 suggest a decrease in the kinetic stability of  $Q_B^-$  in treated membranes. The semi-logarithmic plots of Fig. 25 at pH 6.5 and pH 7.5 yield two linear components for the treated membranes. The initial linear component at pH 6.5 was found to have a  $t_{1/2}$  of 665  $\mu$ s and an amplitude of 21%. At pH 7.5 the initial component had a  $t_{1/2}$  of 464  $\mu$ s and an amplitude of 37%. The corresponding values for treated membranes after a single flash in Fig. 24 are at pH 6.5: 550  $\mu$ s and 30%, and at pH 7.75: 460  $\mu$ s and 54%. Therefore, the half-times at each pH appear to represent the same process, and the ratio of the pH 7.5 to pH 6.5 amplitudes for the initial linear components in both Figs. 24 and 25 are 1.8. In addition, the pH dependence for the overall half-time for  $Q_A^-$  oxidation following two actinic flashes in Fig. 26(b) is identical to that observed for  $K_O$ . It therefore appears that the initial linear component after two actinic flashes does reflect centers undergoing electron transfer between  $Q_A^-$  and  $Q_B^-$  rather than  $Q_A^-$  and  $Q_B^-$ . Furthermore, the removal of  $Q_B^-$  cannot be explained by an increased fraction of centers undergoing a back reaction with  $S_2$  since  $Q_A^-$  oxidation in treated membranes reaches the level seen in control membranes in approximately 100 ms. However, Figs. 27 and 28 clearly show that the back reaction from  $Q_A^-$  with  $S_2$  is slowed from 1.25 s to approximately 5 s at acid pH.

The amplitude of centers undergoing a first order reaction between  $Q_A^-$  and  $Q_B^-$  is approximately 70% in control and restored membranes between pH 6.25 and pH 7.5 (Figs. 25 and 26(b)) At pH 7.5 the association constant,  $K_O$ , in treated membranes approaches that observed in the

restored and control membranes (Table 4). Therefore, the introduction of a 37% amplitude for a process characteristic of  $Q_A^-$  being oxidized by  $Q_B$  after the second actinic flash suggests that the apparent kinetic stability of  $Q_B^-$  in the control and restored membranes has been significantly reduced. This result in fact implies that half of the  $Q_B^-$  present in the control and restored membranes has been lost over a time period of 1 s.

Additional experimental evidence is available to support this conclusion. Velthuys and Amesz [7] have shown that the redox state of  $Q_B$  can be monitored by measuring the fluorescence rise induced by the addition of DCMU. The period-of-two oscillation observed in normal thylakoids is diagnostic of the operation of the two-electron gate (see review in Ref. [47]). This experiment has been performed on  $HCO_3^-$ -depleted or anion inhibited membranes with the result that the period-of-two oscillation was not observed [13,48]. The conclusion from these experiments is that the two-electron gate mechanism is impaired in treated membranes. However, in both reports the DCMU-inducible fluorescence following a single actinic flash is substantially reduced with respect to restored and control samples. The reduction was found to be between 30-50% suggesting that between 30-50% of the  $Q_B^-$  present in the control had been lost. The DCMU in these studies was injected approximately 2 s after the actinic flash in the presence of hydroxylamine to prevent any back reaction with the donor side. Therefore, the oxidation of  $Q_B^-$  on the time scale of 1 or 2 s observed in these experiments is possibly due to a decrease in the kinetic stability of  $Q_B^-$  in these centers. Such a decrease in the kinetic stability of  $Q_B^-$  may also explain why the shift in the equilibrium constant for the sharing of an

electron between  $Q_A$  and  $Q_B$  is not particularly evident in Fig. 22(a).

An apparent contradiction is raised by this interpretation. Vermaas et al. [43] reported that the back reaction of  $Q_B^-$  with  $S_2$  was unaffected in treated membranes. Thus, a decrease in the kinetic stability of  $Q_B^-$  would be reflected in the amplitude of centers undergoing a back reaction with  $S_2$ . Vermaas et al. detected the decay of  $S_2$  to be biphasic with a fraction of centers undergoing a fairly rapid reduction of  $S_2$ . Between 20 and 25% of  $S_2$  decayed with a half-time of approximately 1.5 s. This fast phase is completely abolished in the absence of  $HCO_3^-$  but is restored upon addition of 5 mM  $HCO_3^-$  [43]. Vermaas et al. suggested that the plastoquinol-like thylakoid component which gives rise to EPR signal  $II_G$  [49] may be responsible for the fast phase in the reduction of  $S_2$  [43]. Our data would be consistent with the interpretation that this fast phase represents a fraction of centers with a relatively fast back reaction of  $Q_B^-$  with  $S_2$ . In treated membranes the kinetic stability of these centers is possibly so altered that  $Q_B^-$  is oxidized via a separate mechanism not associated with  $S_2$ .

The discussion so far has assumed that the truncated initial linear component in treated membranes represents a decrease in the fraction of centers having  $Q_B$  bound before the first actinic flash (see Tables 2 and 4). A second plausible explanation exists. The mechanism of electron transfer from  $Q_A^-$  to  $Q_B$  is thought to involve the association of a proton with  $Q_B^-$  (see  $K_3$  in Fig. 3, Chapter I). The pK for this protonation has been estimated to be 7.9 in control membranes [34].

It is apparent from Tables 2 and 4 and Figs. 14, 22 and 24, that the treated membranes tend to behave in a similar fashion to that of the unprotonated control at alkaline pH. However, the  $t_{1/2}$  of the treated membranes at pH 7.75 and pH 8.00 may also contain a contribution from

the rapid component ( $t_{1/2} < 100 \mu\text{s}$ ) detected in the presence of DCMU after a single flash in treated samples (Fig. 29). Evidence in support of this interpretation is found in Table 3. The initial linear component shown for treated membranes in this Table is suggested to represent centers where  $Q_A^-$  is being oxidized by  $Q_B$  after a second flash. This is thought to arise as a consequence of a decreased kinetic stability of  $Q_B^-$  in treated samples. The  $t_{1/2}$  for this initial component remains in the region of  $500 \mu\text{s}$  between pH 7.5 and pH 8.0. This compares with a half-time of  $200 \mu\text{s}$  for the treated case at pH 8.0 in Table 2. This is consistent with the result in Fig. 29 which demonstrated that the additional fast DCMU insensitive component of  $Q_A^-$  oxidation is only seen following the first actinic flash.

Despite this criticism the explanation that the truncated initial linear component of  $Q_A^-$  oxidation in treated membranes reflects an effect on  $K_3$  rather than  $K_0$  is quite successful at explaining the results obtained in this chapter. The pH dependent operating redox potential for the  $Q_B/Q_B^-$  couple is entirely consistent with protons being unable to participate in the protonation of  $Q_B^-$  after the first actinic flash. The observed shift in the  $Q_A^-Q_B \rightleftharpoons Q_AQ_B^-$  equilibrium at pH 6.0 is again consistent with an altered  $K_3$  as is the apparent decrease in the kinetic stability of  $Q_B^-$ . Furthermore, since the amplitude of the initial linear component is reduced as the pH is reduced (see Table 2), this interpretation also suggests that the site of protonation associated with  $Q_B^-$  is not readily accessible to the bulk phase. This is consistent with the assignment of some of the very slow components associated with  $Q_A^-$  oxidation in Chapter III (i.e., those in the 0.1-1 s range) to very slow rates of protonation.

## 2. $\text{HCO}_3^-$ and the $\text{Fe}^{2+}/\text{Fe}^{3+}$ Couple

The  $\text{HCO}_3^-$ -reversible inhibition in treated membranes in the presence of DCMU seen in Fig. 28 is probably a consequence of interactions between  $\text{Q}_\text{A}^-$  and the  $\text{Fe}^{2+}/\text{Fe}^{3+}$  couple. There are several lines of evidence to support this:

(a) The iron in the reaction center of Rps. viridis is liganded to 4 histidines and to a glutamate. In PS II the glutamate is not present on D2 and  $\text{HCO}_3^-$  has been suggested to serve as the ligand in its place [50]. In addition, no  $\text{HCO}_3^-$ -reversible anionic inhibition was observed on quinone mediated electron transfer in Rps. rubrum reaction center preparations [51].

(b) In PS II particles prepared from spinach, the  $\text{Q}_\text{A}^-$ - $\text{Fe}^{2+}$  EPR signal at  $g = 1.82$  increased ten to twelve-fold upon  $\text{HCO}_3^-$  removal in the presence of formate. No such effect was observed in chromatophores from Rps. rubrum [39,52,53].

(c) The redox midpoint potential of the  $\text{Q}_\text{A}^-/\text{Q}_\text{A}$  couple is unaffected by  $\text{HCO}_3^-$ -depletion [38].

(d) The  $\text{Fe}^{2+}/\text{Fe}^{3+}$  couple has been identified as the  $\text{Q}_{400}/\text{Q}_{400}^+$  couple by Petrouleas and Diner [54]. Oxidation of this couple by exogenous oxidants in the presence of DCMU is dependent on a strict order of addition. Addition of DCMU prior to the exogenous oxidant prevents  $\text{Fe}^{2+}$  or  $\text{Q}_{400}$  oxidation [54-56]. Reversal of the inhibition seen by  $\text{HCO}_3^-$ -depletion in the presence of formate is only possible in Fig. 28 when  $\text{HCO}_3^-$  is added before the DCMU (see also [57]).

(e) Electron transfer between  $\text{Q}_\text{A}^-$  and  $\text{Q}_{400}^+$  is inhibited when formate is present following  $\text{HCO}_3^-$ -depletion [58]. On the other hand, if formate is washed out, electron transfer between  $\text{Q}_\text{A}^-$  and  $\text{Q}_{400}^+$  is restored

[59], although linear electron transport remains inhibited approximately two-fold when excess formate is removed until  $\text{HCO}_3^-$  readdition [60,61].

The  $\text{Fe}^{2+}/\text{Fe}^{3+}$  couple has an  $E_{m,7}$  of 400 mV varying by approximately -60 mV per pH unit [54]. The observed effect of pH in the treated membranes in Fig. 28 may therefore result from the interaction of  $\text{Q}_A^-$  with iron changing as the midpoint for the  $\text{Fe}^{2+}/\text{Fe}^{3+}$  couple becomes more reducing. Furthermore, Petrouleas and Diner [54] found that oxidation of  $\text{Fe}^{2+}$  to  $\text{Fe}^{3+}$  occurred, particularly at high pH, and they concluded that electron transfer from  $\text{Q}_A^-$  to  $\text{Fe}^{3+}$  probably occurs in PS II. It is therefore plausible to suggest that the rapid oxidation of  $\text{Q}_A^-$  shown in Fig. 29 is by this route. Fig. 29(b) demonstrates that this phenomenon is only observed after a single actinic flash, and attempts to influence the amplitude of the process by resetting the S-states with 30  $\mu\text{M}$  hydroxylamine had no effect (data not shown).

Interaction between  $\text{Q}_A^-$  and the  $\text{Fe}^{2+}/\text{Fe}^{3+}$  couple may also account for the staggered curves observed in Fig. 26(a). The transition between pH 6.75 and pH 7.0 in the treated membranes correlates with the onset of the pH dependent portion of the curve in the treated membranes in Fig. 28 which are undergoing a back reaction with  $\text{S}_2$ . It is possible that the state of protonation in the  $\text{Q}_A^-$ -iron domain, which is responsible for the pH dependent midpoint potential of the  $\text{Fe}^{2+}/\text{Fe}^{3+}$  couple, may cause a conformational change so as to alter the interaction between  $\text{Q}_A^-$  and iron as the pH is increased. This may explain the fact that at pH 6.0, in both restored and control membranes, the half-time for  $\text{Q}_A^-$  oxidation is slowed for both the forward and back reaction with respect to the rates at pH 6.5. This phenomenon would appear shifted approximately 0.5 pH units in a basic direction in treated membranes (Figs. 26(a) and 28).

## E. Summary and Conclusions

Our findings here demonstrate that: (1) the operating redox potential of the  $Q_B/Q_B^-$  couple is pH independent following  $HCO_3^-$ -depletion in the presence of inhibitory anions; (2) the apparent kinetic stability of  $Q_B^-$  appears to be significantly reduced in treated membranes; (3) the equilibrium for the sharing of an electron between  $Q_A$  and  $Q_B$  is decreased by a factor of 4 at pH 6.0 in treated membranes and (4) the oxidation of  $Q_A^-$  in the presence of DCMU shows a rapid ( $t_{1/2} < 100 \mu s$ ),  $HCO_3^-$  sensitive oxidation in approximately 50% of the centers following a single actinic flash. The oxidant is not known, but  $Fe^{3+}$  is suggested as a candidate.

These results are consistent with  $HCO_3^-$ -depletion or anion inhibition causing a major conformational change in the quinone acceptor complex and/or decreasing  $K_3$ , the equilibrium constant for a proton in association with  $Q_B^-$ . Following [50] and as suggested previously [28], these results are interpreted as implicating  $HCO_3^-$  as a ligand to  $Fe^{2+}$  in the PS II reaction center. The pH dependence for a number of the parameters and rate constants studied here in treated membranes may reflect the pH dependence observed for the  $Fe^{2+}/Fe^{3+}$  couple.

Points (1) through (4) above do not readily explain the rate-limiting step observed in steady-state oxygen electrode measurements on treated membranes. After a single actinic flash the half-time for  $Q_A^-$  oxidation is extended from 547  $\mu s$  to 2.8 ms at pH 6.5 in treated membranes (Fig. 22). After a second actinic flash at pH 6.5, the half-time for  $Q_A^-$  oxidation is extended from 600  $\mu s$  to 11 ms (Fig. 23). A difficulty arises, however, since we have estimated that the rate-limiting step in treated membranes, as seen for the Hill reaction, is of the

order of 45 ms per electron at pH 6.5 (Chapter II). In addition, we have shown that the kinetics of  $Q_A^-$  oxidation in treated membranes depend on the actinic flash number, the actinic flash frequency and the pH (Chapter III). The pH dependence in treated membranes is such that the kinetics of  $Q_A^-$  oxidation, after one or two actinic flashes, are accelerated when the pH is increased. This dependence is then reversed after four actinic flashes. That is, after two turnovers of the reaction center the rate of  $Q_A^-$  oxidation becomes sensitive to the bulk pH and is slowed at alkaline pH.

It is possible to reconcile these data by proposing the existence of two  $HCO_3^-$  binding sites (see Chapter V). The first is a ligand to  $Fe^{2+}$  and is characterized by a dissociation constant of approximately 80  $\mu M$  [61,62]. The second  $HCO_3^-$  is involved in protonation reactions and is bound very tightly such that even after extensive  $HCO_3^-$ -depletion procedures in the presence of inhibitory anions, a bound  $HCO_3^-$  may still remain. A role for  $HCO_3^-$  in protonation reactions was first suggested by Good [63], and we have previously advocated such a role in the reactions of the two-electron gate [29,37]. Shipman [64] has proposed that an arginine residue is the most probable ligand for  $HCO_3^-$ . The hydroxyl moiety of the bound  $HCO_3^-$  is envisaged as a proton donor, and at least two independent models are in development incorporating a bound  $HCO_3^-$  acting as a proton donor at the  $Q_B$  site [65,66]. Stemler and Murphy ([67] and see also [68]) found evidence for two  $HCO_3^-$  binding sites from competitive binding studies between atrazine and  $HCO_3^-$ . These workers concluded that both sites had a dissociation constant of the order of 80  $\mu M$ . The interpretation here would suggest that the tight binding site associated with protonation would have been missed by this study since these workers were looking at a concentration range

above  $50 \mu\text{M H}^{14}\text{CO}_3^-$ . However, the interpretation that  $\text{HCO}_3^-$  depletion affects  $K_3$  allows for the results in this thesis to be explained by a single  $\text{HCO}_3^-$  binding site (see Chapter V).

The results of the study presented in this chapter suggest that  $\text{HCO}_3^-$  is not involved with the protonation of  $\text{Q}_B^{2-}(\text{H}^+)$  since the calculated values for the redox potential of the  $\text{Q}_B^-/\text{Q}_B^{2-}$  couple and the equilibrium constant for the oxidation of  $\text{Q}_A^-$  by  $\text{Q}_B^-$  did not show any significant change in the treated membranes. It is concluded therefore that  $\text{HCO}_3^-$  may be involved in the mechanism of  $\text{Q}_B^-$  protonation.

However, when  $\text{HCO}_3^-$  is removed and no formate nor other inhibitory anion is present, the Hill reaction is inhibited only two-fold (Fig. 28 and Chapter II). This suggests that if an inhibitory anion is not bound to the  $\text{HCO}_3^-$  binding site(s), protonation from other sources is more efficient. This implies that any role for  $\text{HCO}_3^-$  in the protonation steps associated with  $\text{Q}_B$  reduction is purely catalytic. Such a suggestion has also been put forward by Stemler [68] and Jursinic and Stemler [60] by drawing an analogy with the participation of  $\text{HCO}_3^-$  in protonation reactions associated with the activity of carbonic anhydrase (see also [69]). Interestingly, the dissociation constant associated with restoring maximal activity of both the Hill reaction and normal rates of  $\text{Q}_A^-$  oxidation was found to be between  $70\text{-}100 \mu\text{M HCO}_3^-$  in the absence of any inhibitory anions [60,61].

The binding of  $\text{HCO}_3^-$  to PS II, however, does appear to have physiological significance beyond a possible catalytic role in the protonation reactions. Figure 13 in Chapter II clearly demonstrates that an irreversible loss of activity is associated with  $\text{HCO}_3^-$ -depletion in the absence of inhibitory anions. With respect to this observation, Pet-

rouleas and Diner [54] detected irreversible changes in the PS II preparations accompanying the oxidation of  $\text{Fe}^{2+}$  to  $\text{Fe}^{3+}$ . The possibility that  $\text{HCO}_3^-$  may in fact be a ligand to  $\text{Fe}^{2+}$  would support the interpretation that the inhibition seen in Chapter II, Fig. 13 is in fact due to irreversible changes associated with the formation of  $\text{Fe}^{3+}$ .

#### References

1. Deisenhofer, J., Epp, O., Miki, K., Huber, R. and Michel, H. (1984) *J. Mol. Biol.* 180, 385-398
2. Michel, H. and Deisenhofer, J. (1986) in *Encyclopedia of Plant Physiology* (Staehelein, A.C. and Arntzen, C.J., eds.), New Series, Vol. 19, pp 371-381, Springer-Verlag, Berlin
3. Deisenhofer, J., Epp, O., Miki, K., Huber, K. and Michel, H. (1985) *Nature* 318, 618-623
4. Trebst, A. and Draber, W. (1986) *Photosynthesis Res.* 10, 381-392
5. Nanba, D. and Satoh, K. (1987) *Proc. Natl. Acad. Sci USA* 84, 109-112
6. Bouges-Bocquet, B. (1973) *Biochim. Biophys. Acta* 314, 250-256
7. Velthuys, B.R. and Amesz, J. (1974) *Biochim Biophys. Acta* 333, 85-94
8. Velthuys, B.R. (1981) *FEBS Lett.* 126, 277-281
9. Wraight, C.A. (1981) *Israel J. Chem.* 21, 348-354
10. van Rensen, J.J.S. (1982) *Physiol. Plant.* 54, 515-521
11. Crofts, A R. and Wraight, C.A. (1983) *Biochim. Biophys. Acta* 726, 149-185
12. Kyle, D.J. (1985) *Photochem. Photobiol.* 41, 107-116
13. Govindjee, Pulles, M.P.J., Govindjee, R., van Gorkom, J.H. and Duysens, L.M.N. (1976) *Biochim. Biophys. Acta* 449, 602-605

14. Jursinic, P., Warden, J. and Govindjee (1976) *Biochim. Biophys. Acta* 440, 322-330
15. Jursinic, P. and Stemler, A. (1982) *Biochim. Biophys. Acta* 681, 419-428
16. Robinson, H.H., Eaton-Rye, J.J., van Rensen, J.J.S. and Govindjee (1984) *Z. Naturforsch.* 39C, 382-385
17. Jursinic, P. and Stemler, A. (1987) *Photosynthesis Res.*, in the press
18. Govindjee, Nakatani, H.Y., Rutherford, A W. and Inoue, Y. (1984) *Biochim. Biophys. Acta* 766, 416-423
19. Khanna, R., Pfister, K., Keresztes, A., van Rensen, J J.S. and Govindjee (1981) *Biochim. Biophys. Acta* 681, 419-428
20. Vermaas, W.F.J., van Rensen, J.J.S. and Govindjee (1982) *Biochim. Biophys. Acta* 681, 242-247
21. Eaton-Rye, J.J. and Govindjee (1987) in *Progress in Photosynthesis Research* (Biggins, J., ed.), Vol. II, pp. 433-436, Martinus Nijhoff, Dordrecht
22. Vermaas, W.F.J. and Govindjee (1981) *Photochem. Photobiol.* 34, 775-793
23. Cramer, W.A. and Crofts, A.R. (1982) in *Photosynthesis: Energy Conversion by Plants and Bacteria* (Govindjee, ed.), Vol. I, pp. 387-467, Academic Press, New York
24. Crofts, A.R., Robinson, H.H. and Snozzi, M. (1983) in *Advances in Photosynthesis Research* (Sybesma, C., ed.), Vol. I, pp. 461-468, Martinus Nijhoff/Dr. W. Junk Publishers, The Hague
25. Govindjee and van Rensen, J.J.S. (1978) *Biochim. Biophys. Acta* 505, 183-213
26. Vermaas, W.F.J. and Govindjee (1981) *Proc. Indian Natl. Sci. Acad.*

B47, 581-605

27. van Rensen, J.J.S. and Snel, J.F.H. (1985) *Photosynthesis Res.* 6, 231-246
28. Eaton-Rye, J.J., Blubaugh, D.J. and Govindjee (1986) in *Ion Interactions in Energy Transfer Biomembranes* (Papageorgiou, G.C., Barber, J. and Papa, S., eds.), pp. 263-278, Plenum Publishing Corporation, New York
29. Govindjee and Eaton-Rye, J.J. (1986) *Photosynthesis Res.* 10, 365-379
30. Joliot, A. (1974) in *Proceedings of the Third International Congress on Photosynthesis* (Avron, M., ed.), Vol. I, pp. 315-322, Elsevier, Amsterdam
31. Robinson, H.H. and Crofts, A.R. (1983) *FEBS Lett.* 153, 221-226
32. Robinson, H.H. and Crofts, A.R. (1987) in *Progress in Photosynthesis Research* (Biggins, J., ed.), Vol. II, pp. 429-432, Martinus Nijhoff, Dordrecht
33. Saygin, O., Gerken, S., Meyer, B. and Witt, H.T. (1986) *Photosynthesis Res.* 9, 71-78
34. Robinson, H.H. and Crofts, A.R. (1983) in *Advances in Photosynthesis Research* (Sybesma, C., ed.), Vol. I, pp. 477-480, Martinus Nijhoff/Dr. W Junk Publishers, The Hague
35. Wydrzynski, T.J. (1982) in *Photosynthesis: Energy Conversion by Plants and Bacteria* (Govindjee, ed.), Vol. I, pp. 469-506, Academic Press, New York
36. Wydrzynski, T. and Govindjee (1975) *Biochim. Biophys. Acta* 387, 403-408
37. Eaton-Rye, J.J. and Govindjee (1984) *Photobiochem. Photobiophys.* 8,

279-288

38. Vermaas, W.F.J. and Govindjee (1982) *Biochim. Biophys. Acta* 680, 202-209
39. Vermaas, W.F.J. and Rutherford, A.W. (1984) *FEBS Lett.* 175, 243-247
40. Yocum, C.F. and Guikema, J.A. (1977) *Plant Physiol.* 59, 33-37.
41. Vermaas, W.F.J. (1984) Ph.D. Thesis, Agricultural University, Wageningen, The Netherlands
42. Renger, G., Hagemann, R. and Dohnt, G. (1981) *Biochim. Biophys. Acta* 636, 17-26
43. Vermaas, W.F.J., Renger, G. and Dohnt, G. (1984) *Biochim. Biophys. Acta* 764, 194-202
44. Joliot, P. (1972) *Methods Enzymol.* 24, 123-134
45. Knaff, D.B. (1975) *FEBS Lett.* 60, 331-335
46. Mitchell, P. (1976) *J. Theor. Biol.* 62, 327-367
47. van Gorkom, H.J. (1986) in *Light Emission by Plants and Bacteria* (Govindjee, Ames, J. and Fork, D.C., eds.), pp. 267-289, Academic Press, Orlando
48. Stemler, A., Murphy, J. and Jursinic, P. (1984) *Photobiochem. Photobiophys.* 8, 289-304
49. Babcock, G.T. and Sauer, K. (1973) *Biochim. Biophys. Acta* 325, 483-503
50. Michel, H. and Deisenhofer J. (1987) in *Progress in Photosynthesis Research* (Biggins, J., ed.), Vol. I, pp. 353-362, Martinus Nijhoff, Dordrecht
51. Shopes, R.J., Blubaugh, D.J., Wraight, C.A. and Govindjee (1986) unpublished observations
52. Rutherford, A.W. (1987) in *Progress in Photosynthesis Research* (Biggins, J., ed.), Vol. I, pp. 277-283, Martinus Nijhoff, Dor-

drecht

53. Beijer, C. and Rutherford, A.W. (1987) *Biochim. Biophys. Acta*,  
submitted
54. Petrouleas, V. and Diner, B.A. (1986) *Biochim. Biophys. Acta* 849,  
264-275
55. Ikegami, I. and Katoh, S. (1973) *Plant Cell Physiol.* 14, 829-836
56. Wraight, C.A. (1985) *Biochim. Biophys. Acta* 809, 320-330
57. Blubaugh, D.J. and Govindjee (1984) *Z. Naturforsch* 39C, 378-381
58. Radmer, R. and Ollinger, O. (1980) *FEBS Lett.* 110, 57-61
59. Jursinic, P.A. and Stemler, A. (1984) *Biochim. Biophys. Acta*, 170-  
178
60. Jursinic, P.A. and Stemler, A. (1986) *Photochem. Photobiol.* 43,  
205-212
61. Snel, J.F.H. and van Rensen, J.J.S. (1984) *Plant Physiol.* 75, 146-  
150
62. Stemler, A. and Murphy, J.B. (1983) *Photochem. Photobiol.* 38, 701-  
707
63. Good, N.E. (1963) *Plant Physiol.* 38, 298-304
64. Shipman, L.L. (1981) *J. Theor. Biol.* 90, 123-148
65. Blubaugh, D.J. and Govindjee (1987) in preparation
66. Robinson, H.H. and Crofts, A.R. (1987) in preparation
67. Stemler, A. Murphy, J.B. (1984) *Plant Physiol.* 76, 179-182
68. Stemler, A. (1985) in *Inorganic Carbon Transport in Aquatic Photo-  
synthetic Organisms* (Berry, J. and Lucas, W., eds.), pp. 377-387,  
*American Society of Plant Physiologists*
69. Yeagle, P.L., Lochmuller, C.H. and Henkens, R.W. (1975) *Proc. Natl.  
Acad. Sci. USA* 72, 454-458

## V. SUMMARY AND FINAL CONCLUSIONS

The  $\text{HCO}_3^-$  anion regulates electron transfer through the plastoquinone acceptors ( $\text{Q}_A$  and  $\text{Q}_B$ ) of photosystem II (PS II). Depletion of  $\text{HCO}_3^-$  results in an approximately two-fold inhibition of electron transport rates supported by a Hill oxidant. In the presence of monovalent anions such as  $\text{HCO}_2^-$ ,  $\text{NO}_2^-$  or acetate,  $\text{HCO}_3^-$ -depletion can depress electron transport rates as much as ten-fold. The addition of  $\text{HCO}_3^-$  is able to restore electron transport rates to the level of non-depleted controls. An overview of the  $\text{HCO}_3^-$  effect is presented in Chapter I. The major conclusions of this thesis are listed in Table 5 along with the chapters, figures and tables where supporting evidence is presented. The major conclusions are also discussed in the following sections.

### A. The Site of Action of $\text{HCO}_3^-$ in Electron Transport

Contradictory conclusions to those outlined above were reported in the literature when methyl viologen was used as the Hill oxidant in measurements of linear electron transport. This reaction was found to exhibit only a two-fold  $\text{HCO}_3^-$  effect even in the presence of formate. In addition, partial reactions employing artificial electron donors to PS II, thereby bypassing the oxygen evolving complex (OEC), were found to be insensitive to  $\text{HCO}_3^-$ . This suggested a major site of  $\text{HCO}_3^-$  action on the OEC.

The initial objective of this thesis was to establish the major site of  $\text{HCO}_3^-$  action (Chapter II). A six to seven-fold stimulation of the  $\text{H}_2\text{O}$  to methyl viologen reaction was observed following the addition of  $\text{HCO}_3^-$  to samples depleted in the presence of either formate or nitrite. Artificial electron donors to PS II in such  $\text{HCO}_3^-$ -depleted

TABLE 5  
MAJOR CONCLUSIONS

<u>Conclusions</u>	<u>Location of Supporting Evidence</u>
1. There is no $\text{HCO}_3^-$ effect in the electron flow from duroquinol to methyl viologen, but there is a large effect in the electron flow from $\text{H}_2\text{O}$ to methyl viologen. Thus, $\text{HCO}_3^-$ affects electron transport at a site which precedes the step involving the reoxidation of plastoquinol.	Chapter II Fig. 8 Table 1
2. No conclusion could be made about the site of $\text{HCO}_3^-$ action from electron flow measurements from artificial electron donors to PS II. In control samples with artificial electron donors to PS II the electron transport rates to methyl viologen were not significantly different from the rates observed in $\text{HCO}_3^-$ -depleted samples for the $\text{H}_2\text{O}$ to methyl viologen reaction.	Chapter II Table 1
3. Measurements on Chl <u>a</u> fluorescence decays with hydroxylamine as the electron donor do show a site of $\text{HCO}_3^-$ action on the acceptor side of PS II.	Chapter II Fig. 9
4. Nitrite can easily substitute for formate in replacing $\text{HCO}_3^-$ from the membrane as demonstrated by the slowing of the decay of Chl <u>a</u> fluorescence and thus $\text{Q}_A^-$ oxidation.	Chapter II Figs. 10, 11
5. The dissociation constant for nitrite was found to be 5 mM.	Chapter II Fig. 11
6. A six-fold $\text{HCO}_3^-$ effect can	Chapter II

TABLE 5 (Continued)

<p>be observed on the half-time of <math>Q_A^-</math> reoxidation in the absence of formate or nitrite, and this compares to a &gt; thirty-fold effect in the presence of inhibitory anions.</p>	<p>Figs. 9, 10, 12</p>
<p>7. A <math>HCO_3^-</math> effect of approximately two-fold, instead of six to ten-fold, can be observed in the <math>H_2O</math> to methyl viologen reaction in the absence of formate or nitrite. However, removal of bound <math>HCO_3^-</math> in the absence of other anions causes irreversible inhibition of electron flow.</p>	<p>Chapter II Figs. 12, 13</p>
<p>8. The oxidation of <math>Q_A^-</math> by <math>Q_B</math> or <math>Q_B^-</math> following 1 or 2 actinic flashes respectively, exhibits a smaller overall half-time at pH 7.5 than at pH 6.5 in treated membranes.</p>	<p>Chapters III and IV Figs. 14, 15, 17, 18 22, 23, 24, 25, 26</p>
<p>9. The characteristic oscillations observed in the fluorescence flash pattern, generated by assaying the Chl <math>a</math> variable fluorescence at specific times after an actinic flash and plotting these data as a function of flash number, are entirely lost in treated membranes.</p>	<p>Chapter III Figs. 15, 16</p>
<p>10. The slowest oxidation of <math>Q_A^-</math>, as indicated by the overall half-time parameter, depends on both pH and flash number in treated membranes.</p>	<p>Chapter III Figs. 15, 16, 17, 18</p>
<p>11. The overall half-time parameter also depends on the actinic flash frequency in treated membranes.</p>	<p>Chapter III Figs. 19, 20, 21</p>
<p>12. The operating redox potential for the <math>Q_B/Q_B^-</math> couple</p>	<p>Chapter IV Table 4</p>

TABLE 5 (Continued)

- is not pH dependent in treated membranes.
13. The equilibrium for the sharing of an electron between  $Q_A$  and  $Q_B$  is decreased by a factor of 4 at pH 6.0 in treated membranes. Chapter IV  
Figs. 27, 28  
Table 4
  14. The back reaction between  $Q_A^-$  and the  $S_2$ -state of the OEC is inhibited approximately four-fold below pH 7.0 but is unaffected above pH 7.5 in the presence of DCMU in treated membranes. Chapter IV  
Figs. 27, 28
  15. A back reaction with a half-time of  $< 100 \mu s$  is present at pH 8.0 in the presence of DCMU in approximately half of the PS II centers in treated membranes. Chapter IV  
Fig. 29
  16. The kinetic stability of  $Q_B^-$  is reduced in treated membranes. Chapter IV  
Figs. 23, 25, 26
  17.  $HCO_3^-$  is a ligand to  $Fe^{2+}$  in the PS II reaction center. Chapter IV  
Figs. 27, 28, 29
  18. In treated membranes the rate-limiting step in electron flow is the protonation of  $Q_B^-$ . This suggests that the  $HCO_3^-$  anion participates in this protonation step. Chapters IV and V

membranes, and even in control samples, exhibited a rate-limiting step of donation on the order of the rate-limiting step due to  $\text{HCO}_3^-$ -depletion. No conclusion on the site of  $\text{HCO}_3^-$  action could, therefore, be inferred from such studies. However, the oxidation of the primary quinone acceptor ( $\text{Q}_A$ ) of PS II was dramatically inhibited in these artificial donor systems. Thus, the  $\text{HCO}_3^-$  effect on the electron acceptor side of PS II was confirmed.

The dibromothymoquinone-sensitive partial reaction, duroquinol to methyl viologen, was insensitive to  $\text{HCO}_3^-$ , thus firmly indicating that the site of  $\text{HCO}_3^-$  action is before the site of plastoquinol oxidation. This, taken together with other published results confirmed the notion that the site of  $\text{HCO}_3^-$  action is at the level of charge transfer through the quinone acceptors of PS II.

In the presence of both formate and nitrite a large and reversible  $\text{HCO}_3^-$  effect on  $\text{Q}_A^-$  oxidation was consistently observed. In addition,  $\text{Q}_A^-$  oxidation was inhibited, although to a much lesser degree, when inhibitory anions were omitted from the  $\text{HCO}_3^-$ -depletion system. Prolonged incubation, however, resulted in irreversible inhibition not observed when formate or nitrite were present. This result is presented in Chapter II.

#### **B. The Participation of $\text{HCO}_3^-$ in Electron Transfer Through the Two Electron Gate**

Two principal hypotheses exist to account for the action of  $\text{HCO}_3^-$  on PS II. These are: (1) that  $\text{HCO}_3^-$  is directly involved in the protonation reactions associated with plastoquinone reduction at the  $\text{Q}_B$ -site ( $\text{Q}_B$  is the secondary quinone acceptor of PS II) and (2) that  $\text{HCO}_3^-$  is required in maintaining the conformational integrity of PS II to allow

for efficient transfer of electrons through the quinone acceptor complex to the plastoquinone pool.

Experiments were performed (see Chapter III) to understand the effect of  $\text{HCO}_3^-$ -depletion on  $\text{Q}_\text{A}^-$  oxidation as a function of actinic flash number, actinic flash frequency and pH. This approach addressed the objective of developing an understanding of the mechanism of the  $\text{HCO}_3^-$  effect leading to an appreciation of its role in the reactions associated with the two-electron gate.

Some typical values for  $\text{Q}_\text{A}^-$  oxidation in  $\text{HCO}_3^-$ -depleted (treated) membranes and control membranes follow. The inhibitory effect of  $\text{HCO}_3^-$ -depletion was fully reversible with the addition of 5 mM  $\text{HCO}_3^-$ . At pH 6.5 the overall half-times for  $\text{Q}_\text{A}^-$  oxidation following actinic flashes 1, 2 and 5 given at 1 Hz were 2.8 ms, 11 ms and 22 ms respectively in treated membranes. The corresponding control membranes exhibited half-times of 547  $\mu\text{s}$ , 600  $\mu\text{s}$  and 550  $\mu\text{s}$  respectively. At pH 7.5 the overall half-times of  $\text{Q}_\text{A}^-$  oxidation in treated membranes were 1.5 ms and 3.6 ms after one or two actinic flashes spaced at 1 s (1 Hz). After five actinic flashes given at 1 Hz the overall half-time was 47 ms. The corresponding control membranes exhibited overall half-times of 400  $\mu\text{s}$ , 633  $\mu\text{s}$  and 580  $\mu\text{s}$  for  $\text{Q}_\text{A}^-$  oxidation after 1, 2 or 5 actinic flashes, given at 1 Hz, respectively. When the actinic flash frequency was 5 Hz the kinetics of  $\text{Q}_\text{A}^-$  oxidation in treated membranes were slowed further. At pH 6.5 the  $t_{1/2}$  was 182 ms and at pH 7.6, 240 ms. The respective half-times in the controls were 550  $\mu\text{s}$  and 480  $\mu\text{s}$ .

The above results show that in treated membranes the oxidation of  $\text{Q}_\text{A}^-$  by  $\text{Q}_\text{B}$  or  $\text{Q}_\text{B}^-$ , following 1 or 2 actinic flashes exhibits a smaller overall half-time at pH 7.5 than at pH 6.5. Furthermore, the slowest oxidation of  $\text{Q}_\text{A}^-$ , as indicated by the overall half-time parameter,

depends on both pH and flash number. After five actinic flashes, given at 1 Hz,  $Q_A^-$  oxidation is slower at pH 7.5 than at pH 6.5. The transition for this reversal of the pH dependence was found to occur with the oxidation of  $Q_A^-$  following the third flash. The overall half-time parameter also depends on the actinic flash frequency.

In Chapter IV a detailed study of the decay of variable chlorophyll a fluorescence after 1 or 2 actinic flashes in the presence or absence of DCMU (3-(3,4-dichlorophenyl)-1,1-dimethylurea) produced the following results in treated membranes: (1) the pH dependence of the operating redox potential for the  $Q_B/Q_B^-$  couple was not observed; (2) the equilibrium for the sharing of an electron between  $Q_A$  and  $Q_B$  was decreased by a factor of 4 at pH 6.0; (3) the back reaction between  $Q_A^-$  and the  $S_2$ -state of the OEC was inhibited approximately four-fold below pH 7.0 but was unaffected above pH 7.5 in the presence of DCMU, (4) a back reaction with a half-time of less than 100  $\mu$ s was present at pH 8.0 in the presence of DCMU in approximately half of the PS II centers and (5) the kinetic stability of the tightly bound  $Q_B^-$  semiquinone was significantly reduced.

Two hypotheses emerge from these results particularly with respect to the pH independent operating redox potential of the  $Q_B/Q_B^-$  couple in treated membranes. These are: (1) that two distinct  $HCO_3^-$  binding sites are present on PS II and (2) that only a single site is present. Each of these will be presented separately.

#### 1. The Two Site Hypothesis

In control and  $HCO_3^-$ -restored membranes a semi-logarithmic plot of the decay of  $[Q_A^-]$  following a single actinic flash yields an initial linear decay with an amplitude of approximately 70% (see Fig. 24 and

Ref. [24] in Chapter IV). This component is thought to reflect the fraction of PS II that has a plastoquinone from the PQ pool bound at the  $Q_B$ -site. This fraction is therefore described by the association constant,  $K_0$ , for  $Q_B$ , the secondary plastoquinone acceptor of PS II. In treated membranes the fraction of centers with  $Q_B$  bound appears to decrease as the pH becomes more acid. The values of  $K_0$  in treated, restored and control membranes are presented as a function of pH in Table 4.

The equilibrium constant for sharing an electron between  $Q_A$  and  $Q_B$  is given by equation (1):

$$K_{app} = \frac{[Q_A Q_B^-] + [Q_A Q_B^-(H^+)]}{[Q_A^-] + [Q_A^- Q_B]} \quad (1)$$

and the redox potential of the  $Q_B/Q_B^-$  couple can be determined from the following relationship using a known value for the  $Q_A/Q_A^-$  couple:

$$E_m(Q_B/Q_B^-) - E_m(Q_A/Q_A^-) = \frac{RT \ln K_{app}}{F} \quad (2)$$

where R is the gas constant, F is the Faraday constant and T is the absolute temperature.

In Ref. [24] of Chapter IV, Crofts et al. have shown that  $K_{app}$  and  $K_0$  are related by equation (3):

$$K_{app} = \frac{K_E(1 + 10^{-pH} \cdot 10^{pK_3})}{\left(1 + \frac{1}{K_0 \cdot [PQ]}\right) (1 + 10^{-pH} \cdot 10^{pK_a})} \quad (3)$$

where  $K_E$  is the equilibrium constant for the sharing of an electron between  $Q_A^-Q_B \rightleftharpoons Q_AQ_B^-$  and  $K_3$  describes the equilibrium of a  $H^+$  with  $Q_B^-$  (see Fig. 3, Chapter I).  $K_a$  in equation 3 describes the equilibrium of a  $H^+$  with  $Q_B$  in its oxidized form.

Therefore it can be seen from equations 1, 2 and 3 that the pH independent operating redox potential for the  $Q_B/Q_B^-$  couple observed in treated membranes may arise from the apparent pH dependent decrease observed for  $K_0$  in these samples.

Two modes of action associated with the  $HCO_3^-$  anion were outlined above. These were (1) that  $HCO_3^-$  is directly involved in the protonation reactions associated with plastoquinone reduction at the  $Q_B$ -site and (2) that  $HCO_3^-$  is required in maintaining the conformational integrity of PS II to allow for efficient transfer of electrons through the quinone acceptor complex to the plastoquinone pool.

The pH dependence seen for  $Q_A^-$  oxidation after 1 or 2 actinic flashes and the apparent pH dependence observed for  $K_0$  in treated membranes can be understood from the perspective of the conformational hypothesis. Were  $HCO_3^-$  to be acting as a proton donor the pH dependence would be expected to be the opposite of that seen, since increasing the bulk proton concentration by lowering the pH would be expected to substitute, at least in part, for the normal native proton donor.

In treated membranes the kinetics of  $Q_A^-$  oxidation at pH 6.5 after 1 or 2 actinic flashes, 2.8 ms and 11 ms respectively, as described above are problematic. A difficulty arises since the rate-limiting step as determined for the Hill reaction at pH 6.5 is on the order of 45 ms per electron (Chapter II). The pH dependence is such that the kinetics of  $Q_A^-$  oxidation, after 1 or 2 actinic flashes, are accelerated when the pH is increased. This dependency is then reversed after three or four

actinic flashes. That is, after two turnovers of the reaction center the rate of  $Q_A^-$  oxidation becomes sensitive to the bulk pH and is slowed at alkaline pH. It is also only after three or four turnovers of the reaction center that the kinetics of  $Q_A^-$  oxidation are slowed to the degree that they can account for the estimated rate-limiting step in linear electron transport (Chapter III).

To reconcile these data, the existence of two  $HCO_3^-$  binding sites is proposed. These are defined as site 1 and site 2. Site 1 is suggested to incorporate  $HCO_3^-$  as a ligand to  $Fe^{2+}$  (see Chapter IV) and is characterized by a dissociation constant of approximately 80  $\mu M$  (see overview in Chapter I). This hypothesis can then account for the apparent pH dependence on  $K_D$ , the reduction in the kinetic stability of  $Q_B^-$  and the other  $HCO_3^-$ -reversible effects associated with the back reaction from  $Q_A^-$  in the presence of DCMU by suggesting that they arise from a conformational change in the quinone acceptor complex accompanying the removal of  $HCO_3^-$ , in the presence of inhibitory anions, from site 1.

Site 2 is suggested to be involved in the protonation reactions associated with  $Q_B$  reduction. Bicarbonate at this site would be expected to be bound very tightly such that even after extensive  $HCO_3^-$ -depletion procedures in the presence of inhibitory anions, a bound  $HCO_3^-$  may still remain.

However,  $HCO_3^-$  does not appear to be involved with the protonation of  $Q_B^{2-}(H^+)$  since the calculated values for the redox potential of the  $Q_B/Q_B^{2-}$  couple and the equilibrium constant for the oxidation of  $Q_A^-$  by  $Q_B^-$  did not show any significant change in the treated membranes. Bicarbonate is therefore suggested to be involved in the mechanism of  $Q_B^-$  protonation.

After the protonation of  $Q_B^-$  following a single actinic flash,  $CO_3^{2-}$  may dissociate from a putative arginine binding ligand (see Chapter IV). In treated membranes no  $HCO_3^-$  is available to rebind, so following a third actinic flash, protonation must result from protons arriving from other sources. The observed dependencies on actinic flash number and actinic flash frequency reflect the kinetics of this protonation and are therefore dependent on the bulk pH (Chapters III and IV).

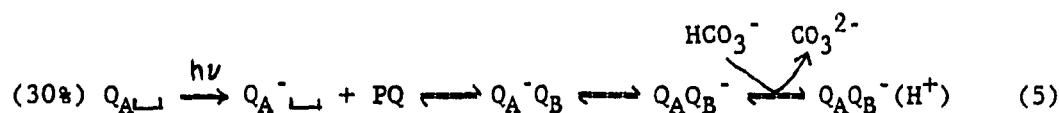
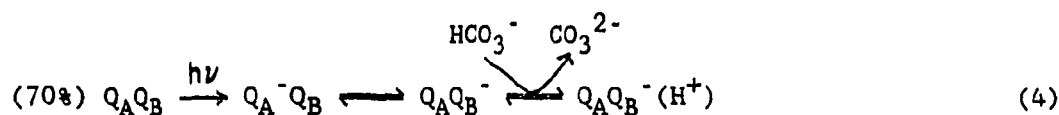
However, when  $HCO_3^-$  is removed and no formate or other inhibitory anion is present, the Hill reaction is only inhibited two-fold (see Chapter II). This suggests that if an inhibitory anion is not bound to the suggested tight  $HCO_3^-$  binding site protonation from other sources is more efficient. This implies that any role for  $HCO_3^-$  in the protonation steps associated with  $Q_B$  reduction is catalytic or regulatory.

The binding of  $HCO_3^-$  to PS II does appear to have physiological significance beyond a possible regulatory role in the protonation reactions. Irreversible loss of activity is associated with  $HCO_3^-$ -depletion in the absence of inhibitory anions. The possibility that  $HCO_3^-$  may in fact be a ligand to  $Fe^{2+}$  supports the interpretation that this irreversible change is associated with the formation of  $Fe^{3+}$ .

The equations that follow illustrate the above mechanism and refer back to the appropriate experimental results in the preceding chapters.

In Table 4 in Chapter IV the  $K_0$  for  $Q_B$  is seen to be  $420 M^{-1}$  and unaffected between pH 6.5 and pH 7.75 in undepleted control membranes or  $HCO_3^-$ -restored membranes. A  $K_0$  of this value corresponds to 70% of the reaction centers having  $Q_B$  bound before the actinic flash. Therefore, since in our preparations we have attempted to oxidize any  $Q_B^-$  in the dark adapted samples, we have for control membranes at pH 6.5 or 7.5 after a single actinic flash the following equations:

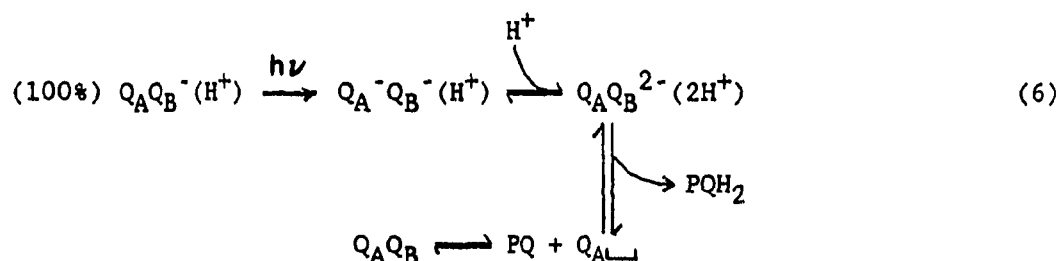
Flash 1



The  $\text{HCO}_3^-$  anion shown in equations 4 and 5 represents the  $\text{HCO}_3^-$  bound to site 2. This  $\text{HCO}_3^-$  is envisioned to participate in the protonation of  $\text{Q}_B^-$ . As suggested above, after donating its proton,  $\text{HCO}_3^-$  then would dissociate as  $\text{CO}_3^{2-}$ . In control or  $\text{HCO}_3^-$ -restored membranes  $\text{CO}_3^{2-}$  may become reprotonated (it has a pK of 10.2 at 25° C) or another available  $\text{HCO}_3^-$  may rebind to this site.

Equations 4 and 5 indicate that all centers would be in the state  $\text{Q}_A\text{Q}_B^-(\text{H}^+)$ . Thus assuming the simplest case (i.e., all centers with  $\text{Q}_B^-$  protonated), the equation for the second flash is:

Flash 2



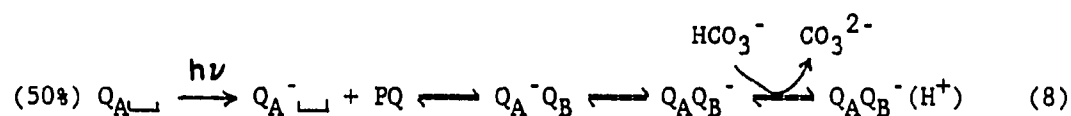
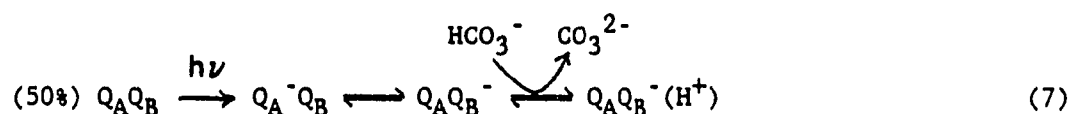
where the second protonation does not involve  $\text{HCO}_3^-$ . Neither the estimated redox potential for the  $\text{Q}_B^-/\text{Q}_B^{2-}$  couple nor the equilibrium constant for the reaction  $\text{Q}_A^-\text{Q}_B^- \rightleftharpoons \text{Q}_A\text{Q}_B^{2-}$  was found to be significantly influenced by  $\text{HCO}_3^-$ -depletion in Chapter IV. Equation 6 returns the centers to the initial starting point, and therefore flash 3 resembles

flash 1 and flash 4 resembles flash 2, etc.

Turning to the treated case, and considering first the situation at pH 7.5, equations 7 through 16 describe the proposed sequence of states associated with the acceptor side following the removal of  $\text{HCO}_3^-$ .

As discussed in Chapter IV, the  $\text{HCO}_3^-$ -depletion process appears to remove a  $\text{HCO}_3^-$  which is a ligand to  $\text{Fe}^{2+}$  in PS II. A large conformational change in the quinone acceptor complex may result, and, as shown in Table 4 in Chapter IV, the association constant for  $\text{Q}_B$  is decreased from  $420 \text{ M}^{-1}$  to  $230 \text{ M}^{-1}$  at pH 7.5. This corresponds to a reduction in the bound  $\text{Q}_B$  fraction from 70% to 50%. Therefore for flash 1 we have:

Flash 1



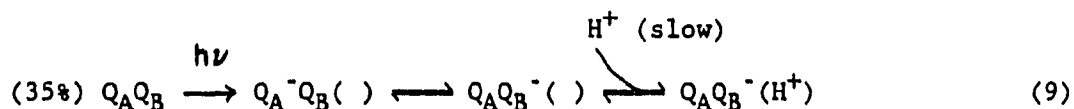
The  $\text{HCO}_3^-$  bound to the tight binding site (site 2) and involved in  $\text{Q}_B^-$  protonation, is assumed to not be removed by the  $\text{HCO}_3^-$ -depletion process in this scheme. The increase in overall  $t_{1/2}$  for  $\text{Q}_A^-$  oxidation in treated membranes may thus be largely associated with the increased fraction of centers undergoing a second-order reaction with respect to  $\text{Q}_B$  binding. As the pH is increased so the association constant approaches that of the control and the overall half-time is decreased (Figs. 14 and 22).

The formation of  $\text{Q}_B^-$  is shown to be thermodynamically unstable in  $\text{HCO}_3^-$ -depleted, restored and control membranes in Chapter IV. The characteristic long life of this species is therefore attributed to kinetic stability. The kinetic stability appears significantly reduced

in treated membranes (e.g., Figs. 25 and 26 and discussion in Chapter IV). An additional indication of the reduced kinetic stability associated with  $Q_B^-$ , and discussed in Chapter IV, is the level of DCMU-induced Chlorophyll a fluorescence following a single turnover actinic flash. However, the DCMU-induced fluorescence level following the third or fifth actinic flashes is essentially the same in treated, restored and control membranes. This would appear to indicate that the kinetic stability is only altered after the first turnover of the reaction center and that the process involves a component that when reduced is only reoxidized on a very slow time scale. In Fig. 25 35% of the decay of  $Q_A^-$  at pH 7.5 after two actinic flashes, spaced at 1 s, is shown to be by a process resembling oxidation by  $Q_B$  rather than  $Q_B^-$ . That is, 35% of the decays resemble the decay observed for centers with  $Q_B$  bound before a single actinic flash.

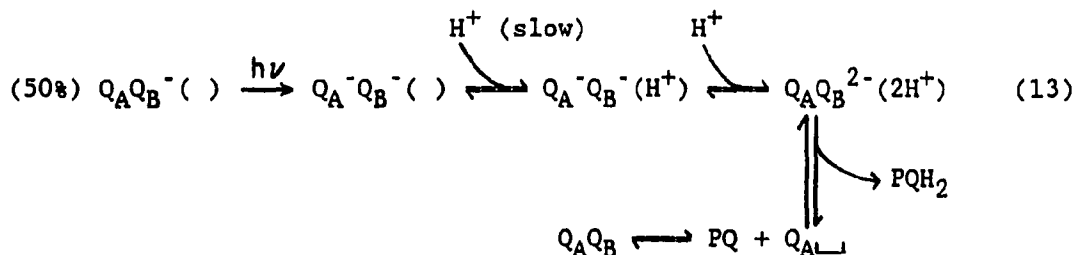
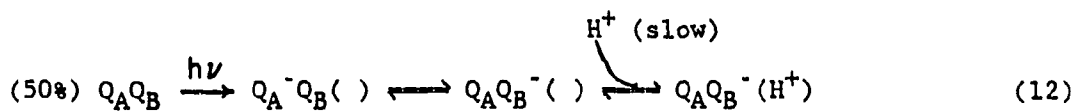
If it is assumed that 50% of the centers remain in the state  $Q_A Q_B^-(H^+)$  after the first flash, then a value for  $K_O$  of  $220 M^{-1}$  can be calculated when 35% of the remaining centers have  $Q_B$  bound before the second actinic flash. This is in good agreement with the value of  $230 M^{-1}$  given in Table 4 in Chapter IV. Thus after the second flash we have:

Flash 2



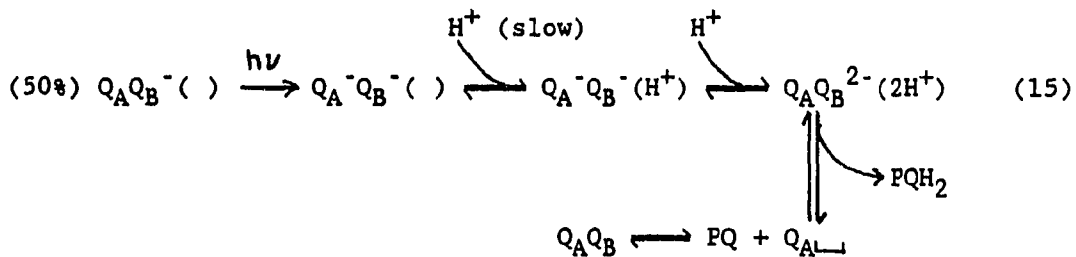


Flash 3



Then assuming no protonation at the rate-determining step in equations 12 and 13, we have:

Flash 4



and again assuming no protonation at the rate-limiting step in 15 we have:

Flash 5

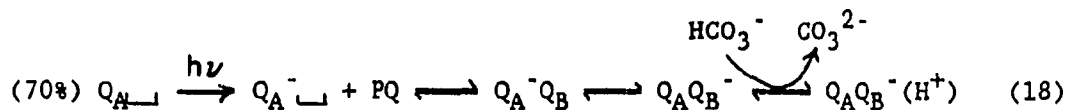
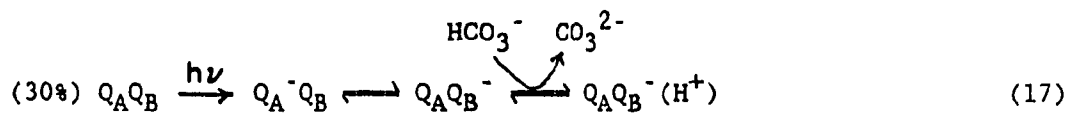


Therefore, the maximum inhibition in  $\text{Q}_A^-$  oxidation would occur after the fifth actinic flash. This scheme satisfactorily explains the data for treated membranes at pH 7.5 in Figs. 15-18. However, it should

be pointed out that the kinetics of  $Q_A^-$  oxidation after flash 4 in this scheme should be identical with those observed following the fifth flash. In Figs. 15-18 the flash frequency was 1 Hz and presumably the degree of protonation occurring between successive actinic flashes is reflected in the somewhat faster overall decay of  $Q_A^-$  indicated after the fourth actinic flash as compared to the decay after the fifth and subsequent turnovers. A similar set of arguments as used for equations 7 through 16 readily explain the observed data in Chapter III for  $Q_A^-$  oxidation in treated membranes at pH 6.5.

The association constant in treated membranes at pH 6.5 was found to be  $80 \text{ M}^{-1}$  (Table 4, Chapter IV). This corresponds to a fraction of 30% of the centers having  $Q_B$  bound before the flash. Therefore we have

Flash 1

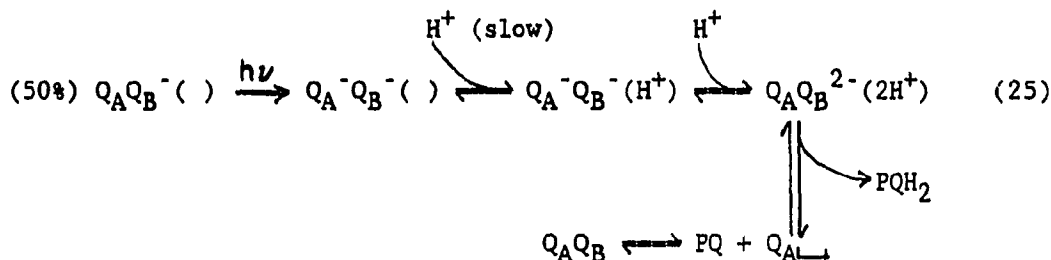


Then assuming the same effect on the kinetic stability of  $Q_B^-$  after one flash as discussed above (i.e., that 50% of centers have  $Q_B^-$ ) and following the results of Figs. 25 and 26(b) which indicate that 20% of centers have  $Q_B$  bound 1 s after the initial actinic flash, then a value of  $55 \text{ M}^{-1}$  is obtained for  $K_0$ . This is in reasonable agreement with the value of  $80 \text{ M}^{-1}$  given in Table 4, Chapter IV. The equations after the second flash then become:



again assuming no protonation at the rate-determining step for flash 4 we have:

Flash 4



and thus for flash 5:

Flash 5



As discussed above, the decay kinetics reflecting  $\text{Q}_A^-$  oxidation are predicted to be identical by this model following the fourth flash and subsequent turnovers. This result was obtained for the kinetics of  $\text{Q}_A^-$  oxidation monitored by either the absorbance change at 320 nm in a train of actinic flashes given at 20 Hz or by the decay of Chl a fluorescence when a train of actinic flashes were given at 25 Hz (see Ref. [81], Chapter I).

The results obtained for  $\text{Q}_A^-$  oxidation at pH 6.5 in Figs. 15-18 therefore demonstrate that a significant amount of protonation at the rate-determining step can occur, even in the presence of inhibitory anions, when the actinic flashes are delivered in a train at 1 Hz. This dependency on actinic flash frequency is clearly shown in Fig. 21. As

the actinic flash frequency is increased from 1 Hz to 5 Hz the overall  $t_{1/2}$  at pH 6.5 approaches that measured at pH 7.6.

The model described in equations 4 through 26 therefore allows us to conclude that the rate-determining step in linear electron transfer, in membranes depleted of  $\text{HCO}_3^-$  in the presence of inhibitory anions, is the protonation of  $\text{Q}_B^-$ . This occurs as a result of removing  $\text{HCO}_3^-$  from site 2.

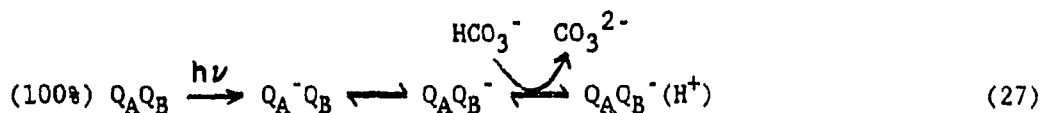
## 2. The Single Site Hypothesis

The two site hypothesis just described assumes that the initial linear component of  $\text{Q}_A^-$  oxidation (see Fig. 24) reflects centers that have  $\text{Q}_B$  bound before the first actinic flash. A second plausible explanation exists. The mechanism of electron transfer from  $\text{Q}_A^-$  to  $\text{Q}_B$  is thought to involve the association of a proton with  $\text{Q}_B^-$  (see  $K_3$  in Fig. 3, Chapter I). The  $\text{pK}$  for this protonation has been estimated to be 7.9 in control membranes (see Ref. [34] in Chapter IV). Furthermore, Tables 2 and 4 and Figs 14, 22 and 24 all demonstrate that the treated membranes tend to behave in a similar fashion to that of the unprotonated control at alkaline pH.

The truncated initial linear component in treated membranes may therefore reflect an effect on  $K_3$ , the equilibrium constant for the association of a proton with  $\text{Q}_B^-$  rather than an effect on  $K_0$ . Since the amplitude of the initial linear component is reduced as the pH is reduced, this interpretation also suggests that the site of protonation associated with  $\text{Q}_B^-$  is not readily accessible to the bulk phase.

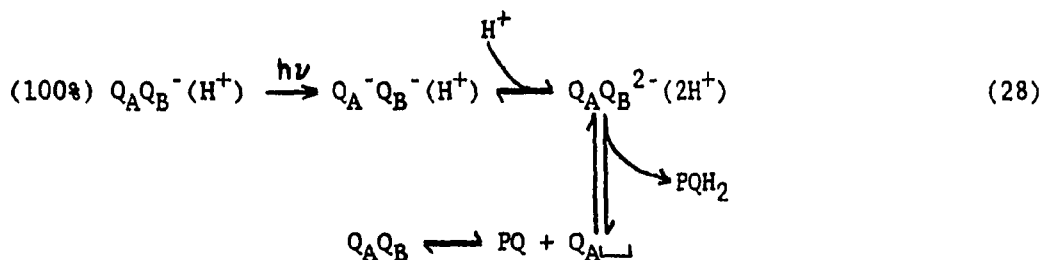
Neglecting  $K_0$ , equations 27 and 28 are essentially the same as equations 4-6 and describe the control case with  $\text{HCO}_3^-$  participating in the protonation of  $\text{Q}_B^-$ .

Flash 1



and assuming all centers are in the state  $\text{Q}_A\text{Q}_B^-(\text{H}^+)$  before the second flash, we have:

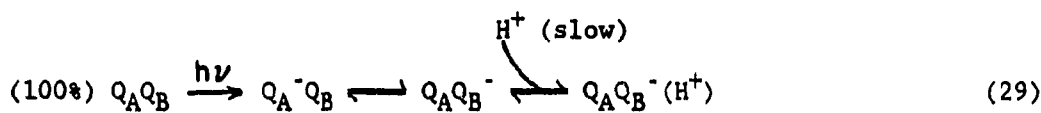
Flash 2



and hence flash 3 would be as flash 1 and flash 2 as flash 4, etc.

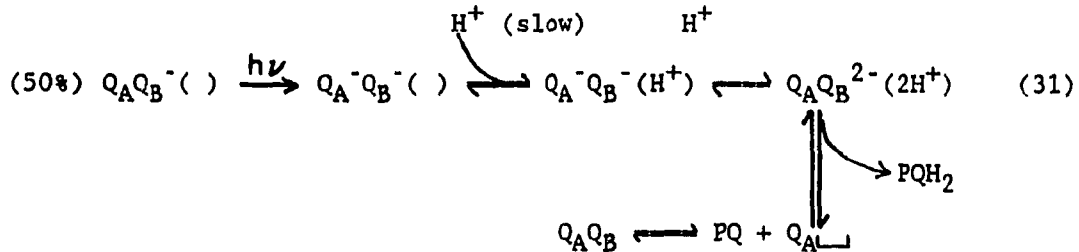
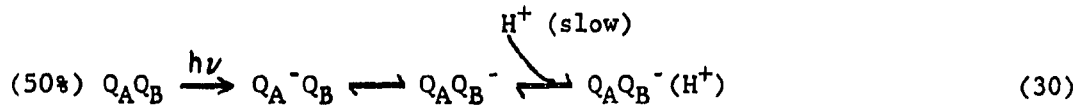
Equations 29-34 depict the expected sequence of events for treated membranes using the single site hypothesis. Again, neglecting  $K_0$  for flash 1 we have:

Flash 1



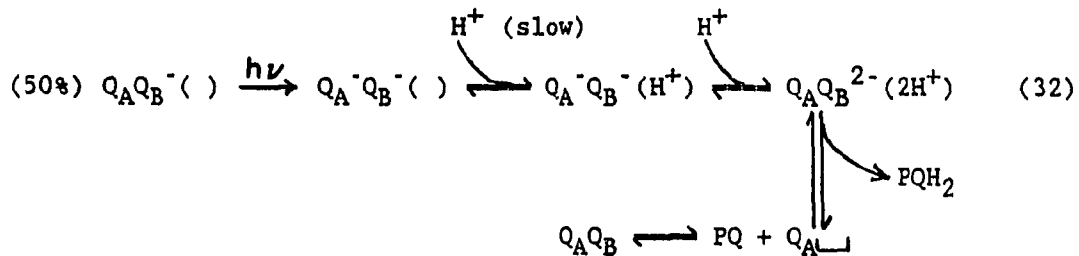
From Fig. 25 and Tables 2 and 3 it can be estimated that approximately 47% of  $\text{Q}_B^-$  is lost between flash 1 and 2 when a dark time of 1 s is given. This is assumed to be due to a decreased kinetic stability of  $\text{Q}_B^-$  in treated membranes following a single actinic flash. Thus for flash 2 we have:

Flash 2



and assuming no protonation at the rate-determining steps in equations 30 and 31 we have for flash 3:

Flash 3



and again assuming no protonation at the rate-determining step we have for flash 4:



Equations 29-34 therefore predict that the maximum inhibition observed for  $\text{Q}_A^-$  oxidation will depend on flash number, frequency and pH. This is apparent since some protonation accompanying  $\text{Q}_B$  reduction is expected to occur even when  $\text{HCO}_3^-$  has been removed and replaced by inhibitory anions. The one site hypothesis is thus also seen to be

consistent with the findings of Chapter III. In addition, the assignment of a large portion of the slow decay associated with  $Q_A^-$  oxidation to protonation in Chapter III is consistent with the notion that the site of protonation is fairly inaccessible to protons in the bulk phase.

The single site hypothesis is also quite successful at explaining the additional results of Chapter IV. The pH dependent operating redox potential for the  $Q_B/Q_B^-$  couple is entirely consistent with protons being unable to participate in the protonation of  $Q_B^-$  after the first actinic flash. The reported shift in the  $Q_A^-Q_B \rightleftharpoons Q_AQ_B^-$  equilibrium at pH 6.0 is again consistent with an altered  $K_3$  as is the apparent decrease in the kinetic stability of  $Q_B^-$ .

The discussion of  $HCO_3^-$  acting as a ligand to  $Fe^{2+}$  in Chapter IV is equally applicable to both the single site and the two site hypotheses. Both approaches to the findings of this thesis suggest that the rate-determining step in linear electron flow following  $HCO_3^-$  depletion, in the presence of inhibitory anions, is the protonation step associated with  $Q_B$  reduction to  $Q_B^-$ . While further experimentation will lead to additional refinements in our appreciation of the function of  $HCO_3^-$  in PS II, the results of this work do represent a new understanding. The notion that the rate-determining step represented centers locked in the state  $Q_A^-Q_B^{2-}$  and unable to exchange  $Q_B^{2-}$  with the PQ pool, either as a result of protonation or a conformational change, is not supported by this study.

## VITA

Julian Eaton-Rye was born on January 31, 1957 in Hastings, East Sussex, England. He obtained a Bachelor of Science degree in Botany from Manchester University in 1981. He joined the Plant Biology Department at the University of Illinois in 1981 and later transferred into the Plant Physiology Doctoral Program. During his graduate studies he has held research assistantships in the Department of Physiology and Biophysics and teaching assistantships in the Department of Plant Biology.

He is a coauthor of the following publications:

1. The Effects of Bicarbonate Depletion and Formate Incubation on the Kinetics of Oxidation-Reduction Reactions of the Photosystem II Quinone Acceptor Complex, *Z Naturforsch.* 39C, 382-385 (1984)
2. A Study of the Specific Effect of Bicarbonate on Photosynthetic Electron Transport in the Presence of Methyl Viologen, *Photobiochem. Photobiophys.* 8, 279-288 (1984)
3. Action of Bicarbonate on Photosynthetic Electron Transport in the Presence or Absence of Inhibitory Anions, In: *Ion Interactions in Energy Transfer Membranes* (Papageorgiou, G.C., Barber, J. and Papa, S., eds.), pp. 263-278, Plenum Publishing Corporation, New York (1986)
4. Electron Transfer Through Photosystem II Acceptors. Interactions with Anions, *Photosynthesis Res.* 10, 365-379 (1986)
5. The pH Dependence of  $Q_A^-$  Reoxidation in Anion Inhibited Photosystem II Centers, In: *Proceedings of the VII International Congress on Photosynthesis* (Biggins, J. ed.), Vol. II, pp. 433-436, Martinus Nijhoff, Dordrecht (1987)
6. Book Review. D.O. Hall and K.K. Rao; *Photosynthesis*, 4th Edition,

1987, Edward Arnold Publishers, Photosynthesis Res. (1987), in the  
press